University of Stavanger

Faculty of Science and Technology

MASTER'S THESIS

Study Program/ Specialization: M.Sc. Petroleum Engineering Specialization: Reservoir Engineering	Spring Semester, 2010 Open Access
Writer: Usman Aslam	*Usman Aslam*
Faculty supervisor: Professor Svein M. Skjæveland External supervisor(s): Ingebret Fjelde (Senior Research Scientist at IRIS), Arild Lohne (Senior Research Engineer at IRIS)	
Titel of thesis: **Numerical Simulation of Surfactant Flooding in Mixed Wet Reservoirs**	
Credits (ECTS): 30 ECTS	
Key words: Simulation, IFT, Wettability	Pages: 110 + Enclosure: 9 Stavanger, June 15, 2010

DEDICATION

This work is dedicated to my beloved country Pakistan, all of my teachers, my family and fiancé.

ACKNOWLEDGEMENTS

TABLE OF CONTENTS

LIST OF FIGURES

LIST OF TABLES

NOMENCLATURE

A = Area

ASP = Alkaline Surfactant Polymer Flooding

CDC = Capillary Desaturation Curve

CL = Capillary Limit

EOR = Enhanced Oil Recovery

FOPR = Field Oil Production Rate

FOPT = Field Cumulative Oil Production

FWCT = Field Water Cut

g = Acceleration due to gravity

h = Thickness

H = Mean Curvature of Interface

IFT = Interfacial Tension

IOR = Improved Oil Recovery

JowI = Dimensionless Imbibition Capillary Pressure

JowD = Dimensionless Drainage Capillary Pressure

K = Absolute Permeability

K_{eff} = Effective Permeability

K_r = Relative Permeability

K_{ro} = Oil Relative Permeability

K_{rw} = Water Relative Permeability

L = Length

N_c / N_{ca} = Capillary Number

N_{vc} = Local Capillary Number

$(N_{vc})_c$ = Critical Capillary Number

$(N_{vc})_t$ = Desaturation Capillary Number

P_w = Wetting Phase Pressure

P_{nw} = Non Wetting Phase Pressure

P_{cow} = Oil–Water Capillary Pressure

PV = Pore Volume Injected

Q_w = Water Flow Rate

r = Pore Radius

ROS = Remaining Oil Saturation

S_{or} = Residual oil saturation M

S_{nwr} = Residual Saturation of Non Wetting Phase

S_{wr} = Residual Saturation of Wetting Phase

S_{wi} = Initial water saturation

ST = Surface Tension

u = Darcy Velocity

v = Interstitial Velocity

VL = Viscous Limit

μ = Viscosity

σ = Interfacial Tension

θ = Contact Angle

φ = Porosity

ΔP = Pressure drop

ABSTRACT

Surfactants have been considered for enhanced oil recovery either by reduction of oil–water interfacial tension (IFT) or through wettability alteration. This study reveals the effect that reduced interfacial tension has on capillary trapping in heterogeneous reservoirs. This effect has been investigated by running numerical experiments on different synthetic simulation models. Rock capillary pressure is assumed to scale with IFT. Capillary contrast on the scale of a few centimeters to few tens of meters is reduced in the presence of surfactant. This reduction in IFT potentially may result in increased or accelerated oil production from mixed–wet reservoirs.

The main focus of this study is to simulate the displacement process (water flood) at various IFT using Eclipse (Surfactant Model). Simulation studies of different mechanisms which are believed to occur in mixed–wet reservoirs are presented. The surfactant flooding model was applied to the synthetic reservoir models. Simulation results indicate that surfactant flooding has a promising effect on the oil recovery depending upon the types of reservoir.

Detailed fine–scale simulation is carried out with representative relative permeability and imbibitions capillary pressure curves from mixed–wet cores. The efficiency of the surfactant flooding is investigated through sensitivity scenarios on formation rock/fluid parameters (e.g., Permeability, IFT, Flow Rate etc). It was found that the geological heterogeneity (layering, inclusions), imbibitions capillary pressure curve from mixed–wet reservoirs, viscous/capillary balance (N_c), gravitational forces, all have an impact on recovery by surfactant flooding. L_x/L_z (Length to thickness ratio of the model/ reservoir), permeability, IFT, density difference between oil and water and injection flow rates were found to be the critical parameters which influence simulation results.

CHAPTER 1

INTRODUCTION

1.1. Background

Oil recovery operations have traditionally been subdivided into three stages: primary, secondary and tertiary and these stages historically described the production from a reservoir in a chronological sense. Primary production, initial production stage, results from the displacement energy naturally exists in the reservoirs. The natural energy sources are solution–gas drive, gas–cap drive, natural water drive, fluid and rock expansion and gravity drainage. Secondary recovery, a second stage of the operations, is usually implemented after primary recovery stage declines. Traditionally secondary recovery processes are water flooding, pressure maintenance, and gas injection.

Tertiary recovery, the third stage of production, was that obtained after water flooding or whatever processes was implemented under secondary recovery. Tertiary processes include thermal, chemical and/or miscible gas injection after the secondary recovery process become uneconomical. Another descriptive designation commonly used is "improved oil recovery" (IOR) which includes EOR but also encompasses a broader range of activities e.g., reservoir characterization, improved reservoir management and infill drilling.

The flow sheet (Subhash 2002) in Figure 1 shows the types of various EOR processes that are currently employed in the oil industry.

EOR

Thermal	Chemical	Gas	Other
1) Steam	1) Polymer	1) CO_2 miscible/immiscible	1) Microbial
2) Combustion	2) Alkaline	2) HC miscible/immiscible	
3) Hot Water	3) Surfactant	3) Nitrogen	
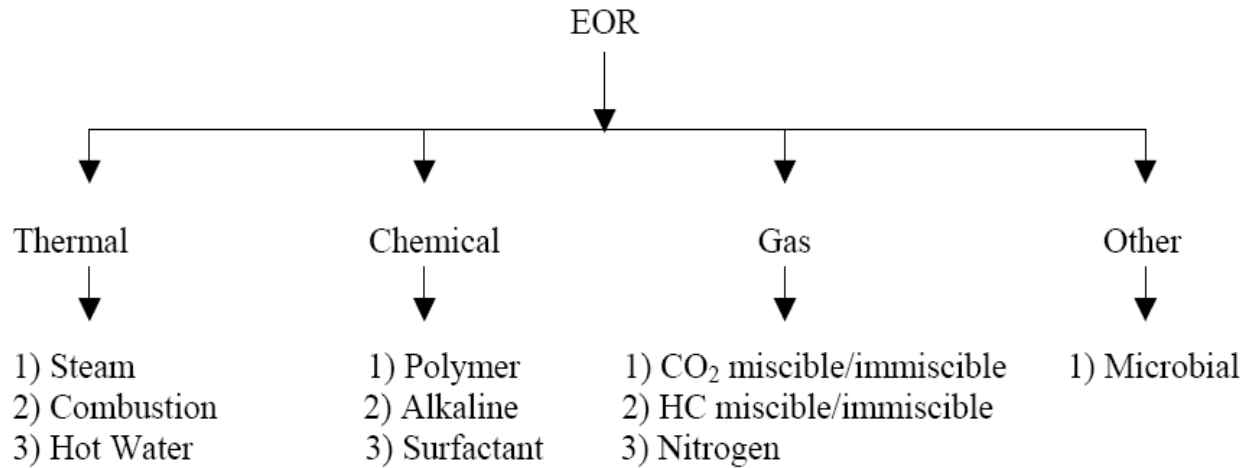
Figure 1: Flow Sheet for EOR Processes (Subhash 2002)

On the basis of types of injectants, EOR processes are classified into three categories (Lake, 1989): thermal (including steam flooding, hot–water injection, surface mining and extraction, etc.), gas (including CO_2 flooding, nitrogen injection, etc) and chemical methods (including alkaline flooding, surfactant flooding, alkaline/surfactant/polymer flooding, gel injection etc). Based on oil–displacement mechanisms and EOR field project results, Taber (1997) summarized the EOR screening criteria. Among the three methods, thermal and gas injection, account for most of the EOR production. However, some chemical methods have great research promise, like surfactant flooding. This study is devoted to figure out effectiveness of surfactant flooding in mixed–wet reservoirs.

Surfactant flooding is one of the three main chemical flooding processes which include polymer flooding, surfactant–polymer flooding and alkaline–surfactant–polymer (ASP) flooding. In the polymer flooding method, water–soluble polymers increase the viscosity of the injected water, leading to a more efficient displacement of moderately viscous oils. Addition of surfactant to the polymer

formulation may, under very specific circumstances, reduce oil–water interfacial tension to almost zero displacing trapped residual oil.

Although no large–scale surfactant–polymer floods have been implemented, the process has considerable potential to recover oil. A variation of this process involves addition of alkaline to the surfactant–polymer formulation. For some oils, alkaline may convert some acids within the oil to surfactants that aid oil recovery. The alkaline may also play a beneficial role in reducing surfactant retention in the rock. For all chemical flooding processes, inclusion of a viscosifier (usually a water–soluble polymer) is required to provide an efficient sweep of the expensive chemicals through the reservoir.

The primary purpose of surfactant flooding is to reduce the interfacial tension but this may also change or modify the wettability of the reservoir creating favorable conditions for increased or accelerated oil production. One of the key oil recovery problems in oil–wet reservoirs is overcoming the surface tension forces that tend to bind the oil to the rock surfaces. In water–wet reservoirs surface tension forces act to create bubbles of oil, which can block pore passages. In mixed–wet reservoir, snap–off of oil is believed to be absent. The surface tension forces are the primary reason why reservoirs become increasingly impermeable to oil relative to water as the water saturation increases. In mixed–wet reservoirs, oil relative permeability has a long tail at higher water saturation indicating that oil becomes less mobile at higher water saturation.

If the interfacial tension can be reduced between the oil and the driving fluid, then the resistance to flow is reduced. By designing and selecting a series of surfactants to lower the interfacial tension to the range of 10^{-3} dynes/cm, a recovery of 10 to 20% of the original oil in place is technically and economically feasible.

1.2. Objectives

Capillary number can be increased by either reducing the interfacial tension (IFT) or letting the value of contact angle (θ) approach 90°, which means an intermediate wettability of the rock–fluid system. The contact angle term in the definition of capillary number has been ignored in previous work by setting Cos θ = 1.0 (or 0° = 0) which is equivalent to assuming perfect water–wet conditions in all reservoirs. In other words, previous literature represents results from water–wet reservoir. It should be noted that there are more non water–wet reservoirs than water–wet ones (Anderson 1987).

The main objective of this work is to study the effect of capillary trapping by varying IFT on oil recovery enhancement whereas effects of wettability have been taken into account during simulation studies by using relative permeability and capillary pressure curves as input from mixed–wet reservoirs.

This study will numerically investigate the effect that reduced IFT has on capillary trapping in heterogeneous reservoirs. Displacement process (Waterflood) at various IFTs has also been simulated using Eclipse 100 (Surfactant Model).

The effects of reduced interfacial tension on three possible mechanisms which are believed to occur in mix–wet reservoirs have been investigated through numerical simulation of different synthetic models. These mechanisms include

1. Change in oil relative permeability (K_{ro}) curvature
2. Gravity segregation
3. Capillary trapping

The effect of reduced IFT has been investigated through remaining oil saturation as a function of capillary number. While simulating the effect of reduced IFT as a result of surfactant flooding on one of the above mentioned mechanisms, the other mechanisms are turned off during simulation runs so that the individual

4

mechanism could be studied. The combined effect of last two mechanisms has not been studied since investigation of gravity segregation require vertically refined model whereas capillary trapping require long model in horizontal direction and their integration requires an upscaled model which is beyond the scope of this work.

1.3. Methodology

The investigation of the effect of reduced IFT on aforementioned mechanisms requires three different types of synthetic models. These models include homogenous model, heterogeneous model (Layered/Stratified Case) and heterogeneous model (Inclusion Case). Inclusion represents a part of the model/reservoir with different permeability in comparison to surrounding matrix.

Relative permeability and capillary pressure curves from mixed–wet reservoir are introduced in each model. Injection of surfactants (Low IFT) is compared with its base case of waterflood (High IFT) in order to investigate the effect of reduced IFT. This reduction in turn increases the capillary number leading to low residual oil saturation. Only one water injection well and one oil production well is considered for the case of simplicity. Eclipse 100 (Surfactant Model) was used to carry out the required simulation studies.

First synthetic simulation model is the simplest model representing a homogeneous reservoir with 200 x 1 x 50 grid blocks. This model represents a vertical cross section of a reservoir since we are interested in investigating the effect of vertical heterogeneity on capillary trapping of oil. In this model the effect of gravity segregation is neglected by setting oil density approximately equal to water density (negligible difference between oil and water density), the effects of gravity were included afterwards separately to investigate the effect of reduced IFT on gravity segregation. The change in oil relative permeability curves was also

turned off by setting equal immiscible and miscible curves during simulation runs. This effect was also investigated later on by introducing different immiscible and miscible curves. The time required for simulation studies was extended to make sure that we capture the effect of surfactant dissolution with the passage of time.

Second model was a stratified (Layered) reservoir representing vertical heterogeneity containing five layers with varying rock characteristics (Permeability and porosity). Average porosity was kept same as in case of homogeneous model in order to get same pore volume so that the results of reduced IFT on capillary trapping could be compared in both cases. Leverett J–function was used in this case for averaging the capillary pressure data for all layers since the lithology of all layers is same. The results from both cases, with and without surfactant injection were compared. The effect of change in oil relative permeability curve was later investigated.

In third synthetic models, heterogeneity was introduced through inclusions. Two different types of inclusion were used in simulation studies. First type of inclusions was low permeable compared to the surrounding matrix whereas second type of inclusion was high permeable. All the inclusions within a model regardless of the type of permeability (low or high) were assigned same permeability to make the case simpler and results understandable. Again both the cases, with and without surfactant injection were compared and investigation. The effect of surfactant adsorption is not taken into consideration during the simulation studies since the emphasis of this study is to capture and develop a clear understanding of the effect of reduced IFT on capillary trapping in mixed–wet heterogeneous porous media. Most of the previous research work in this area has been conducted on water– wet reservoirs.

CHAPTER 2

LITERATURE REVIEW

Some of the basic concepts related to this study are elaborated below.

2.1. Chemical Flooding Effects

In chemical flooding, chemicals are added to achieve one or more of the following effects: interfacial tension reduction, wettability alteration and mobility control. Some fundamental concepts related to this study are presented below.

Interfacial Tension (IFT) is the excess free energy or lateral stress at the interface (C.A. Miller & Neogi, 1985). Interfacial tension develops due to the imbalanced cohesive forces like molecules within each fluid and adhesive forces of dissimilar molecules at phase boundaries. Thus the surface area of the resulting interface is minimized. Interfacial tension is commonly expressed in milli–Newton/meter (mN/m also dynes/cm). At fixed temperature, IFT can be changed by the addition of surface–active material know as surfactants.

Capillary Pressure (Pc) The combined effects of wettability and interfacial tension cause the wetting fluid to be simultaneously imbibed into a capillary tube. This phenomenon is known as capillarity and is significant in a porous medium saturated with two or more immiscible fluids since the interconnected pores of the medium are of capillary dimensions. Capillary pressure represents the pressure differential that must be applied to the non–wetting fluid in order to displace a wetting fluid. For the capillary tube, an often used yet admittedly simplistic representation of a pore throat, capillary pressure can be expressed as:

$$P_c = P_{nw} - P_w = \frac{2\sigma \cos\theta}{r} = (\rho_w - \rho_{nw})gh \quad \ldots\ldots\ldots\ldots 2.1$$

Where σ is the interfacial tension between the two fluids, θ represents the wettability of the capillary tube, r is the radius of the capillary tube, P_w, P_{nw} are the pressures of the wetting and non–wetting phases, respectively, and ρ_w and ρ_{nw} are the wetting and non–wetting phase densities, respectively.

Capillary pressure is caused by curved boundaries between different homogeneous fluid phases in a pore (Lake, 1989). Capillary pressure can be related with interfacial tension, wettability (contact angle), and interfacial curvature by Young–Laplace equation:

$$P_c = 2H\sigma \qquad\text{...} 2.2$$

If we assume pores are cylindrical geometry, then equation 2.2 turns into:

$$P_c = \frac{H\sigma\cos\theta}{R} \qquad\text{...}2.3$$

Where P_c : Capillary pressure

σ : Interfacial tension between two fluid phases

H : Mean curvature of interface

θ : Contact angle

R : Radius of the curvature

The pressure head in the non–wetting fluid must exceed the capillary entry pressure to displace the wetting fluid and enter a pore opening. In oil–wet reservoirs, capillary effect is usually the cause for large amount of oil being trapped in pores which cannot be recovered by water flooding. Capillary forces can be overcome be ultra–low interfacial tension (interfacial tension of about zero) or wettability reversal (which changes the sign of Cosϴ).

Capillary Pressure Curve The capillary pressure curve for a porous medium is a function of pore size, pore size distribution, pore geometry, fluid

8

saturation, fluid saturation history or hysteresis, wettability, and interfacial tension. Fig. 2 shows drainage and imbibitions capillary pressure curves. The drainage capillary pressure curve describes the displacement of the wetting phase from the porous medium by a non–wetting phase, as is relevant for the initial fluid distribution in a water–wet reservoir as well as for the water front advance in an oil–wet reservoir. The imbibitions capillary pressure curve, on the other hand, describes the displacement of a non–wetting phase by the wetting phase, as is relevant for water front advance in a water–wet reservoir. In both cases, the capillary pressure is equal to the non–wetting phase pressure minus the wetting phase pressure as given by Eq. 2.1.

The capillary pressure curve has several characteristic features. Focusing on the drainage curve and describing it in more detail, one finds that the minimum threshold pressure is the displacement pressure that must be applied to the wetting phase in order to displace the non–wetting phase from the largest pore connected to the surface of the medium such that:

$$(P_c)_{displacement} = (P_{nw} - P_w)_{displacement} = 2\sigma \cos\theta / r_{Largest\,pore} \quad \ldots\ldots 2.4$$

Eventually, when the irreducible wetting fluid saturation is reached, the capillary pressure curve becomes nearly vertical. At this stage, the wetting phase becomes discontinuous and can no longer be displaced from the porous medium simply by increasing the non–wetting phase pressure. A lower wetting phase irreducible saturation is generally indicative of relatively larger grains and pores. Generally speaking, therefore, a higher capillary pressure curve describes poorer reservoir quality compared to a lower curve.

The capillary pressure curves for rock samples from the same reservoir having different permeabilities will be different. It is often necessary to average the capillary pressure data for cores from the same reservoir to obtain one capillary

pressure curve representative of the whole reservoir. This can be done through use of a dimensionless capillary pressure relation called the Leverett J–function. In this function, Leverett (1941) used a characteristic pore dimension equal to the square root of the ratio of the permeability and porosity of the medium as an equivalent for the capillary tube radius in the capillary rise expression. In oilfield units, the Leverett J–function is given by:

$$J(S_w) = 6.848 \frac{P_c(S_w)\sqrt{k/\phi}}{\sigma \cos \theta} \quad \ldots\ldots\ldots\ldots\ldots\ldots\ldots\ldots 2.5$$

Where σ is the interfacial tension in dyne/cm, k is the permeability in Darcy, and Pc is the capillary pressure in psi.

It has been confirmed by many researchers that different capillary pressures for cores from the same reservoir rock will yield the same J–function (Leverett et al.). On the other hand, the Leverett J–function for different rock types will be different. The concept of a dimensionless characteristic capillary pressure curve for the reservoir provides the flexibility of making laboratory capillary pressure measurements with more convenient fluids than reservoir fluids. This enables the conversion of core capillary pressure data measured in the laboratory to reservoir conditions even if the fluid combination used in the lab is completely different than the one encountered in the reservoir. Leverett J–function is used while simulating the different heterogeneous synthetic models in our study.
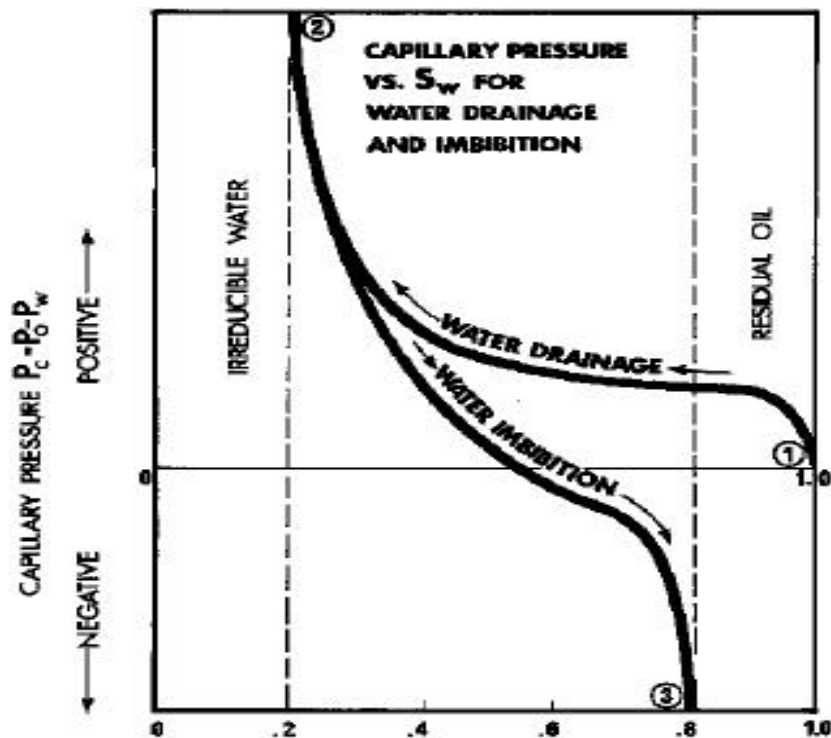
Figure 2: Drainage and Imbibition curves for water–wet system

Mobility Ratio is defined as the ratio of mobility behind and ahead of a displacing front (Lake, 1989). At large mobility ratio, displacing fluid tends to bypass oil which is detrimental to oil recovery. High sweep efficiency is obtained when mobility ratio is smaller than unity but smaller mobility ratio means low injection rate. So a practical mobility ratio is a compromise between mobility control and injection rate. Mobility can be controlled by adding polymers and foam. Mobility ratio is defined by the following formula

$$M = \frac{\mu_o}{\mu_w} \frac{k_{rw}}{k_{ro}}$$ 2.6

Wettability is defined by Craig (1971) as the tendency of one fluid to spread or adhere to a solid surface in the presence of the other immiscible fluids. When the rock is water–wet, there is a tendency for water to occupy the small pores and to

11

contact the majority of the rock surface. The situation is reversed in an oil–wet condition. Is it important to note that the term wettability is used for the wetting preference of the rock and does not necessarily refer to the fluid that is in contact with the rock at any given time. Wettability can be divided into five types: water–wet, oil–wet, intermediate wettability, mixed wettability and fractional wettability. Detail description of each of these wettability types is given by Anderson (1986).

Cleaned sand, glass beads and Berea cores are normally water–wet. The wettability of reservoir rocks varies widely as has been reported by Treiber et al (1971). Reservoir rocks can change from strongly water–wet by adsorption of polar compounds and/or the deposition of organic matter originally present in the crude oil (Denekas et al 1959). Most previous experimental studies of displacement processes in laboratory scale equipment either used water–wet cores and bead packs or have simply ignored the wettability conditions.

Contact Angle as a measure of wettability defines which fluid wets the solid surface. It is usually measured through the denser liquid phase. Through force balance analysis, Fig. 3, equilibrium contact angle is defined by Young's equation:

$$\sigma_{ow} \cos\theta = \sigma_{os} - \sigma_{ws} \quad \ldots\ldots\ldots\ldots\ldots\ldots\ldots\ldots\ldots\ldots\ldots\ldots\ldots 2.7$$
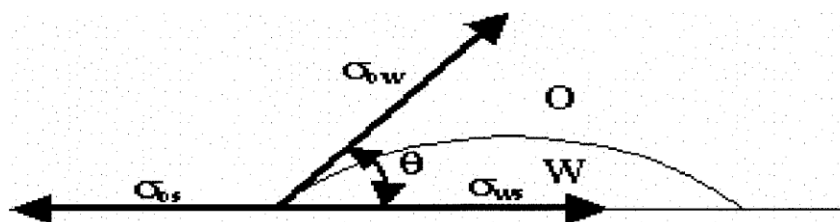
Figure 3: Force balance at three phase contact line

Where σ_{ow} : Interfacial tension between phase oil and water

σ_{ws} : Surface energy between phase water and substrate

σ_{os} : Surface energy between phase oil and substrate

θ : Equilibrium contact angle

12

In crude oil/water/rock system, according to the value of water advancing contact angle (contact angle measured through water phase when water is displacing phase), the wettability of a rock is usually defined as preferentially water–wet, intermediate wet or preferentially oil wet (see Fig. 4, refer to Morrow, 1998).

Oil   Oil   Oil

θ_a Water θ_a Water θ_a Water

$0° < \theta_a < 75°$ $75° < \theta_a < 115°$ $115° < \theta_a < 180°$

Preferentially water–wet   Intermediate–wet   Preferentially oil–wet

Figure 4: Wettability definition with advancing contact angle (θ_a)

The concept of mixed–wettability is proposed by Salathiel in 1973. In mixed–wettability condition, the finer pores and grain contacts are water–wet and the surfaces of larger pores are strongly oil–wet. If these oil–wet paths were continuous through the rock, water would displace oil from the larger pores so that the capillary forces would hold little or no oil in smaller pores or at grain contacts. Willhite (1986) presented additional discussion of intermediate and mixed wettability and described the effect of liquid composition on wettability.

Several parameters like relative permeability's, residual saturations, and capillary depressurization curves change with the wettability state of the reservoir. In addition all these parameters, can greatly impact oil recovery. Thus, there is a need to relate all these parameter to wettability state of the reservoir (Anderson

1986). A relationship between wettability and oil recovery is briefly described below.

2.2. Relationship between Wettability and Oil Recovery

The relative preference of reservoir rock pore surface to be wet by water or oil plays an important role in determining the microscopic distribution of fluids in the pore space of reservoir rocks. As mentioned earlier in a water–wet rock, water will tend to occupy the smallest pores and crevices while the larger pores will be occupied by the oil. Similarly, in an oil–wet rock the oil will occupy the smallest pores, the fluid distribution being the fluids in the pore space of reservoir rocks influence the rates of flow of each fluid as well as recovery efficiency and is therefore very important in oil recovery processes.

The preferential wettability of the reservoir governs, to a large degree, the oil recovery in a waterflood. In water–wet reservoirs, most of the oil is typically displaced before water breakthrough with little or no oil flowing after breakthrough. The residual oil will be trapped by capillary forces as disconnected ganglia. In oil–wet reservoirs, early water breakthrough occurs and appreciable amounts of oil are recovered after breakthrough. Much of the residual oil will be trapped by capillary forces in smaller pores. An accurate knowledge of residual oil saturation and its distribution after a waterflood is imperative for the success of a tertiary recovery process.

The determination of relative permeability values is essential for any recovery process. This is because the relative permeability curves are strongly dependent on wettability. Furthermore, relative permeability data are required in many reservoir engineering calculations.

Many people have studied the effect of wettability on relative permeability. Among them were Donaldson et al (1969), Owen and Archer (1971) and

McCaffery and Bennion (1974). Relative permeability curves are suitable for discriminating between strongly water–wet and strongly oil–wet cores. An example of relative permeability curves for water–wet and oil–wet cores are shown in Fig. 5. There is a significant shift of relative permeability curves due to wettability changes.

The effect of wettability in tertiary recovery process has also been conducted by Mat Hussin (1988). Generally the experimental studies have shown that the injected fluid breakthrough is earlier in water–wet cores than in oil–wet cores. In miscible displacement process residual oil recovery is more efficient in oil–wet rock than in water–wet rock.
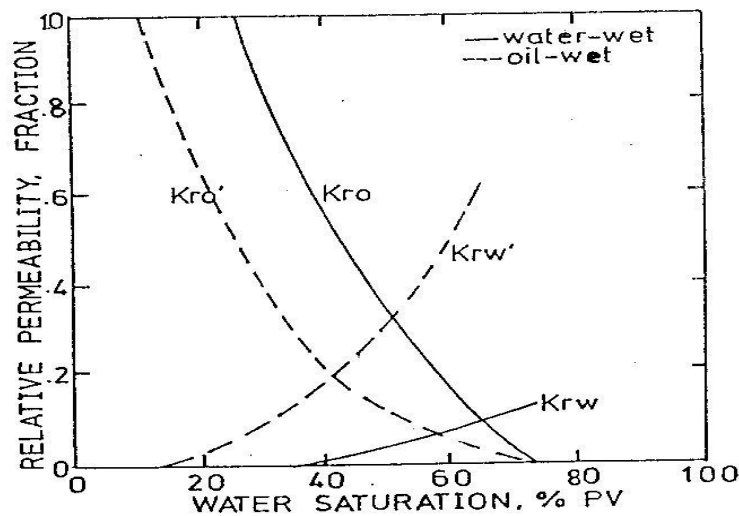
Figure 5: Typical water–oil relative permeability characteristics for strongly water–wet and strongly oil–wet rocks (after Craig, 1971)

2.3. Wettability Effects on Saturation Dependent Parameters

2.3.1. Effect of Wettability on Capillary Pressure

The capillary pressure/saturation relationship depends on the interaction of wettability, pore structure, initial saturation, and saturation history. No simple relationship exists that relates the capillary pressure determined at two different types of wettability. Therefore, the most accurate measurements are made with cores that have native reservoir wettability (Anderson, 1987).

In a uniformly wetted porous medium, pore geometry effects and the extremely rough surface of the porous medium make the capillary pressure curve insensitive to wettability for small contact angles. When the porous medium has fractional or mixed wettability, both the amount and distribution of the oil–wet and water–wet surfaces are important in determining the capillary pressure curve, residual saturation, and imbibition behavior. Imbibition also depends on the interaction of wettability, pore structure, initial saturation, and saturation history.

Because of these interactions, there is a large range of contact angles where neither oil nor water will imbibe freely into a uniform wetted reservoir core. In contrast, it is sometimes possible for both fluids to imbibe freely into a core with fractional or mixed Wettability (Anderson, 1987).

2.3.2. Effect of Wettability on Relative Permeability

The wettability of a core will strongly affect its waterflood behavior and relative permeability. Wettability affects relative permeability because it is a major factor in the control of the location, flow, and distribution of fluid in a porous medium. In uniformly or fractionally wetted porous media, the water relative permeability increase and the oil relative permeability decrease as the system becomes more oil–wet. In a mixed wettability system, the continuous oil–wet paths

in the larger pores alter the relative permeability curves and allow the system to be water flooded to very low residual oil saturation after the injection of many PV's of water. The most accurate relative permeability measurements are made in native–state core, where the reservoir wettability is preserved (Anderson, Nov. 1986).
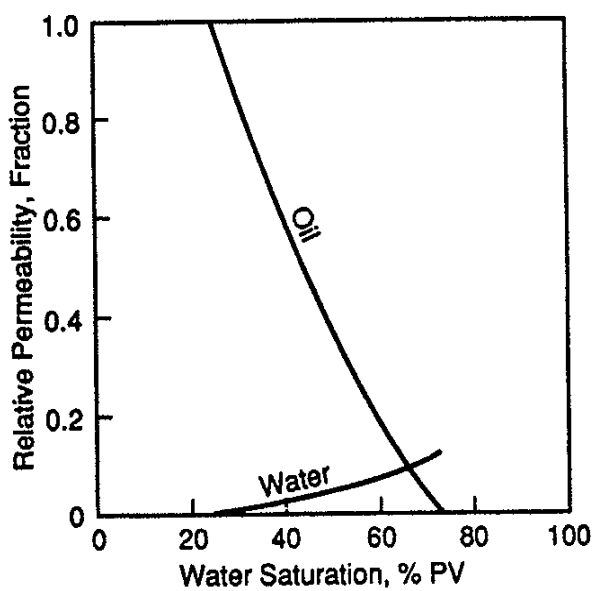
(a) Water-Wet Rock
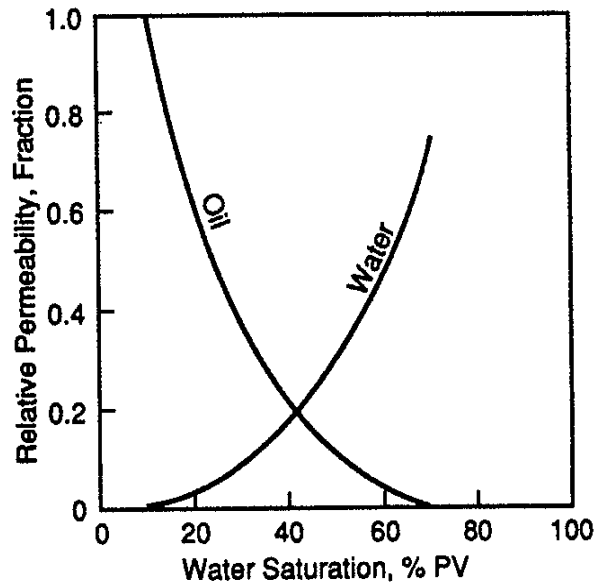
(b) Oil-Wet Rock
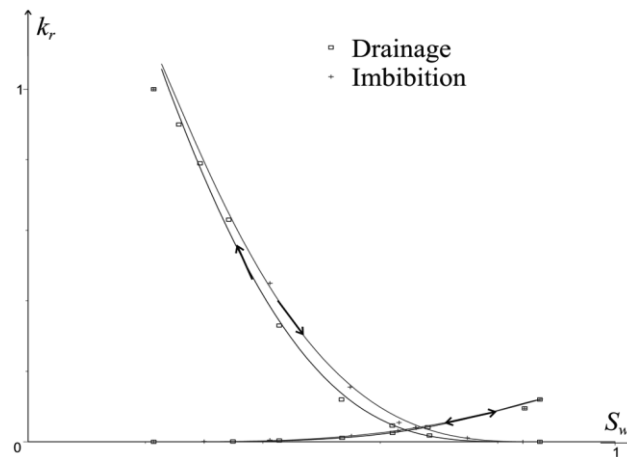
(c) Mixed–Wet Rock

Figure 6: Effect of wettability on relative permeability curves: (a) strongly water–wet rock, (b) strongly oil–wet rock and (c) Mixed Wettability (Skjaeveland et al 2000)

17

2.4. Capillary Number: A Competition between Viscous and Capillary Forces

There is no consensus on how to define the capillary number. A contributing factor to this is that the physical argumentation for defining the capillary number is often absent. A very frequently used definition of the capillary number depends on the viscosity μ, the Darcy velocity v and the interfacial tension σ (Saffman & Taylor 1958, Leal 2007).

$$N_c = \frac{\mu v}{\sigma} \quad \dots\dots\dots\dots\dots\dots\dots\dots\dots\dots 2.8$$

Some authors (Foster 1973, Tiab 1999) have even included porosity and some have included contact angle (Moore and Slobod 1956) leading to a new definitions of capillary number N_c.

$$N_c = \frac{\mu v}{\varphi \sigma} \quad \dots\dots\dots\dots\dots\dots\dots\dots\dots 2.9$$

$$N_c = \frac{\mu v}{\sigma \cos \theta} \quad \dots\dots\dots\dots\dots\dots\dots\dots 2.10$$

From a microscopic point of view, including a contact angle is somewhat questionable, since contact angles are not defined. By substitution of the Darcy velocity using Darcy's law one obtains

$$N_c = \frac{\mu v}{\sigma} = \frac{k_{r,w} K \Delta P / l}{\sigma} \quad \dots\dots\dots\dots 2.11$$

Sometimes, the relative permeability term is excluded in above equation (Foster 1973). Other definitions for the capillary numbers found in literature are

$$N_c = \sqrt{\frac{k}{\varphi}\frac{\nabla p}{p_c}} \qquad \dots\dots\dots\dots\dots\dots\dots\dots\dots 2.12$$

$$N_C = k\frac{|\nabla p + \rho g|}{\sigma\cos\theta} \qquad \dots\dots\dots\dots\dots\dots\dots\dots 2.13$$

$$N_c = k\left|\frac{\nabla p}{\sigma}\right| \qquad \dots\dots\dots\dots\dots\dots\dots\dots 2.14$$

from Leverett (1939), Brownell & Katz (1947) and Larson et al (1981) respectively.

Capillary numbers range from 10^{-5} to 10^{-7} for typical pressures, permeabilities and interfacial tensions, depending on the definition that is being used.

At first sight, the interfacial tension does not play a role in the Darcy description. It is implicitly hidden in the capillary pressure function and in most cases capillary pressure can be neglected. But for enhanced oil recovery (EOR) mechanisms, the important parameter is increasing capillary number, which can be tweaked by increasing the viscosity or by decreasing the interfacial tension. A direct consequence of this is a lower residual oil saturation, and straighter relative permeability function (Lake 1989).

In this thesis, viscosity is kept constant while the effect of increasing velocity and decreasing IFT has been investigated.

2.5. Phase Trapping/Entrapment in Porous Media and Capillary Desaturation

The most common experimental observation regarding phase trapping in actual permeable media is a relationship between residual nonwetting or wetting

phase saturations and a local capillary number. This relationship is called capillary desaturation curve. Fig. 7 shows a schematic of a simple CDC. Typically these curves are plots of percent residual (nonflowing) saturation for the nonwetting (S_{nwr}) or wetting (S_{wr}) phases on the y–axis versus a capillary number on a logarithmic x–axis. The capillary number N_{vc} is a dimensionless ratio of viscous to local capillary forces as described in previous section. At some N_{vc}, designated as the critical capillary number $(N_{vc})_c$, a knee in the curves occurs, and the residual saturation begins to decrease. Complete desaturation – zero residual phase saturation – occurs at the total desaturation capillary number $(N_{vc})_t$, as shown in Fig. 8. Most water floods are well onto the plateau region of the CDC where, as a rule, the plateau S_{wr} is less than S_{nwr}. Frequently, the two CDC curves are normalized by their respective plateau values.

Larry W. Lake (1989) summarized the results of experimentally determined CDC curves from different researchers. But that list is restricted to the flow of two liquid phases in a synthetic or outcrop permeable medium.

The plateau values of S_{nwr} and S_{wr} show considerable variation (there are more nonwetting phase measurements). The $(N_{vc})_c$ and $(N_{vc})_t$ for nonwetting phase are less than the respective values for the wetting phase. For nonwetting phase, $(N_{vc})_c$ is in the 10^{-5} to 10^{-4} range, whereas the $(N_{vc})_t$ is usually 10^{-2} to 10^{-1}. For the wetting phase $(N_{vc})_t$ is roughly equal to the nonwetting $(N_{vc})_t$, whereas the $(N_{vc})_c$ is usually 10^{-1} to 10^{0}. Literature on capillary number does not warranty more precise conclusions because of the variation in N_{vc} definitions and in the experimental conditions.

The range between $(N_{vc})_c$ and $(N_{vc})_t$ is considerably greater for the nonwetting phase (10^{-7} to 10^{-1}) than for the wetting phase (10^{-4} to 10^{0}). Summary of experimental work on Capillary Desaturation Curves by Larry W. Lake's sets forth three general observations based on the CDC curve.

1. Wettability is important. The wetting phase normalized CDC curves should be two to three factors of 10 to the right of a nonwetting phase CDC curve; however, intuitively, the two CDC curves should approach each other at some intermediate wetting condition.

2. Pore size distribution is also important. The critical–total N_{vc} range should increase with increasing pore size distribution for both wetting and nonwetting phases.

3. The critical–total N_{vc} range for the nonwetting phase should be greater than for the wetting phase with, again, a continuous shift between wettability extremes.
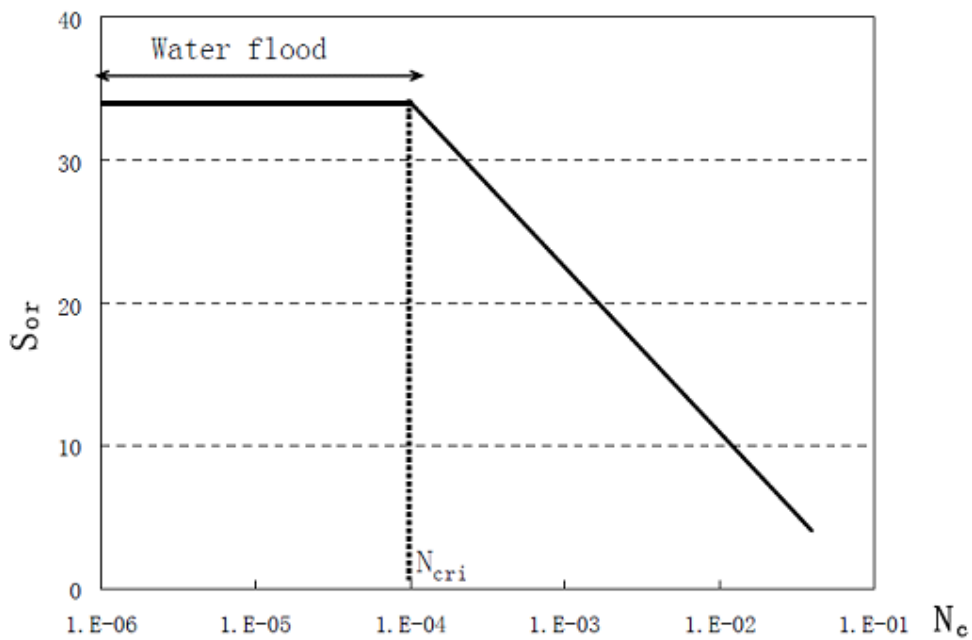
Figure 7: Schematic Capillary Desaturation Curve for Nonwetting Phase
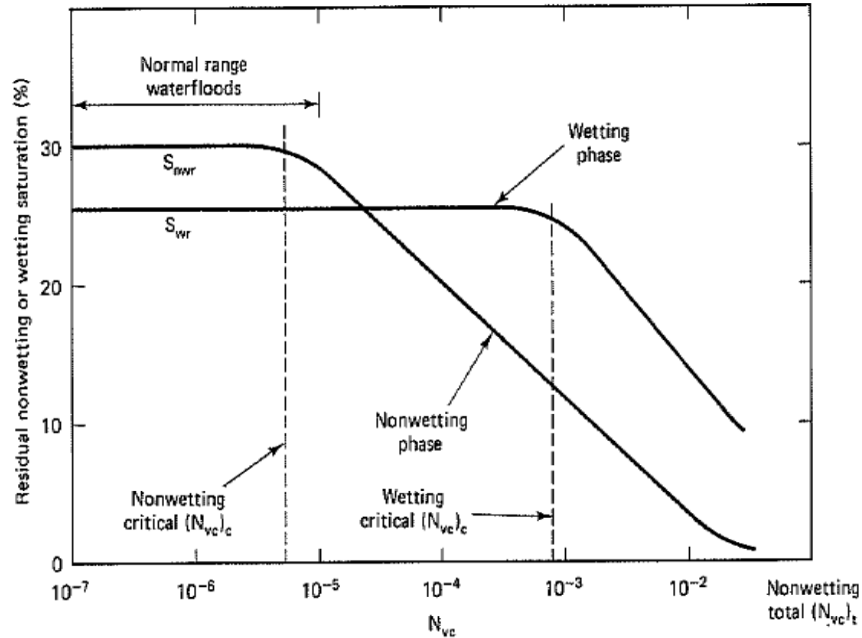
Figure 8: Schematic Capillary Desaturation Curve (from Lake, 1984)

The above plot clearly indicates a reduction in residual oil saturation with an increase in capillary number. A relationship between the capillary number and oil recovery by Chatzis and Morrow (1982) is shown below in Fig. 9.

$$Nc = v\mu/\sigma$$

Nc = Capillary Number

v = Darcy Velocity

μ = Viscosity

σ = Interfacial Tension
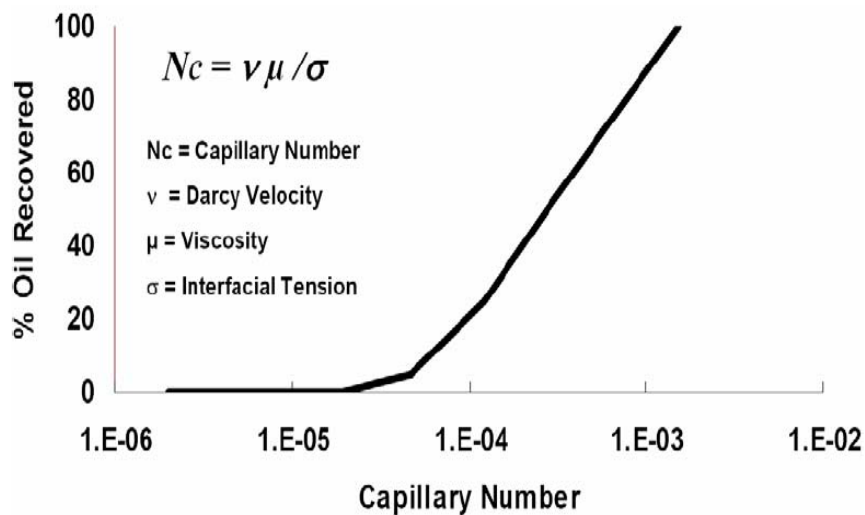
Figure 9: Relationship between Capillary Number and Oil Recovery
(Chatzis and Morrow 1984)

Typical water flood capillary numbers are 10^{-7}. Taber (1979) reported that an increase in capillary number from 10^{-4} to 10^{-3} is essential to improve or enhance the oil recovery. Therefore, it is well recognized that interfacial tension reductions of 1,000 to 10,000 folds are necessary to achieve additional oil recovery by capillary number alteration through the addition of surfactant. Surfactant flooding, one of the ways to release the trapped oil (ROS), is described in the subsequent section.

2.6. Surfactant Flooding

A surfactant is a polar compound, consisting of an amphiphilic molecule, with a hydrophilic part (anionic, cationic, amphoteric or nonionic) and a hydrophobic part. Addition of surfactant to oil–water mixtures reduces interfacial tension and/or alters wettability.

When a surfactant is injected, it disperses into oil and water and lowers interfacial tension thereby increasing the capillary number. As a result, more of the otherwise immobile oil becomes mobile. At the same time, an oil–in–water emulsion may form, blocking the larger pores. This often leads to an improvement in the effective mobility ratio. The injected surfactant continues to mobilize oil and bank it up until the surfactant is diluted or otherwise lost due to adsorption by the rock until it is no longer available to lower the interfacial tension and mobilize oil. At that point, the process degenerates into a water flood. The effect of surfactant adsorption has not been investigated in this thesis study.

The capillary pressure resistance to flow is proportional to oil/water interfacial tension divided by the diameter of the constriction. Viscous forces due to pressure gradients in the reservoir are much lower than the capillary forces. Oil mobilization is achieved if the capillary number is increased. Viscous forces cannot be increased greatly because of the limited pressure resistance of the reservoir.

Hence, the reduction of the interfacial tension by the use of surfactants could produce the desired effect.

However, for significant enhancements in oil recovery, several orders of magnitude reduction in interfacial tension is required. The surfactants capable of generating this reduction are expensive and are required in large quantities, rendering them uneconomical for field application. Hence, our emphasis is to study the effects of reduction in oil–water interfacial tension rather than wettability alteration.

2.7. Surfactant Flooding Mechanism

Surfactant flooding has long been demonstrated to be a prospective improved oil recovery process (for example, Krumrine et al, 1982; Nelson et al, 1984). Quite a few mechanisms are associated with displacement involving surfactants but the main effects anionic surfactant flooding depends on are wettability alteration, ultra–low interfacial tension, and low surfactant retention (Mayer et al., 1983; Lake, 1989; Green and Willhite, 1998).

Taber (Taber, 1968) found through experiments that no residual oil could be displaced until a critical value of $\dfrac{\Delta P}{L\sigma}$ was exceeded, where ΔP is the pressure drop across the distance L and σ is the interfacial tension between the oil and water. This $\dfrac{\Delta P}{L\sigma}$ can translate to an equivalent Capillary Number through Darcy's law (Melrose and Brandner, 1974):

$$N_{ca}^* = \frac{u\mu_w}{\sigma_{ow}}$$

$$N_{ca} = \frac{v\mu_w}{\sigma_{ow}} \quad \text{……….…….….…………2.15}$$

Where $N_{ca}^* = \phi N_{ca}$, u and v represents the Darcy and interstitial velocity respectively.

Stegemeier (Stegemeier, 1977) correlated N_{ca}^* with residual oil saturation for water–wet system. For $N_{ca}^* < 10^{-5}$, there is no mobilization, while as $N_{ca}^* > 10^{-5}$, the fraction of the residual oil mobilized increases sharply with increasing capillary number. The reduction of interfacial tension will result in the increase of capillary number. A brief literature review on reduction in interfacial tension by surfactant flooding is given in subsequent section.

2.7.1 Interfacial Tension Reduction

The effect of capillary number on residual oil saturation (Klins 1984) reveals that an increase of four to five orders of magnitude in capillary number is required in surfactant flooding process in order to reduce the residual oil saturation significantly. An increase in capillary number could either be achieved by reducing interfacial tension or increasing the velocity of the injected fluid. An increase in injection velocity has practical constraints so the best possible way to increase capillary number is to reduce interfacial tension between oil and water phases.

Interfacial tension reduction has long been recognized as one of the most important factors in enhanced oil recovery (Mungan, 1964 & 1966). In fact, in most of the research on alkaline/surfactant/polymer flooding conducted in the last

decade, people look more into the effect of surfactant solution on interfacial tension reduction, without considering wettability alteration (for example, Arihara et al., 1999).

Due to experimental difficulties and the time involved in carrying out displacement measurements at well defined low interfacial tension, relatively few definitive studies of relative permeability properties at low interfacial tensions have been reported in the literature. Lefebvre du Prey (1973) conducted extensive measurements with three types of sintered porous media and fluid pairs having relatively high interfacial tensions, and reported the affect of the ratio of viscous to capillary forces on relative permeabilities and residual saturations. Talash (1976) has provided relative permeability results from water–oil systems containing surfactants, but did not report either the interfacial tensions or the flow rates involved. An earlier investigation by Wanger and Leach (1966) employing near–miscible hydrocarbon phases indicated that the interfacial tension must be reduced to a value lower than 0.07 mN/m (dynes/cm) to achieve an increase in displacement efficiency at field rates. Rosman and Zana (1977) extended this type of study to CO_2–oil system and showed that low interfacial tension displacement by CO_2 is an effective recovery mechanism.

Gupta et al. (1979) provided some correlations of oil recovery verses capillary number for Berea sandstone cores through IFT reduction. However, it should be mentioned that they made extensive attempts in their procedures to minimize or eliminate effects caused by uncontrolled variables; for example, all chemical solutions were pre–equilibrated with the tested oil. Also, they assumed that IFT did not change significantly with dilution by brine, and that partitioning of chemical fluid components into the oil phase was negligible.

An initial study to determine the influence of interfacial tension upon oil–water relative permeabilities in sintered oil–wet porous media was conducted by P.

26

Shen et al. (2006). It was found that the imbibitions relative permeability curves were more significantly affected by a lowering of the interfacial tension from 50mN/m to about 0.01mN/m than were the drainage relative permeability relations. The residual non–wetting phase saturation was also reduced in a manner that generally agreed with previously published correlation between residual oil saturation and the capillary number by Melrose, J.C. and C.F. Brandner (1974) who discussed the role of capillary forces in determining microscopic displacement efficiency for oil recovery by water flooding.

J.P. Batychy and F.G. Mccaffery (1978) during their research on low interfacial tension displacement concluded that interfacial tension reduction causes a reduction and the eventual removal of hysteresis in the measured relative permeability curve. They also concluded that this reduction in interfacial tension also causes relative permeability curves to become less curved. This mechanism has also been included in our simulation studies and the results are presented at the end. We simply considered straight lines as a result of reduced.

In the last two decades, there has been extensive research on alkaline/surfactant flooding, and ultra–low interfacial tension was recognized to be one of the most important mechanisms in the increase of oil recovery (Nelson et al., 1984; Martin et al., 1985; Shuler et al., 1989; Olsen et al., 1990; French and Burchfield, 1990; Falls et al., 1992; Baviere et al., 1994 Baviere et al., 1995; Gao et al., 1995; Song et al., 1995; Al–Hashim et al., 1996; French, 1996; Gao et al., 1996; Wang et al., 1997; Qu et al., 1998; Tong et al., 1998; Wang et al., 1998; Arihara et al., 1999; Wang et al., 1999; Qiao et al., 2000; Vargo et al., 2000; Manrique et al., Hernandez et al., 2001).

2.7.2. Wettability Alteration

Wettability plays a very important role in oil recovery. For decades, much effort has been made towards understanding the relationship between wettability and oil recovery efficiency. Earlier, oil recovery was reported to decrease with increasing oil wettability with sandstone (Donaldson et al, 1969; Owen and Archer, 1971). But Salathiel (Salathiel, 1973) using sandstone presented evidence of higher residual saturation at strongly water–wet conditions compared with that at mixed–wet conditions. Morrow and Jadhunandan (Marrow, 1990; Jadhunandan and Morrow, 1995) with Berea sandstone showed that oil recovery by water flood has a maximum when the wettability is close to neutral–wet.

McDougall and Sorbie (McDougall and Sorbie, 1995) concluded with their simulation results that oil recovery should be maximum if the network consisted of 50% oil–wet and 50% water–wet pores (mixed–wet conditions). Emery et al. (Emery, et al., 1970) found that interfacial tension reduction and breaking of rigid films at oil–water interfaces contribute to the additional oil recovery.

Lake (Lake, 1989) proposed an explanation to the effect of wettability on oil recovery: the change of wettability will result in fluid redistribution in pore structure. The issue of wettability alteration has not been considered and addressed in this study, rather we focused on effect of low interfacial tension on capillary trapping.

CHAPTER 3

THE SURFACTANT SIMULATION MODEL

The surfactant model in Eclipse 100 does not provide the detailed chemistry of a surfactant flooding process, but rather it models the important features of a surfactant flood on a full field basis.

3.1. Surfactant Conservation Equation

The surfactant model in Eclipse 100 models the distribution of injected surfactant by solving a conservation equation for surfactant within the water phase. The surfactant concentrations are updated fully implicitly at the end of each time step after the flows of three phases (oil, water and gas) have been computed. The surfactant is assumed to exist only in the water phase, and the input to the reservoir is specified as a concentration at a water injector.

3.2. Calculation of the Capillary Number

The capillary number is a dimensionless number that measures the ratio of viscous forces to capillary forces as described earlier in section 2.3 of previous chapter. The definition of capillary number used by surfactant model is given by:

$$N_c = C_{unit} \frac{[K.grad\ P]}{ST} \quad \text{...3.1}$$

Where K is the permeability, P is the potential, ST is interfacial tension, C_{unit} is the conversion factor depending upon the units used. The term $[K.grad\ P][K.grad\ P]$ is calculated as

$$[K.grad\ P] = \sqrt{(K_x.grad\ P_x)^2 + (K_y.grad\ P_y)^2 + (K_z.grad\ P_z)^2} \quad \text{......3.2}$$

Where for cell i

$$K_x.grad\,P_x = 0.5\left[\left(\frac{K_x}{D_x}\right)_{i-1,i}.(P_i - P_{i-1}) + \left(\frac{K_x}{D_x}\right)_{i,i+1}.(P_{i+1} - P_i)\right]......3.3$$

and similarly for the y and z direction.

The K/D value is calculated in an analogous manner to the transmissibility and depends on how the geometry was specified. Interfacial tension is a tabulated function of the surfactant concentration.

3.3. Relative Permeability Model

The Relative Permeability model is essentially a transition from immiscible relative permeability curves at low capillary number to miscible relative permeability curves at high capillary number. A table is supplied which describe the transition as a function of $\log_{10}$(Capillary Number).

The relative permeability used at a value of the miscibility function between the two extremes is calculated in two steps. Firstly the end points of the curve are interpolated and both the immiscible and the miscible curves are scaled to honor these points. The relative permeability values are looked up on both curves, and the final relative permeability is taken as an interpolation between these two values. The treatment of the water relative permeability is analogous to the oil case. This procedure is illustrated below for the oil to water
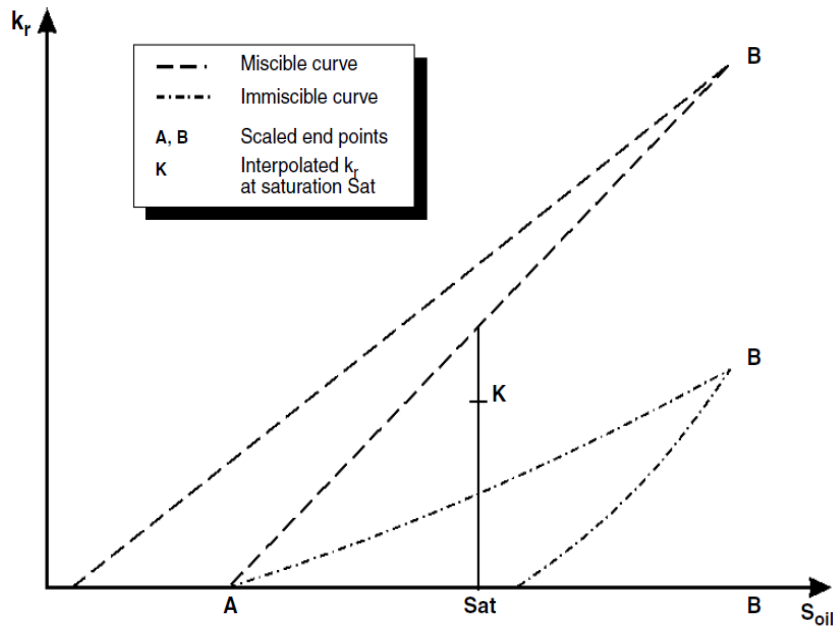
Figure 10: Calculation of relative permeability

3.4. Capillary Pressure

The water oil capillary pressure will reduce as the concentration of surfactant increases; indeed it is the reduction in the oil water capillary pressure that gives rise to the reduction in the residual oil saturation. The oil water capillary pressure is taken as:

$$P_{cow} = P_{cow}(S_w) \frac{ST(C_{surf})}{ST(C_{surf} = 0)} \dots\dots\dots\dots\dots\dots\dots\dots\dots.3.4$$

Where

ST (C_{surf}) is the surface tension at the present surfactant concentration, ST ($C_{surf}=0$) is the surface tension at zero concentration.

3.5. Water PVT Properties

The surfactant modifies the viscosity of the pure water phase. The viscosity of the water (at reference pressure) is given as input as a function of surfactant concentration.

3.6. Treatment of Adsorption

The adsorption of surfactant is assumed to be instantaneous, and the quantity adsorbed is a function of the surrounding surfactant concentration. Eclipse Surfactant Model requires adsorption isotherm as a function of surfactant concentration as input. The quantity of surfactant adsorbed on the rock is given by:

$$Mass\,of\,adsorbed\,surfactant = PORV * \frac{1-\varphi}{\varphi} * MD * CA(C_{surf}) \quad \ldots\ldots 3.5$$

Where PORV is the pore volume of the cell, φ is the porosity, MD is the mass density of the rock and $CA(C_{surf})$ is the adsorption isotherm as a function of local surfactant concentration in solution.

There are two adsorption models that can be selected. The first model ensures that each grid block retraces the adsorption isotherm as the surfactant concentration falls in the cell. The second model assumes that the adsorbed surfactant concentration on the rock may not decrease with time and hence does not allow for any de–adsorption. Since the adsorption of the surfactant is not considered, the adsorption isotherm is not included in simulation study.

3.7. Modeling the Change in Wettability

Surfactant Model is capable of modeling the changes in wettability of the rock due to the accumulation of surfactant. It requires oil–wet immiscible saturation functions as input and permits user to define additional immiscible saturation functions and these are then taken to model the water–wet situation.

In calculating the immiscible relative permeabilities, a weighted average of F times the oil–wet value and (1–F) times the water–wet value is used. The fraction, F, is a function of the adsorbed surfactant concentration, and is defined by tables input. The formula for the new relative permeability is

$$k_r = Fk_r^{ww} + (1-F)k_r^{ow} \qquad \ldots\ldots\ldots\ldots\ldots\ldots\ldots\ldots\ldots.3.6$$

Where F represents weighting of oil–wet to water–wet saturation function, a value of 1.0 implies that only the oil–wet saturation functions will be used and a value of 0.0 implies purely water–wet saturation functions, k_r^{ww} is oil–wet relative permeability and k_r^{ow} is water–wet relative permeability.

CHAPTER 4

SIMULATION RESULTS

This chapter addresses the simulation results from surfactant flooding in mix–wet reservoirs. The basic input data required for simulation runs has been presented followed by the simulation results from three different mechanisms described in objective.

4.1. Synthetic Models

The following synthetic models were used during the simulation studies of surfactant flooding in mixed–wet reservoirs.

1. Homogeneous model
2. Heterogeneous model
   i.   Layered
   ii. Inclusion
        a. Low Permeability Inclusion
        b. High Permeability Inclusion

4.2. Simulation Input Parameters

4.2.1. Fluid Properties

Three phases dead oil, water and surfactant were considered during simulation studies. Different fluid (Oil and water) properties used in simulation studies are tabulated below.

Table 1: Fluid (Oil and gas) Properties

Oil FVF	1.0 rm3/Sm3
Oil Viscosity	0.47 cP
Water FVF	1.0 rm3/Sm3
Water Viscosity	0.34 cP

Oil viscosity, water viscosity and water formation volume factor were considered to be independent of pressure. Oil formation volume factor was almost independent of pressure (Negligible change). Water viscosity was considered to be independent of surfactant concentration.

4.2.2. Saturation Dependent Parameter

Saturation dependent parameters i.e., relative permeability and capillary pressure curves from mixed–wet cores were given input in simulation studies. Capillary pressure was used in dimensionless form using Leveret J–function described earlier. These input relative permeability curves from mixed–wet reservoir are shown in graphical form below.
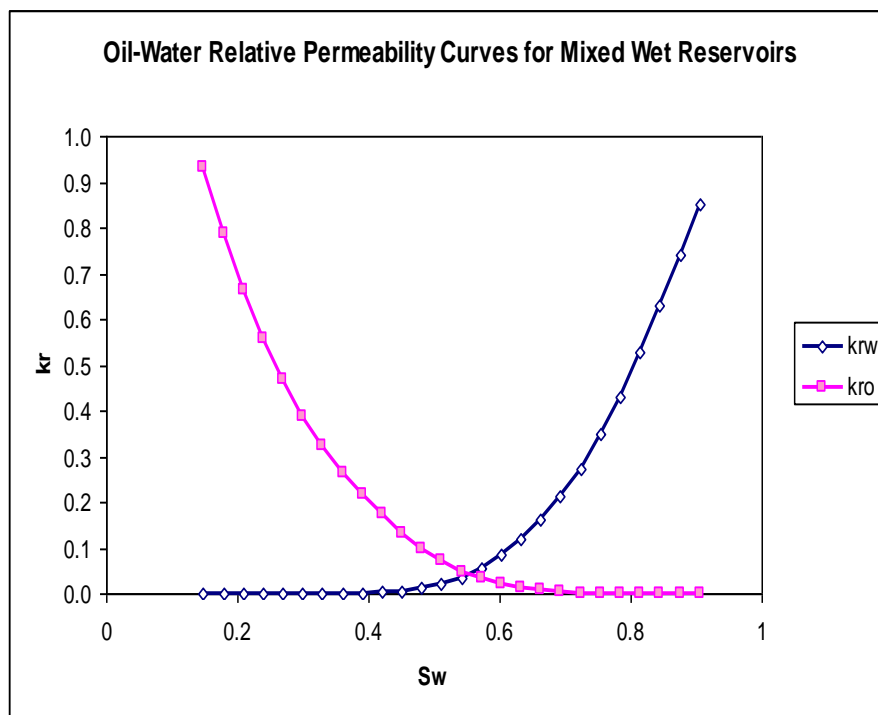

Figure 11: Oil and water relative permeability curves for mixed–wet reservoir used in simulation studies

Oil relative permeability shows a long tail at higher water saturation which is typical in mixed–wet reservoirs. The input capillary pressure curves are shown graphically in Fig. 12 below. Only imbibition capillary pressure data was used in our simulation studies. The relative permeability and capillary pressure data used during simulation can be found in tabular form under sample input data file in Appendix.
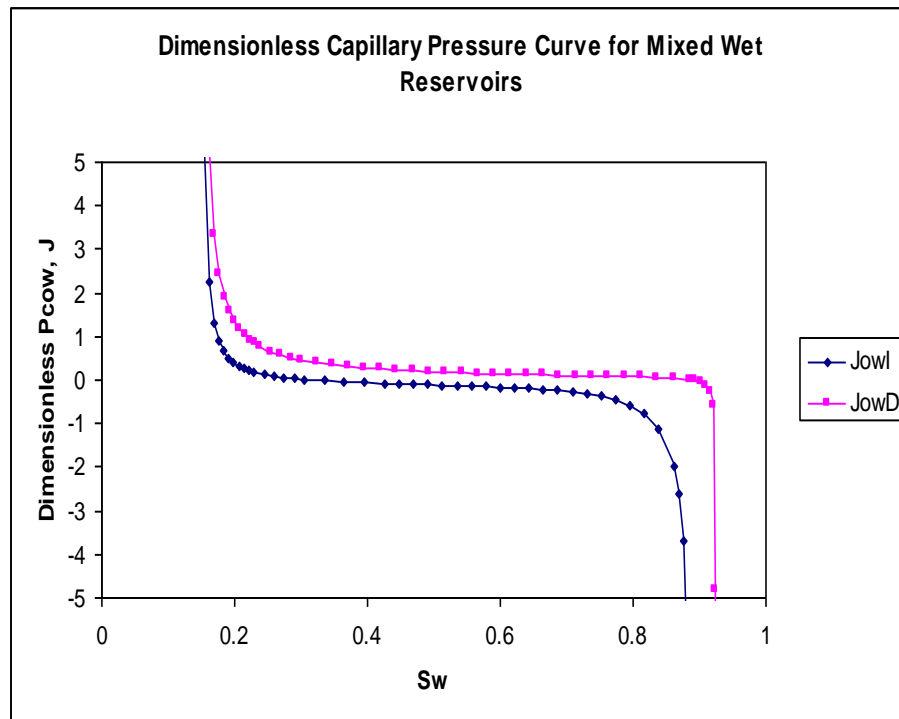

Figure 12: Dimensionless capillary pressure curves for mixed–wet reservoir used in simulation studies

4.2.3. Rock Properties

The following rock properties were used.

Porosity = 0.25

Permeability = 100 mD

Isotropic rock i.e., PermX= PermY= PermZ

The rock compressibility was assumed to have no impact on recovery results

and the average porosity in all models is considered same so that the results from same injected PV can be compared.

4.2.4. Field Properties

Only one injector and one producer were used. Injector was located in first grid block and producer in the last grid block of the model. All the models were perforated all the way to lower most grid block in vertical direction. Producer was controlled by bottom hole pressure whereas injector was controlled through reservoir volume rate during simulation studies. Same volume of water (5*PV) is injected in each case to compare the results from different models.

4.3. Rate Dependency (Flow Rate Sensitivity Analysis)

The rate dependency of two–phase flow can be evaluated in term of a capillary number, as defined by Virnovsky et al. (2004), given below.

$$N_c = \frac{Viscous\ Forces}{Capillary\ Forces} = \frac{\nabla p_g\, l_{pc}}{\Delta P_c} \quad \ldots\ldots\ldots\ldots\ldots 4.1$$

Where, ∇p_g is the global/large–scale pressure gradient attributable to viscous flow, l_{pc} is a characteristic length of the capillary heterogeneity, and ΔP_c is the capillary contrast taken at VL–conditions. The effect of rate on the local saturation distribution across the boundary between two neighboring blocks is illustrated in Fig. 13. The rock has the same relative permeability but different capillary pressure. At low rate, there will be a sharp jump in saturation because P_c is the same in both rocks. At high rate, the fractional flow and the saturation in the two rocks will be equal. In the later case, there will be a jump in P_c between the rocks corresponding to the vertical shift between the two capillary rock curves. This vertical shift represents the capillary force that must be overcome by the viscous force in order to approach VL. CL and VL are most commonly referred to as the

low–rate case and the high–rate case, respectively. From the definition of N_{ca}, we see we can also move from CL to VL by keeping the rate constant and increasing the scale (l_{pc}). In our simulation studies, the effect of characteristic length of capillary heterogeneity is not investigated; rather we focused on rate effect because the effect of an increase in flow rate is similar or analogous to that of a decrease in interfacial tension according to the definition of capillary number.

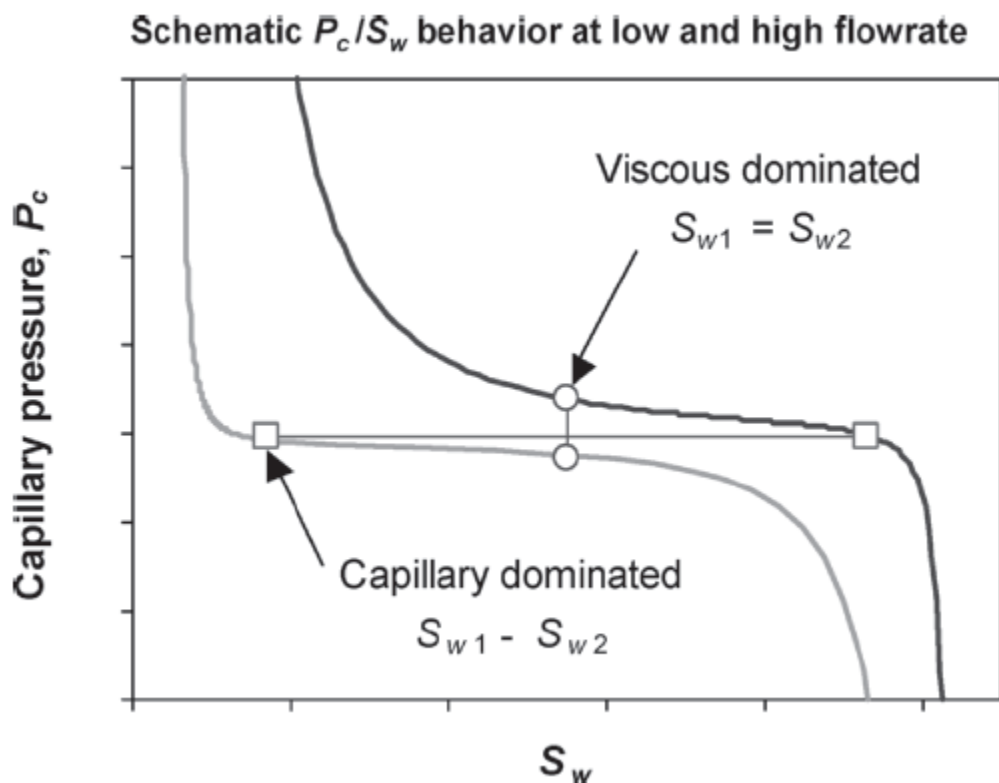Schematic P_c/S_w behavior at low and high flowrate

Figure 13: Saturation in two neighboring rocks with the same relative permeability and different capillary pressure

Since the purpose of our simulation studies is to investigate the effectiveness of surfactant flooding which requires capillary dominance at the beginning of

simulation. A rate sensitivity analysis is conducted to figure out the flow rate required for simulation studies and the results are shown in Fig 14.
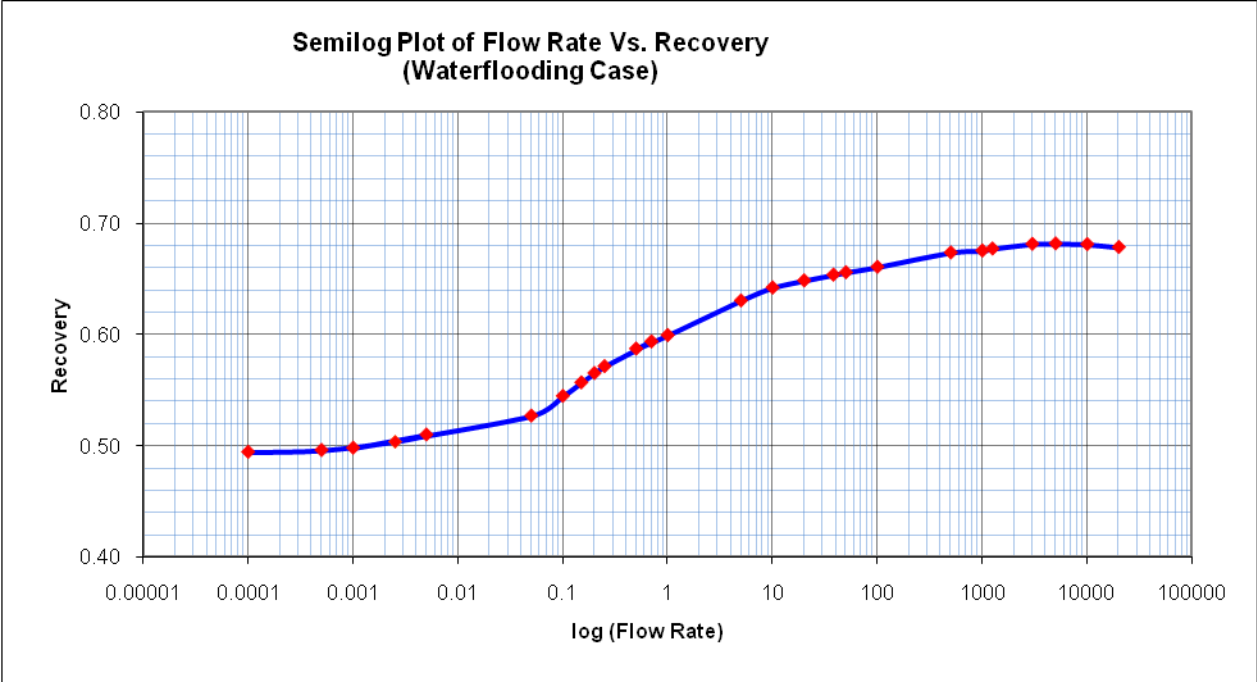

Figure 14: Rate sensitivity analysis

The first part of the above curve (Low flow rates) indicates capillary dominance where as last part (High flow rates) indicates viscous dominance with a transition in between capillary and viscous dominance. Near wells, flow is usually assumed to be viscous–dominated, while some distance away from the well, at typical reservoir rates, capillary dominance is usually assumed. The flow rate to be used in simulation of different scenarios is chosen on the basis of above curve representing capillary dominance at the beginning of the simulation studies.

4.4. Homogeneous Model

After the input simulation data required for surfactant flooding in mixed–wet reservoirs was defined, the validity of surfactant model was checked by simulating a simple homogeneous model. Since it is believed that snap–off of oil does not occur in mixed–wet reservoirs so a reduction in interfacial tension would not lead to an increase in oil recovery. This was verified by simulating homogenous model. Model dimensions are given below

DX = 200, DY = 1, DZ = 50

Length of model = 200 * 2.5 = 500 m

Width of model = 1 * 10 = 10 m

Height of model = 50 * 2.5 = 125 m

Isotropic model with a porosity of 25% and permeability of 100 mD.

The results of the simulation studies are shown below.

Table 2: Effect of reduced IFT in homogeneous model in the absence of gravitational forces

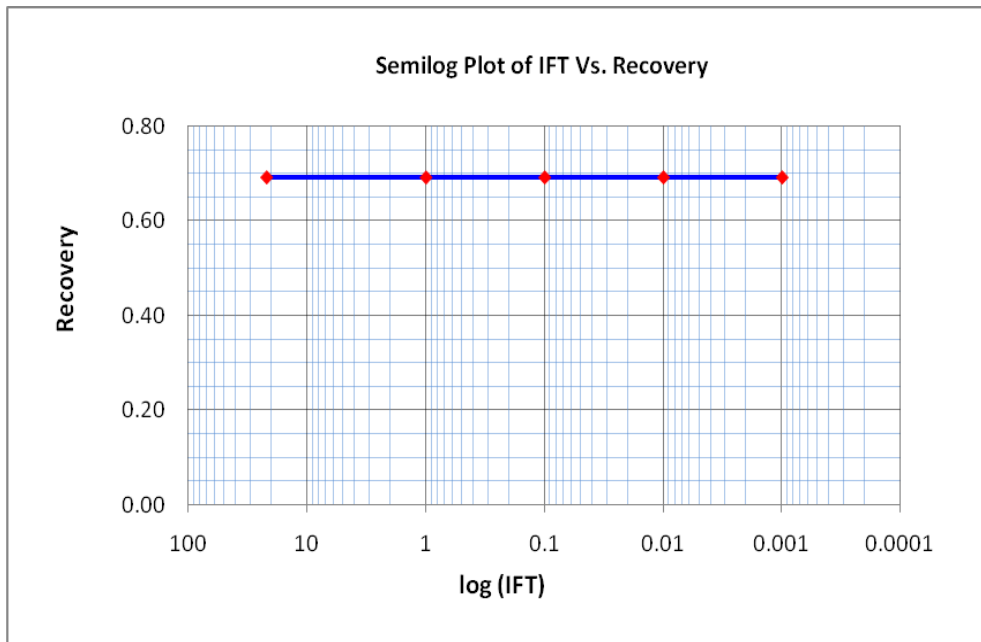| IFT (mN/m)	Recovery Factor	N_c	ROS
22	0.69198	2.3403E–07	0.261311
1	0.69195	5.1540E–06	0.261332
0.1	0.69195	5.1542E–05	0.261332
0.01	0.69196	5.1538E–04	0.261323
0.001	0.69196	5.1538E–03	0.261322

Figure 15: Effect of reduced IFT on recovery from homogeneous model

The above plot clearly indicate no increase in oil recovery with the reduction in interfacial tension which validates our surfactant model.
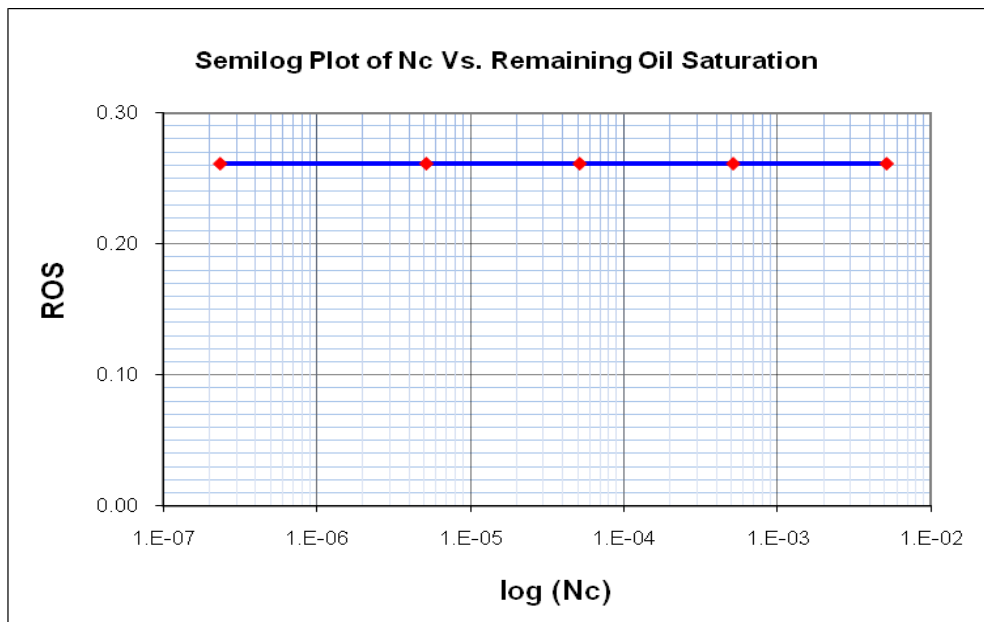

Figure 16: Effect of capillary number on remaining oil saturation from homogeneous model

The second plot is somehow similar to CDC curve where log (N_c) is plotted verses remaining oil saturation instead of residual oil saturation. An increase in capillary number shows no decrease in remaining oil saturation.

The above results were validated with plots from simulation results of Eclipse Office Module which are given below.

Comparison of Field Cumulative Oil Production and Water Cut from Water and Surfactant Flooding
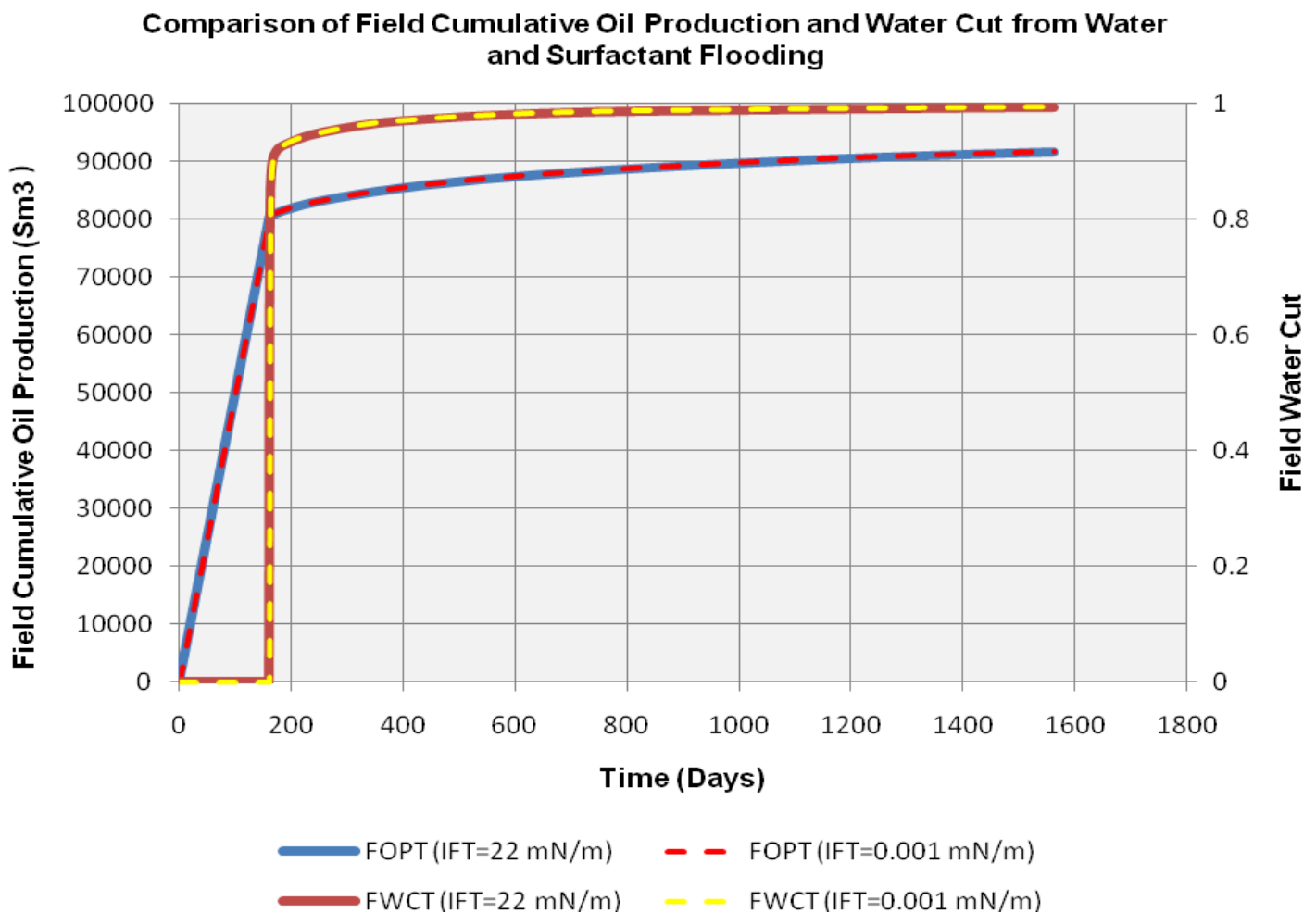

Figure 17: Comparison of field cumulative oil production and water cut at high (water flooding) and low (surfactant flooding) IFT from homogeneous model

The above plot indicates that there is no increase in field cumulative oil production when the interfacial tension is reduced from 22 to 0.001 mN/m as revealed earlier. Field water cut remain the same and show no effect to reduced IFT.

4.5. Heterogeneous Model

4.5.1. Layered/Stratified Case

The same simulation studies were conducted for heterogeneous model (Layered case) as were done for simple homogeneous model described above. A layered reservoir represents a case of vertical heterogeneity which might occurs in real reservoir simulation studies as a result of depositional environment from successive transgression and progression of sea level creating alternative sequence of formation of varying permeability. In this model, quite thin layers were used in order to capture the effect of cross flow between layers. Model dimensions are given below

DX = 200, DY = 1, DZ = 40
Length of model = 200 * 1 = 200 m
Width of model = 1 * 1 = 1 m
Height of model = 40 * 0.01 = 0.4 m

The model was split up into five layers with different permeability. The permeability distribution is shown below in table 3 below.

Table 3: Layer definition in heterogeneous (Layered/Stratified) Model

Layer (Top to bottom)	Layer thickness (m)	Permeability (mD)
1	0.05	10
2	0.10	100
3	0.10	10
4	0.10	100
5	0.05	10

The effective permeability, used in the calculation of capillary number (given in the table below), was obtained through simple arithmetic average of permeability of five layers given in above table. The following formula was used in the calculation of capillary number.

$$N_c = C_f \frac{K_{eff} \Delta P}{L\sigma}$$ …………………………..4.2

Where C_f is the conversion factor.

The results of the simulation studies are shown below.

Table 4: Effect of reduced IFT in heterogenous (Layered/Stratified) model in the absence of gravitational forces

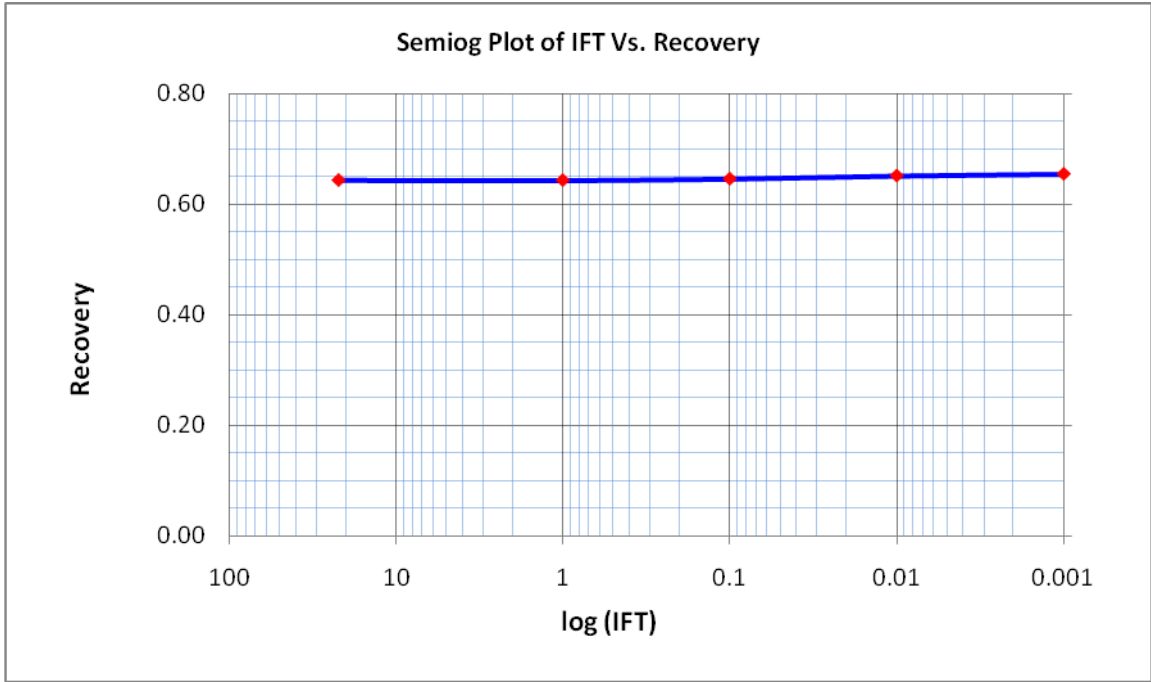| IFT (mN/m)	Recovery Factor	N_c	ROS
22	0.64335	1.097E–06	0.301681
1	0.64313	2.501E–05	0.301875
0.1	0.64591	2.780E–04	0.299516
0.01	0.65175	2.946E–03	0.294578
0.001	0.65499	3.022E–02	0.291842

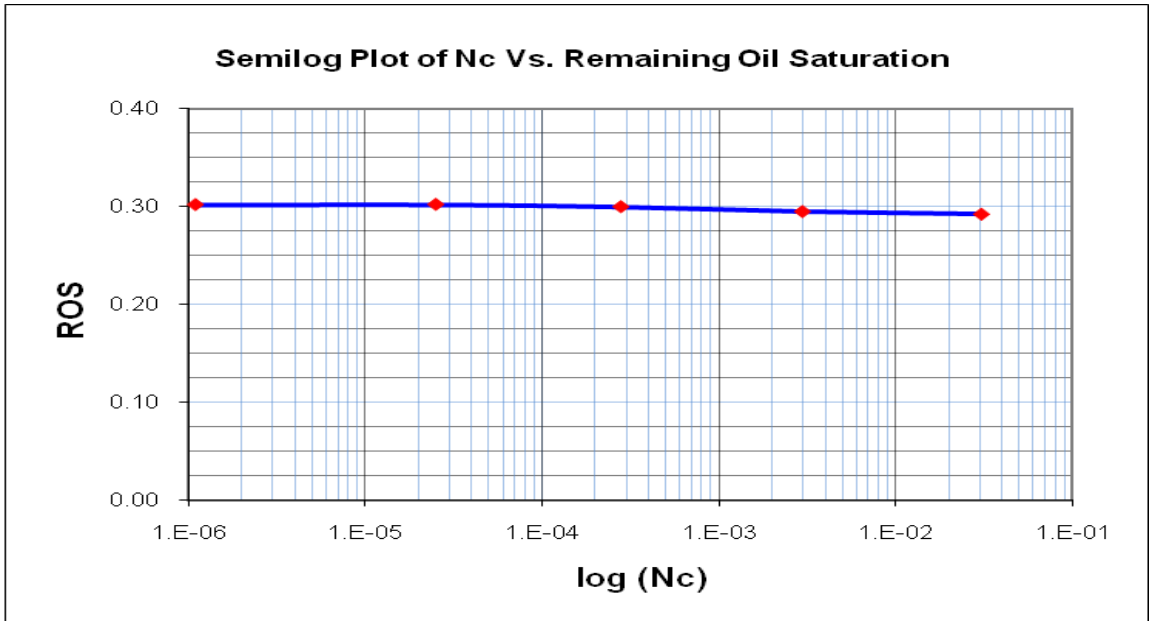Figure 18: Effect of reduced IFT on recovery from stratified model

Figure 19: Effect of capillary number on remaining oil saturation from stratified
model

First plot indicate almost no or negligible effect of reduced IFT on recovery enhancement whereas second plot reveals a very small reduction in remaining oil saturation even though the capillary number is increased to an order of magnitude of 10000 folds. These results correspond to the simulation results as shown below.
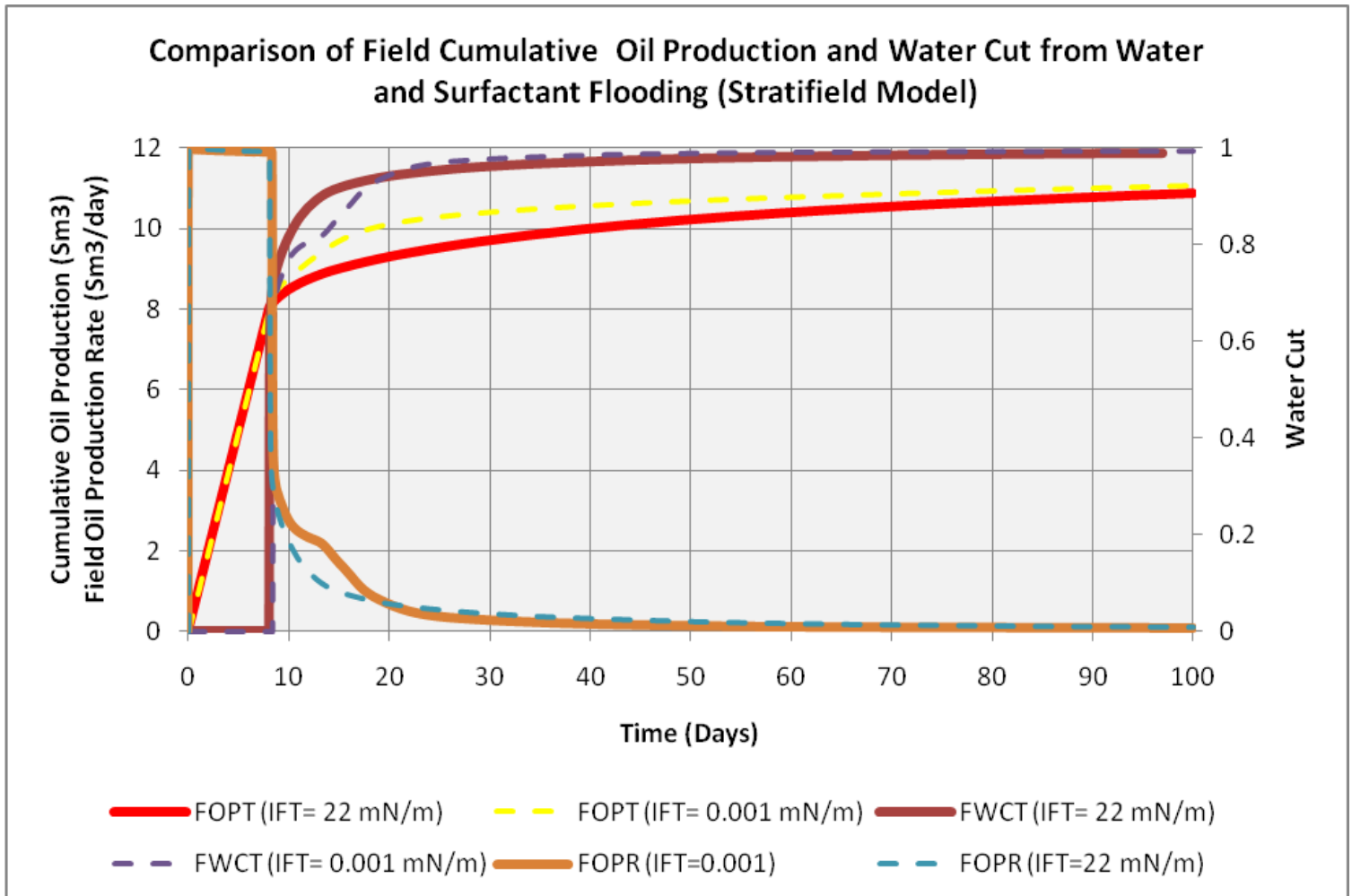

Figure 20: Comparison of field cumulative oil production and water cut at high (water flooding) and low (surfactant flooding) IFT from stratified model

Above plot clearly shows that field cumulative oil production for reduced IFT is little more compared to that of high IFT (Waterflooding) which is analogous

to the results manually calculated and shown in above table in form of remaining oil saturation. High cumulative oil production means less remaining oil saturation as depicted in above table. Reduced IFT also seems to increase field oil production immediately after breakthrough from the one of the layers but this change does not last for long time and come to same rate as in case of water flooding i.e., the increase in production due to reduced IFT is temporary.

4.5.2. Inclusion Case

Inclusions (A part of rock with varying permeability in comparison to surrounding matrix) represent heterogeneity that might occur, for example, in a fluvial channel due to the deposition of clay minerals. In our case, both inclusions and background rock are mixed–wet (same relative permeability and capillary pressure curves are used for both rock types). When oil and water flow under capillary dominance in a heterogeneous porous media, high saturation contrast can, depending on the geometry, significantly reduce the mobility of one or both phases and cause capillary trapping.

High saturation contrast under capillary dominance is also revealed by our simulation studies in this case which is shown in figure below (from Eclipse FloViz Module). In our simulation studies, capillary forces are totally dominant or at least have significant influence at the beginning of simulation since a flow rate representing capillary dominance is used during simulation runs.
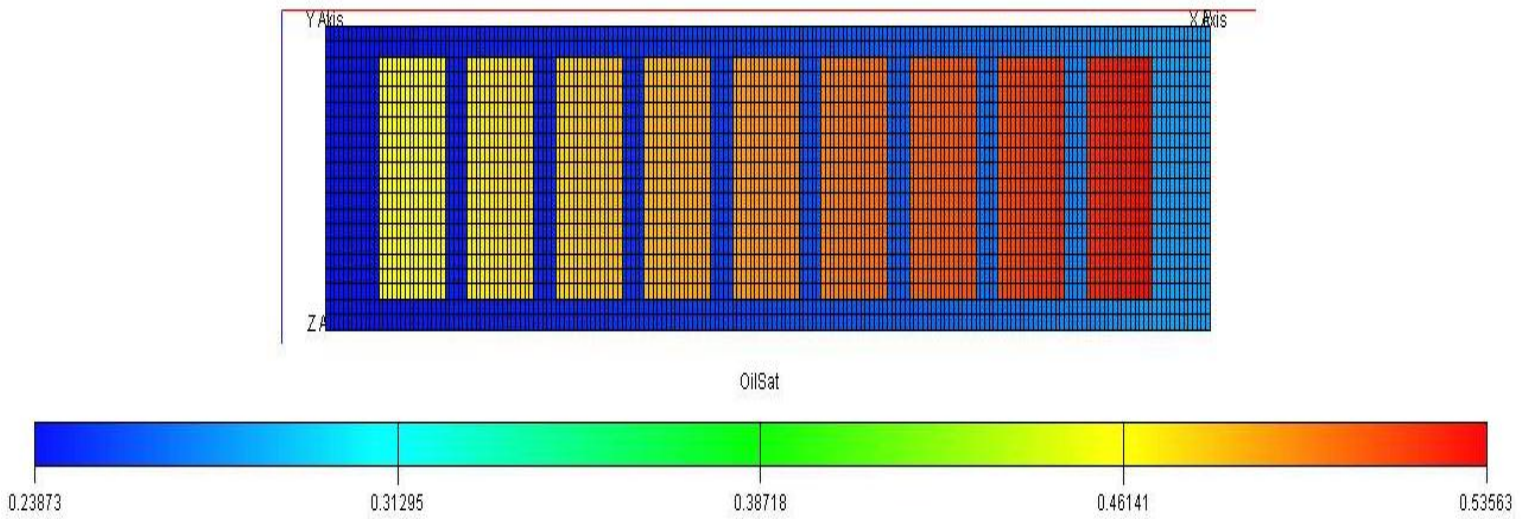
Figure 21: High saturation contrast under capillary dominance in low
permeable inclusion model

Inclusions constitute a significant volume of the model so that they have considerable effect which can be observed in simulation results. Inclusions are oriented perpendicular to flow direction to avoid bypassing of injected water as shown in Fig 21.

Model dimensions are given below

DX = 200, DY = 1, DZ = 20

Length of model = 200 * 0.01 = 2 m

Width of model = 1 * 0.01 = 0.01 m = 1 cm

Height of model = 20 * 0.0025 = 0.05 m = 5 cm

Isotropic model with a porosity of 25%.

As indicated by dimensions of the model, this model represents a core scale model. We have chosen the core scale model because large field scale model revealed neither the effect of reduced IFT on recovery, nor of an increase in capillary number on remaining oil saturation. The reason was that the effects were beyond the range of large scale model.

Two types of inclusions (Low permeability and high permeability inclusions) were simulated to investigate the effect of reduced IFT on capillary trapping due to capillary forces which cause high saturation contrast in different permeability rocks as described earlier. The model definition for both low and high permeable inclusion cases is same except the permeability of the inclusions. The simulation results from low and high permeable inclusion cases are described below.

4.5.2.1. Low Permeability Inclusion

Permeability of surrounding matrix = 100 mD

Permeability of inclusions = 10 mD

Effective permeability, used in the calculation of capillary number (given in table below), was obtained by using simple Darcy's Law. The calculations are shown below.

$$K_{eff} = C_f \frac{Q_w \mu_w \Delta X}{K_{rw} A \Delta P} = 0.27778 * \frac{10 * 0.34 * 200}{1 * 5 * 1.06702} = 35.41 mD$$

Where C_f is the conversion factor.

A significant contrast in permeability of surrounding matrix and inclusions was used to ensure that we capture the effect of reduced IFT on capillary trapping. Low permeability inclusions are analogous to low permeability shale streaks which

presents a restriction to fluid flow in porous media. The simulation results from low permeable inclusions models are shown below.

Table 5: Effect of reduced IFT in heterogenous (Low Permeable Inclusions) model in the absence of gravitational forces

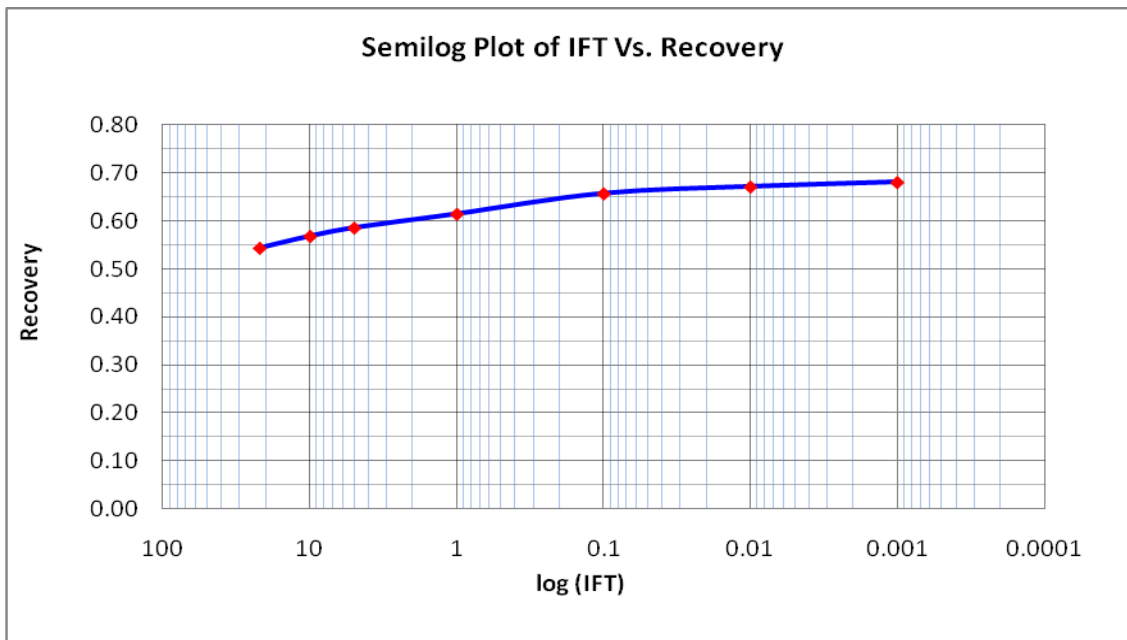| IFT (mN/m)	Recovery Factor	N_c	ROS
22	0.54337	5.095E–07	0.386207
10	0.56821	1.937E–06	0.366515
5	0.58566	6.465E–06	0.352239
1	0.61463	4.841E–05	0.325938
0.1	0.65725	4.969E–04	0.289889
0.01	0.67148	5.399E–03	0.277853
0.001	0.68090	5.997E–02	0.269882

Figure 22: Effect of reduced IFT on recovery from low permeable inclusion model

The above plot indicates that a reduction in interfacial tension to an order of 10^4 results in approximately 14 % increase in recovery, likewise plot below reveals roughly 12 % reduction in remaining oil saturation when capillary number is increased to an order of 10^4. These results clearly reflect effectiveness of surfactant flooding in heterogeneous reservoirs with low permeable inclusions.
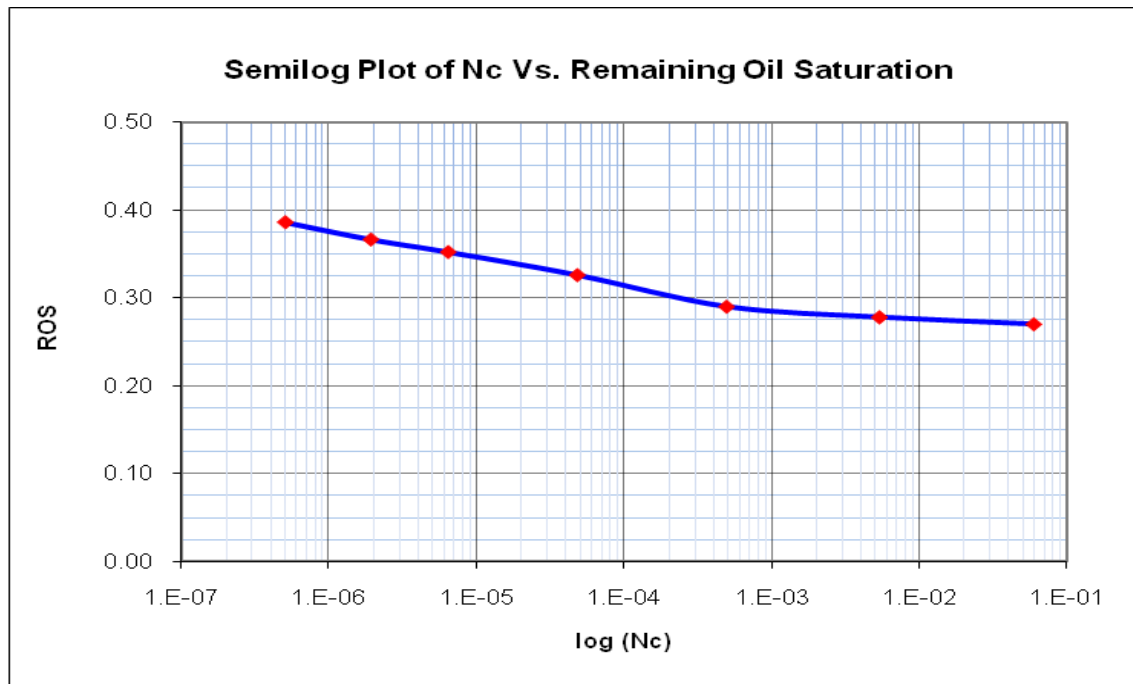

Figure 23: Effect of capillary number (obtained by varying IFT) on remaining oil saturation from low permeable inclusion model

According to the definition of capillary number ($N_c = \frac{v\mu}{\sigma}$), the effect of reduced IFT is analogous to increased flow rate which has technical constraints since flow rates cannot be increased beyond certain limit. The effect of flow rate on recovery, capillary number and remaining oil saturation is shown below which corresponds to the results described above.

Table 6: Effect of flow rate in heterogenous (Low Permeable Inclusions) model in the absence of gravitational forces

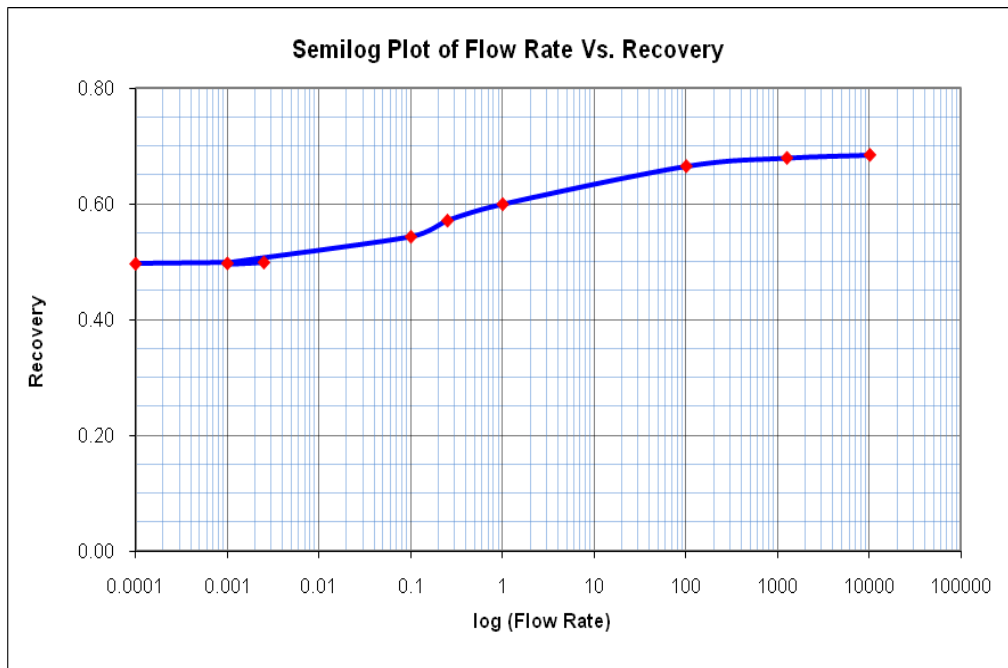| Q (cm^3/hr)	Recovery Factor	N$_c$	ROS
0.0001	0.49694	3.219E–10	0.425475
0.0025	0.49932	8.610E–09	0.423461
0.001	0.49776	3.460E–09	0.424778
0.1	0.54337	5.095E–07	0.386207
0.25	0.57116	2.401E–06	0.362703
1	0.59936	1.964E–05	0.338850
100	0.66478	2.379E–03	0.283523
1250	0.67898	3.346E–02	0.271511
10000	0.68408	2.774E–01	0.267193

Figure 24: Effect of flow rate on recovery from low permeable inclusion model
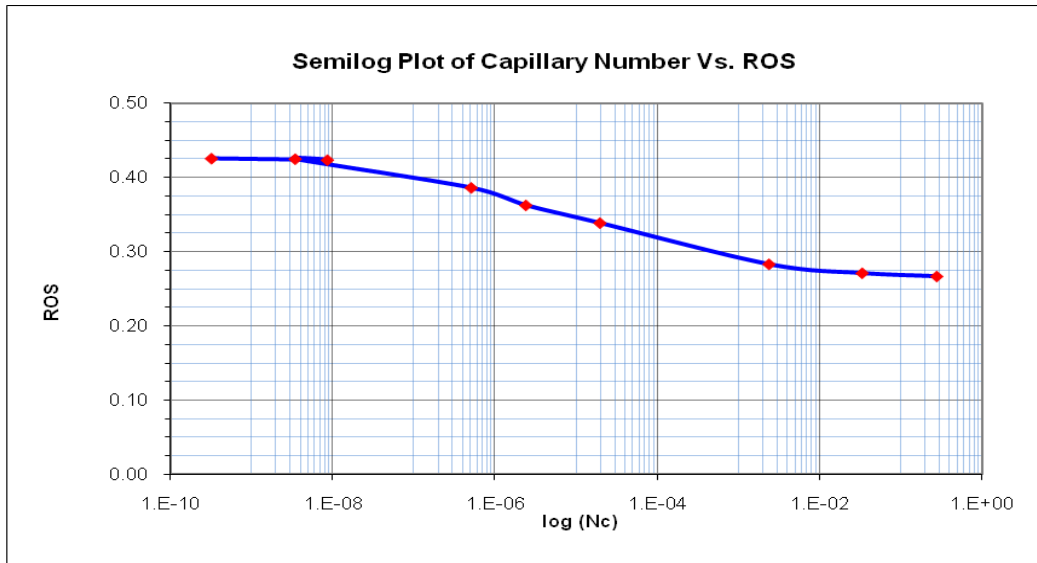
Figure 25: Effect of capillary number (obtained by varying flow rate) on remaining oil saturation from low permeable inclusion model
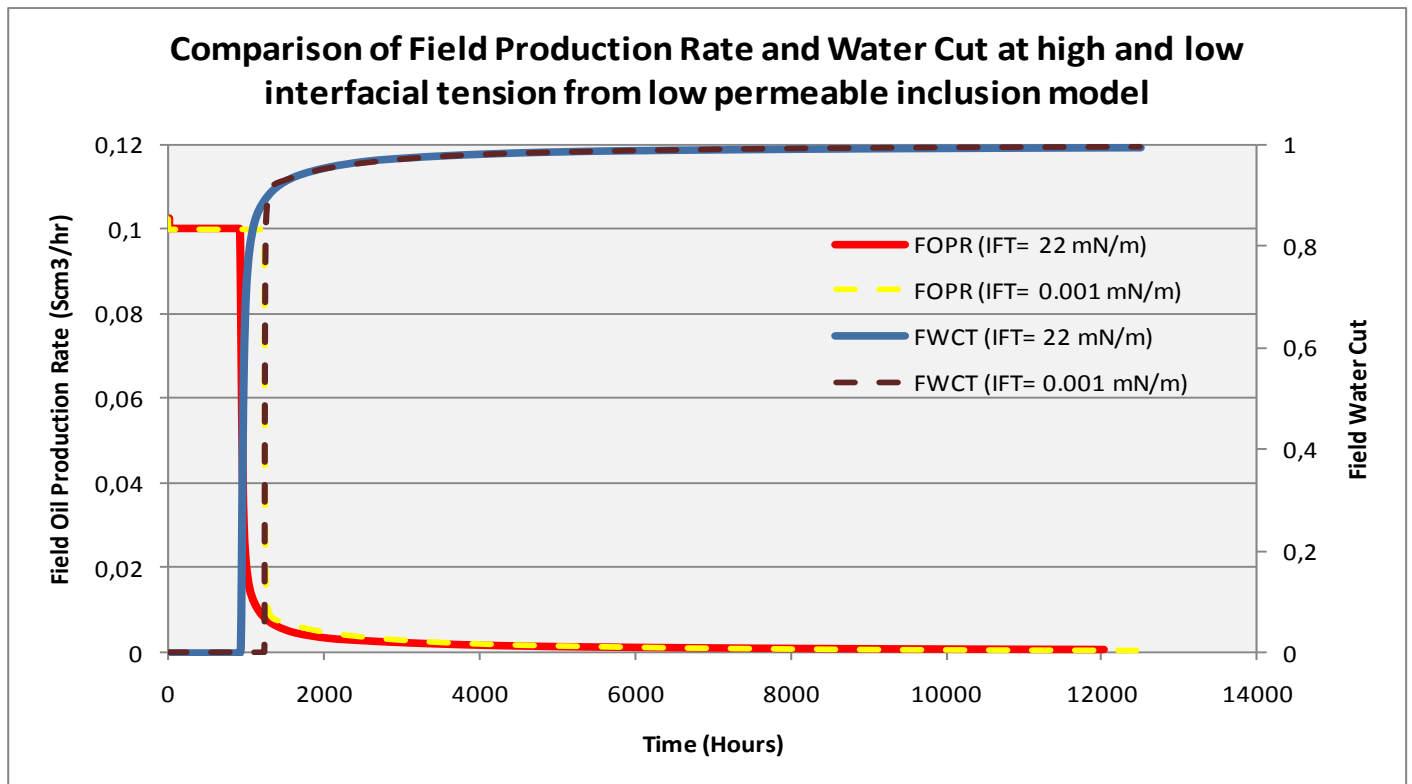

Figure 26: Comparison of field production rate and water cut at high (water flooding) and low (surfactant flooding) IFT
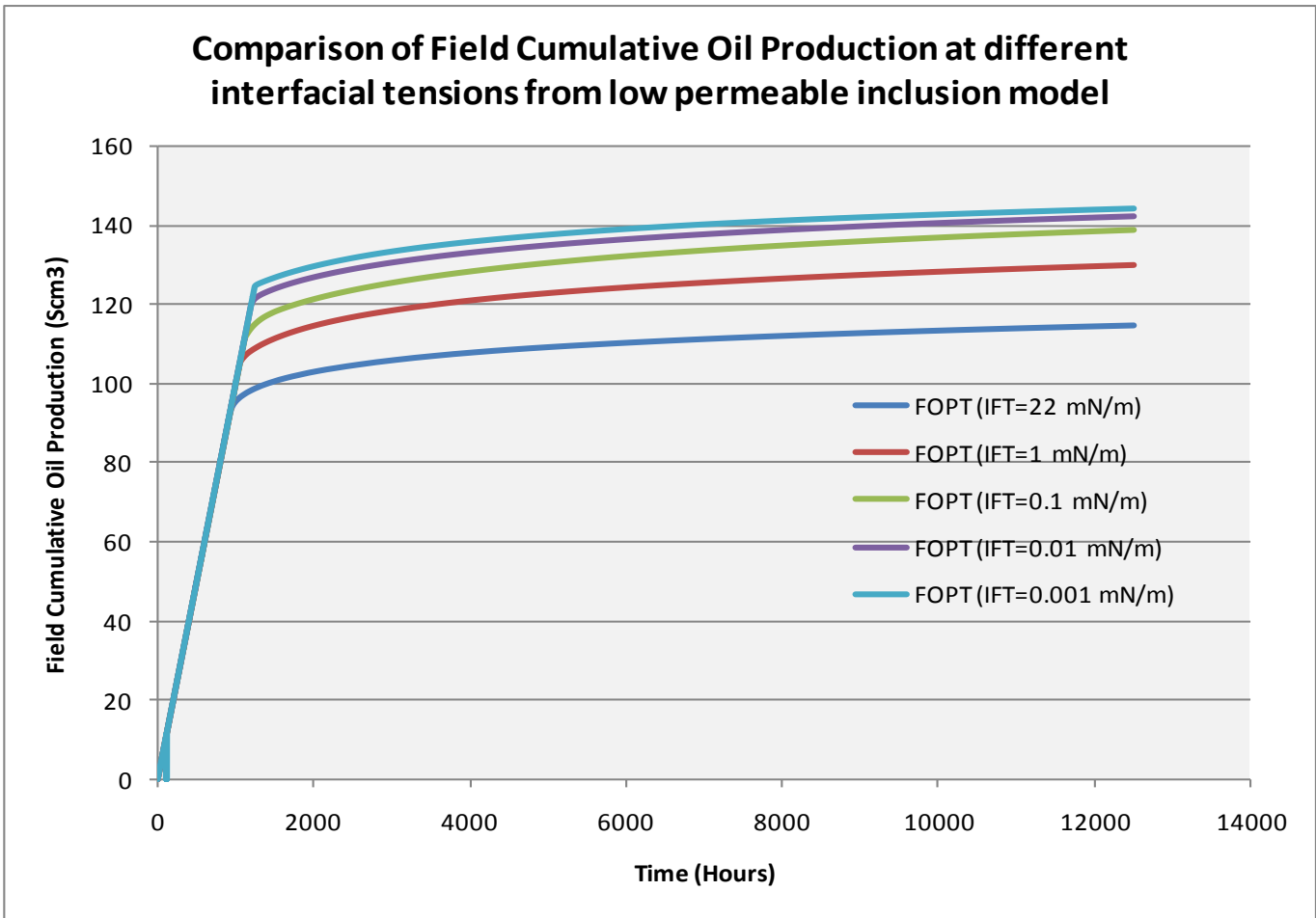
Figure 27: Comparison of field cumulative oil production at different IFTs from low permeable inclusion model

The plot shown in Fig. 26 and Fig. 27 validates our results shown earlier for low permeable inclusion model. Figure 27 clearly reveals an increase in field cumulative oil production (hence recovery) by reducing interfacial tension.

Saturation distribution field at high interfacial tension (water flooding) in this case indicates entrapment of oil in low permeable inclusions. Capillary forces are stronger in low permeable inclusions compared to surrounding matrix which tend to bind oil in low permeable inclusions as indicated by high oil saturation in inclusions in Fig. 28 below compared to surrounding matrix, a significant contrast exists. A reduced interfacial tension (surfactant flooding) causes a reduction in capillary forces and release oil from such low permeable zones of the reservoir. So a reduction in interfacial tension in this case has a positive impact on oil recovery. The saturation distribution in low permeable inclusion model at high (22 mN/m) and low (0.001 mN/m) IFTs are shown below.

OilSat

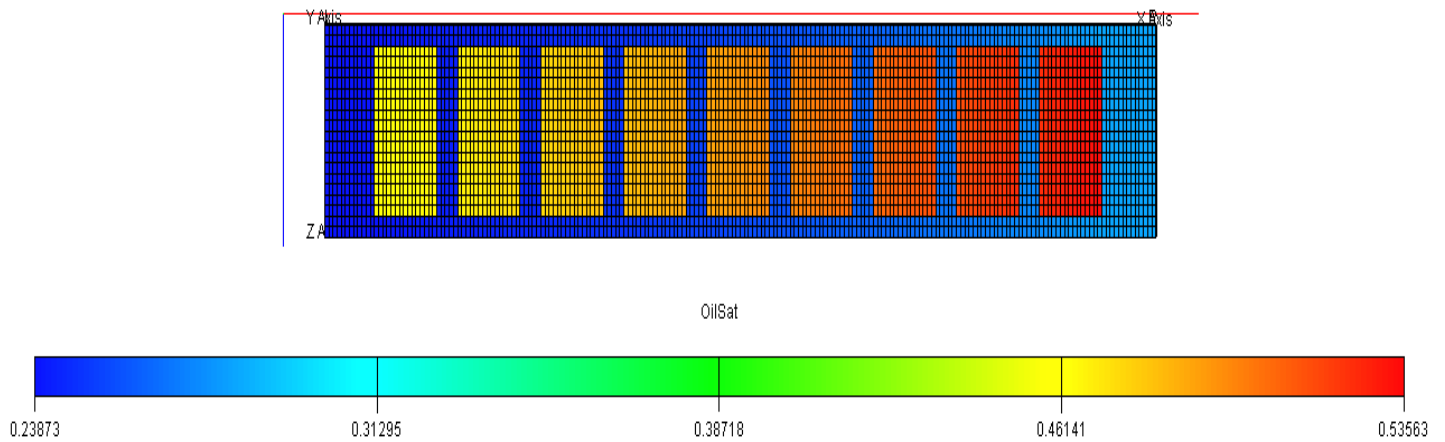| 0.23873 | 0.31295 | 0.38718 | 0.46141 | 0.53563 |

Figure 28: Oil saturation field (From Eclipse FloViz Module) from water flooding (High IFT) revealing entrapment of oil in low permeable inclusions
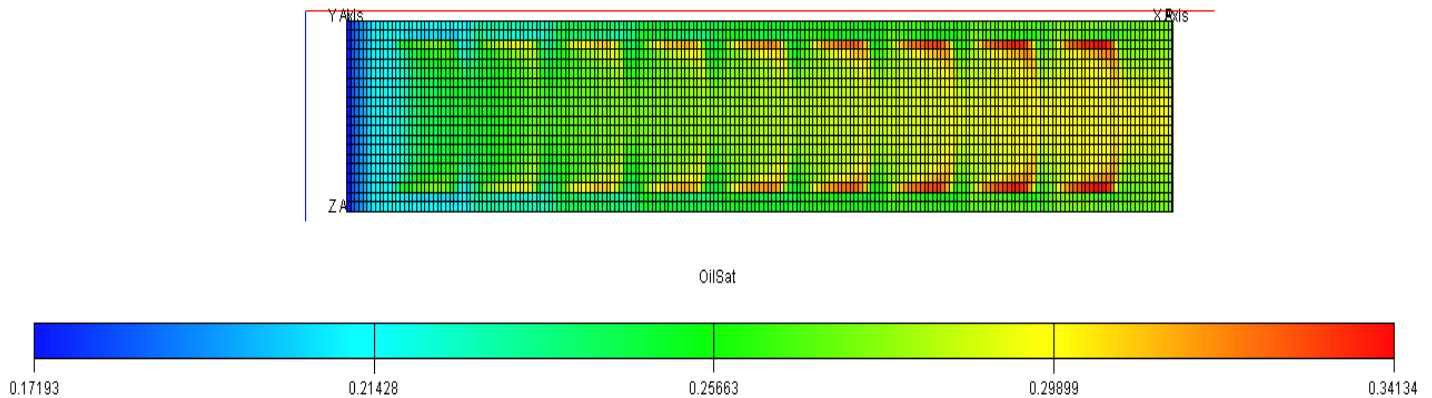
Figure 29: Oil saturation field (From Eclipse FloViz Module) from surfactant flooding (Low IFT) revealing reduction in oil saturation in low permeable inclusions

4.5.2.2. High Permeability Inclusion

Permeability of surrounding matrix = 100 mD

Permeability of inclusions = 1000 mD

Effective permeability, used in the calculation of capillary number (given in table below), was obtained by using Darcy's Law. The calculations are shown below.

$$K_{eff} = C_f \frac{Q_w \mu_w \Delta X}{K_{rw} A \Delta P} = 0.27778 * \frac{10*0.34*200}{1*5*0.1558} = 242.46\,mD$$

High permeable inclusions could exist as fracture in reservoirs. Simulation results from high permeable inclusion model are shown below.

Table 7: Effect of reduced IFT in heterogenous (High Permeable Inclusions) model in the absence of gravitational forces

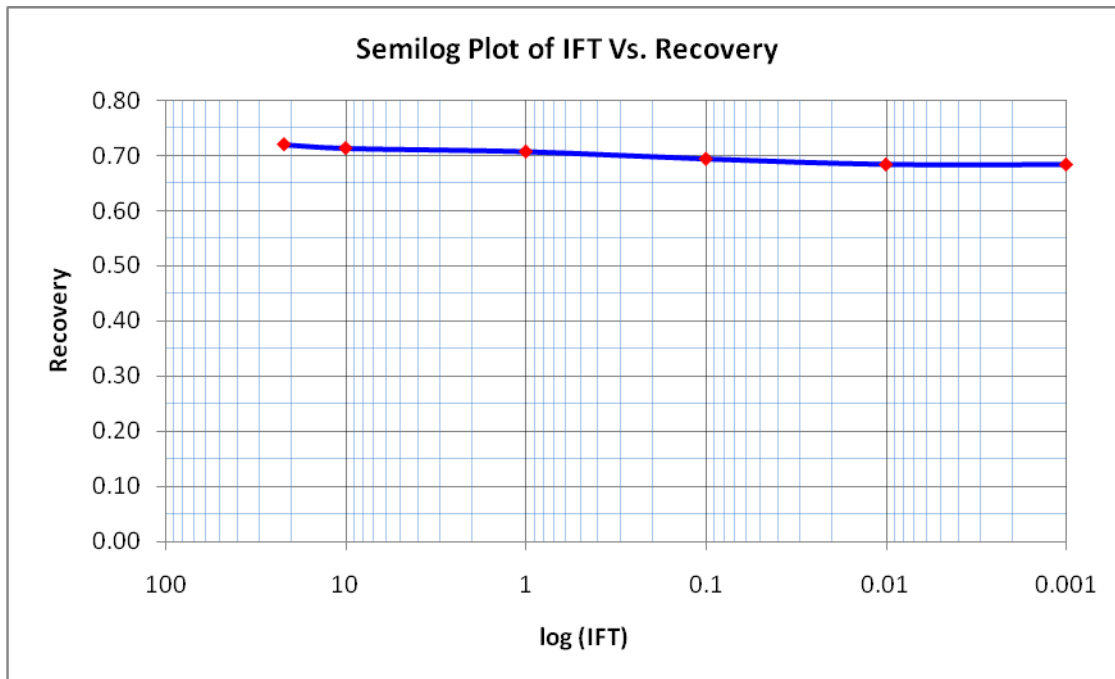| IFT (mN/m)	Recovery Factor	N_c	ROS
22	0.72039	9.795E–06	0.237547
10	0.71344	1.635E–05	0.243807
1	0.70712	7.687E–05	0.248825
0.1	0.69346	6.340E–04	0.260428
0.01	0.68310	5.817E–03	0.269231
0.001	0.68297	5.954E–02	0.269344

Figure 30: Effect of reduced IFT on recovery from high permeable inclusion model
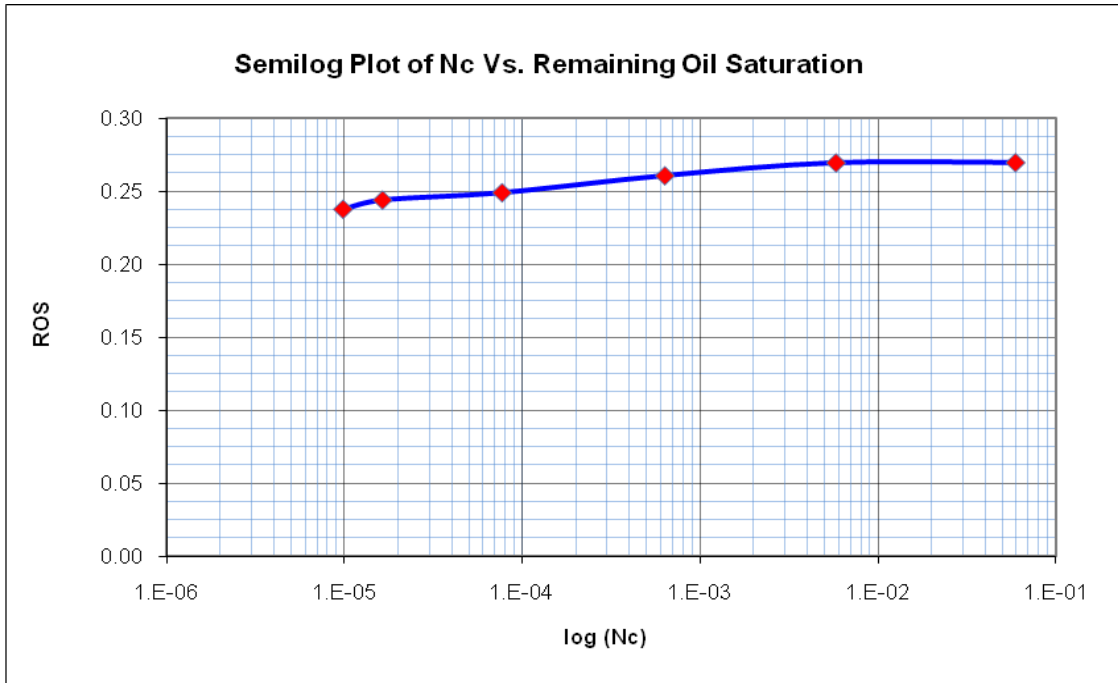
Figure 31: Effect of capillary number (obtained by varying IFT) on remaining oil saturation from high permeable inclusion model

Results in this case are quite opposite to the ones we obtained in low permeable inclusion case i.e., a reduction in IFT leads to decrease in oil recovery and an increase in capillary number leads to an increase in remaining oil saturation. This suggests that surfactant flooding is detrimental to recovery in high permeable inclusion reservoirs, but this result is limited to effect of capillary trapping since we have yet not included the effect of gravity. A similar trend must be expected through an increase in flow rate. The effect of increasing flow rate on recovery, capillary number and remaining oil saturation is shown below.

Table 8: Effect of flow rate in heterogenous (High Permeable Inclusions) model in the absence of gravitational forces

Q (cm^3/hr)	Recovery Factor	N_c	ROS
0.0001	0.73879	1.102E–08	0.221918
0.001	0.73856	1.080E–07	0.222110
0.1	0.72039	9.795E–06	0.237547
0.25	0.71296	1.762E–05	0.243865
1	0.70708	4.118E–05	0.248861
100	0.68164	2.714E–03	0.270471
1250	0.68231	3.354E–02	0.269897
10000	0.68597	2.743E–01	0.266794
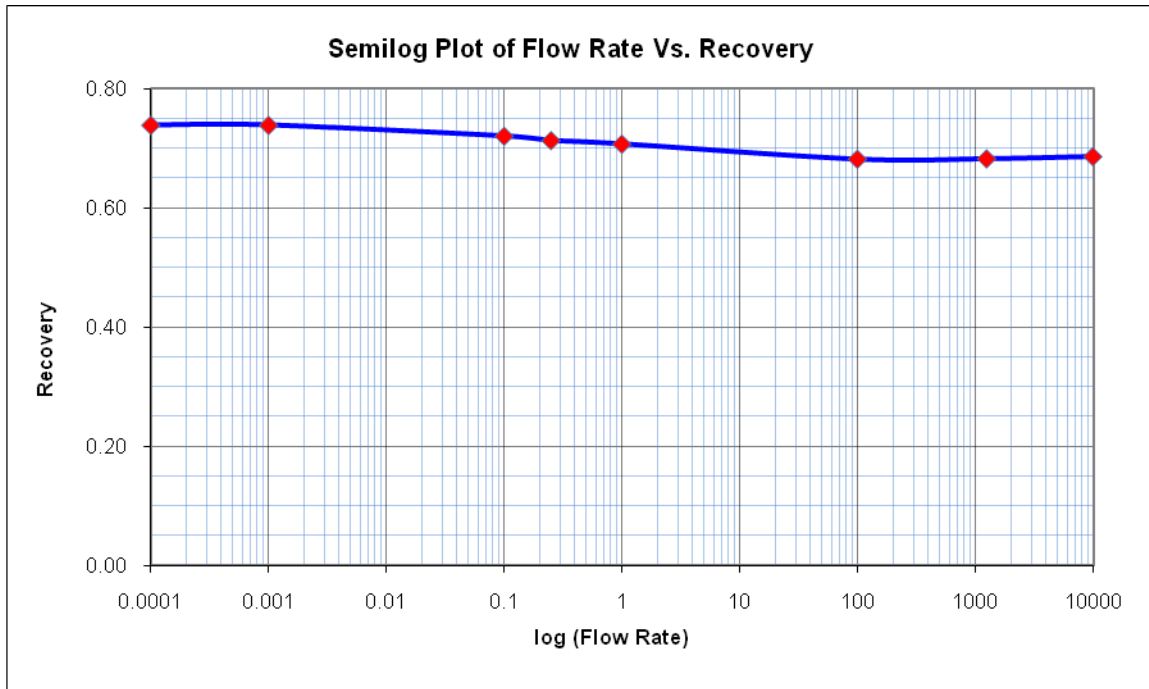
Figure 32: Effect of flow rate on recovery from high permeable inclusion model
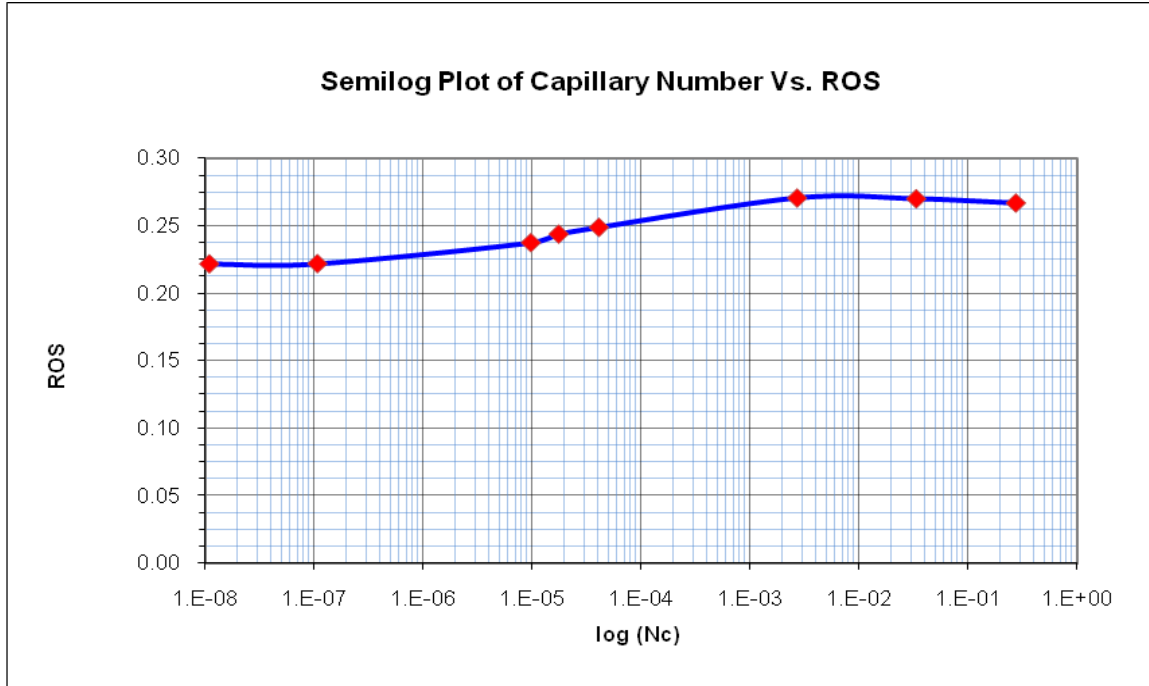
Figure 33: Effect of capillary number (obtained by varying flow rate) on remaining

oil saturation from high permeable inclusion model

These results are pretty similar to ones obtained by reduction in interfacial tension. The effect of gravity in simulation results discussed above was made negligible by setting oil and water density approximately equal since our sole purpose was to just investigate the effect of reduced IFT on capillary trapping in heterogeneous porous media. The effect of gravity on recovery is discussed in subsequent section.
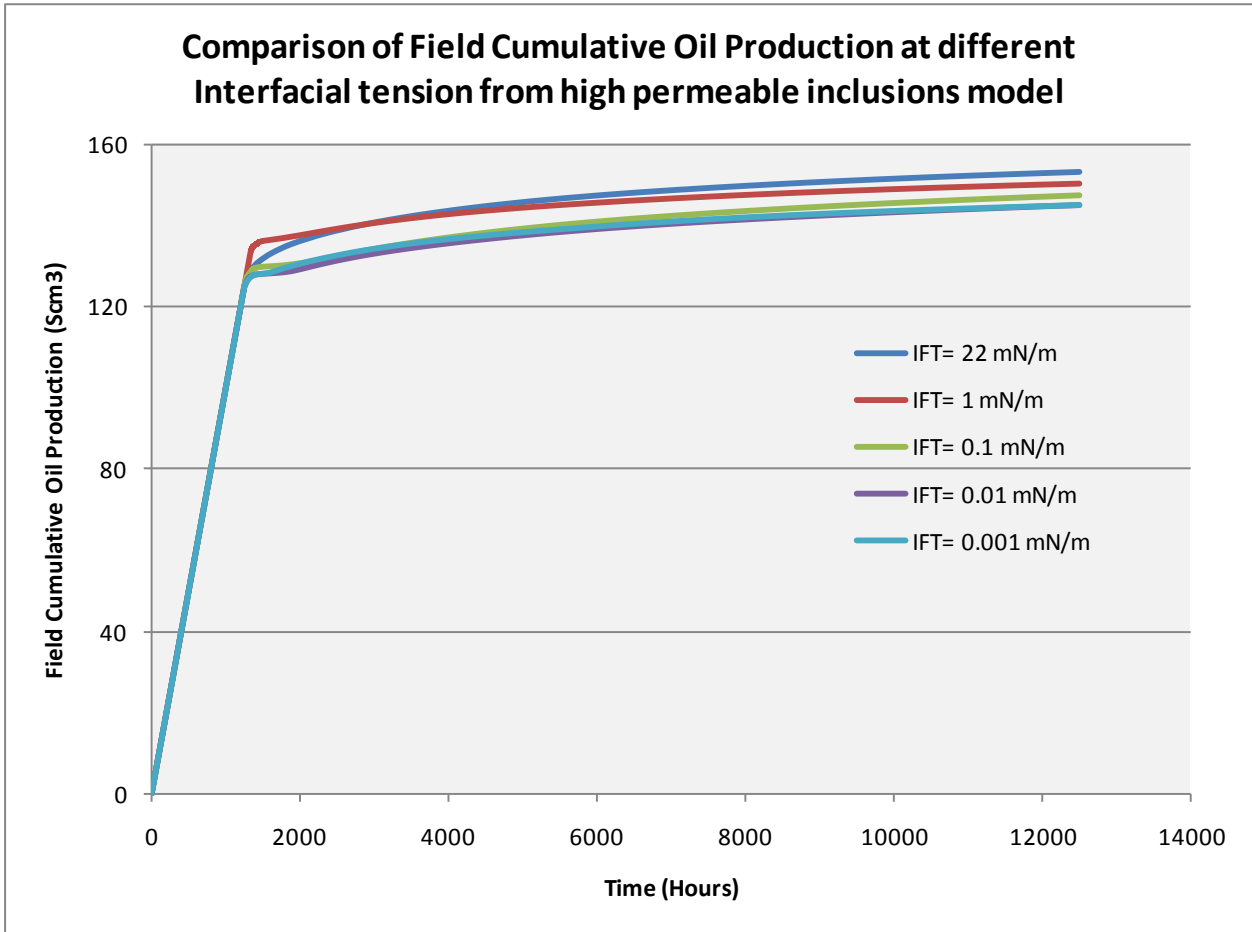
Figure 34: Comparison of field cumulative oil production at different IFTs from high permeable inclusion model

The above plot indicates a decrease in oil recovery with a reduction in interfacial tension which is consistent with results discussed and shown earlier. A comparison oil production and water cut in case of water flooding and surfactant flooding in shown below.
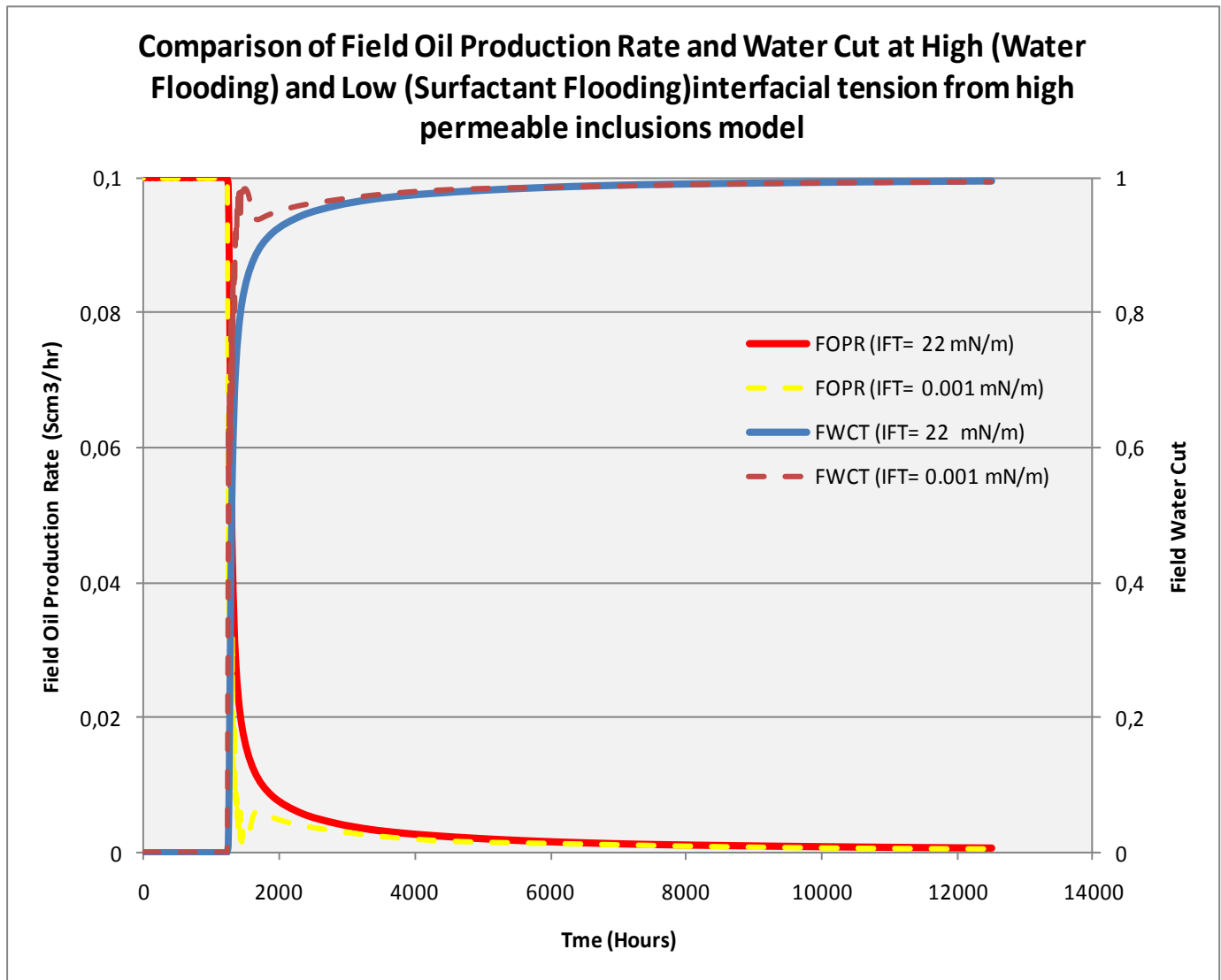
Figure 35: Comparison of field oil production and water cut at high (waterflooding) and low (surfactant flooding) IFT from high permeable inclusion model

The above comparison shows that the reduced IFT causes an increase in water cut immediately after breakthrough but it starts following the same trend as in case of waterflooding soon after.

The oil saturation field at high and low IFTs in this case are shown below which suggests oil entrapment as a result of reduction in interfacial tension. A reduced IFT in this case also reveals bypassing of oil below and above high permeable inclusions which affects the oil recovery. Since the distance between top of model and top of inclusion and bottom of model and bottom of inclusions is quite less so recovery results in such case depends upon the distribution of inclusions whereas geometry and frequency of inclusions also affects the recovery results. In our case, inclusions constitute significant volume of the model.
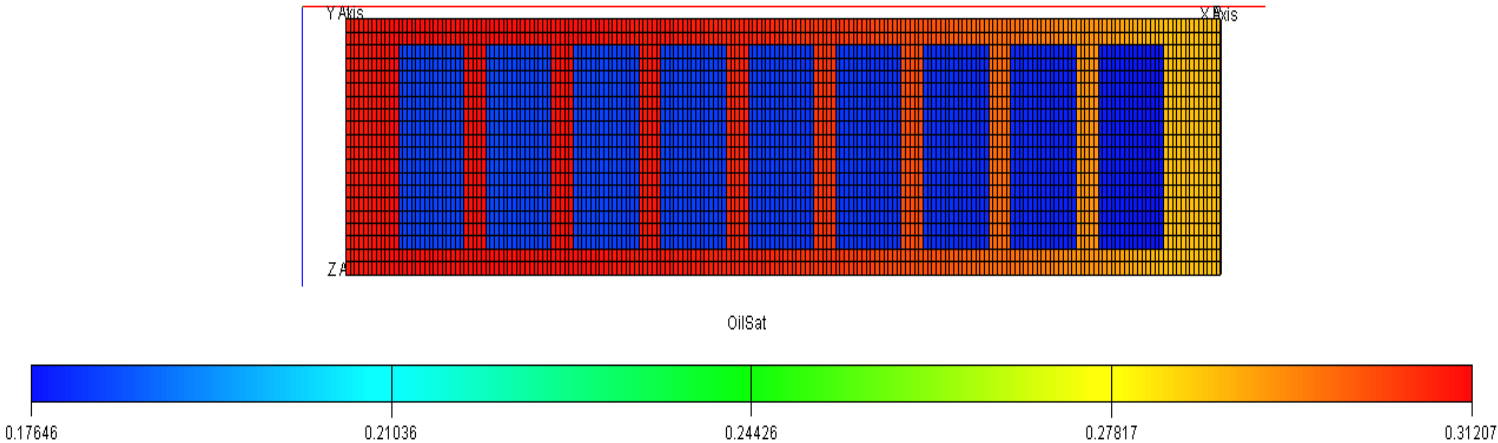

Figure 36: Oil saturation field (From Eclipse FloViz Module) in high permeable inclusion model from waterflooding
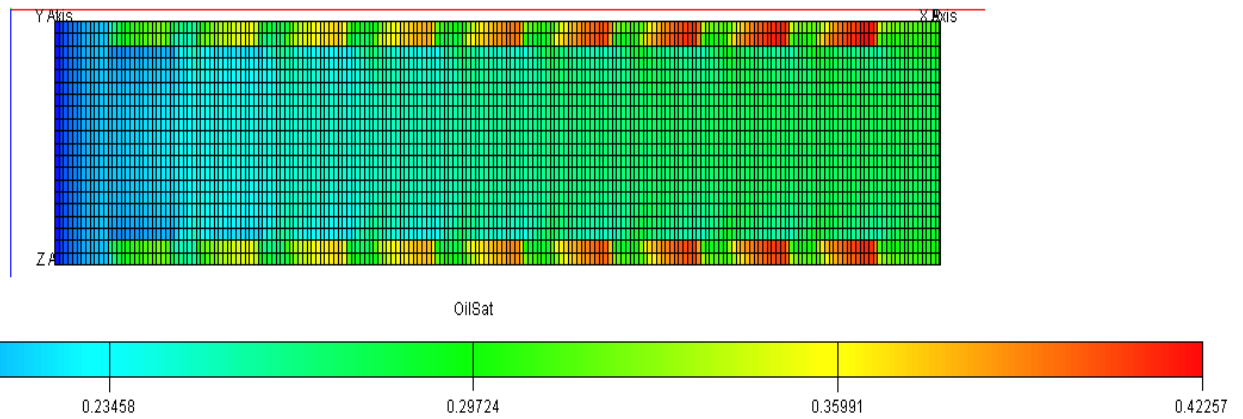
Figure 37: Oil saturation field (From FloViz Module) revealing bypassed oil above and below inclusions from surfactant flooding

4.6. Effect of Gravity Segregation

For many years, gravity segregation in reservoir processes was not accounted for because it could not be adequately handled in reservoir engineering calculations. The advent of reservoir simulation provided the capability to handle gravity, and it became apparent that gravity effects could significantly affect reservoir performance.

Craig et al. (1957) did experimental work to study the effects of gravity segregation during water, gas, and solvent flooding. As a result of their studies, they concluded that segregation of fluids due to gravity effects could result in oil recoveries at breakthrough as low as 20 percent of those otherwise expected. They also concluded that performance may in some cases be influenced to a greater degree by heterogeneity than by gravity effects. They were not able to directly compare performance under a given set of conditions with and without gravity.

Gravity segregation as a result of reduced interfacial tension could occur in heterogeneous porous media. This effect can be quantified through a ratio of viscous to gravitational forces which depends upon injection rates as a proportion

of pore volume, absolute horizontal permeability of reservoir and vertical permeability, density difference.

The effect of gravity segregation is only investigated in simple homogeneous model since it makes it easier to comprehend the results and draw conclusion. Two different models with and without impermeable shale streaks were used to capture segregation effect. Impermeable shale streaks restrict the further vertical movement of oil segregated due to gravity and let it accumulate just beneath them. This accumulated oil beneath impermeable layers might or might not have considerable effect on oil recovery depending upon the injection rate during water flooding (higher the injection rate, lesser the segregation and less increase in oil recovery and vice versa) and amount of segregated oil. The vertical thickness of both models was kept same in order to get same pore volume so that the results could be compared after injection of certain pore volume. These models and simulation results are elaborated below.

4.6.1. Model without Impermeable Shale Streaks

The homogeneous model used earlier, where effect of gravity segregation was absent, contained thick grid layers in vertical direction. A new homogeneous model is defined where the thickness of the layers or grids in vertical direction has been reduced since it's hard to capture the effect of gravity segregation in thicker layers. Top most and bottom most layers of the model were made comparatively thinner to visualize the effect of water and oil accumulation caused by gravity segregation as can be seen in table below. Model dimensions for new homogeneous model are given below

DX = 200, DY = 1, DZ = 32

Length of model = 200 * 2.5 = 500 m

Width of model = 1 * 10 = 10 m

Isotropic model with a porosity of 25%, same as used in earlier homogeneous and all other models. The thickness of layers/grid blocks in vertical direction with their respective connection transmissibility factor (used in simulation) is given in table below.

Table 9: Definition of new homogeneous model to capture of gravitational effects

Layers (Grids in vertical direction)	Grid vertical thickness (m)	Connection Transmissibility Factor
1 to 5	0.1	6.8216
6 to 7	0.5	34.108
8 to 25	1	68.216
26 to 27	0.5	34.108
28 to 32	0.1	6.8216

As can be seen from above table, model represents a symmetric case in vertical direction with a total thickness of 21 meters which is probably the suitable model to capture gravity segregation effects. A sensitivity analysis on both flow rate and IFT was conducted using Eclipse Surfactant Model and the results are shown in table below.

Table 10: Effect of reduced IFT and flow rate to capture gravitational effect in homogeneous model in the absence of impermeable shale streaks

Flow Rate (m^3/day)	Recovery without Impermeable Shale Steaks		
	22E–3 N/m	1E–3 N/m	0.001E–3 N/m
20000	0.68882	0.68937	0.68858
15000	0.68918	0.68869	0.68979
10000	0.68777	0.68963	0.68904
5000	0.68952	0.69156	0.69178
2000	0.69199	0.69493	0.69520
1000	0.69876	0.70582	0.70612
500	0.71249	0.72136	0.72167
200	0.73589	0.74490	0.74504
100	0.75314	0.76346	0.76363
20	0.78923	0.80090	0.80122
2	0.82159	0.83550	0.83651
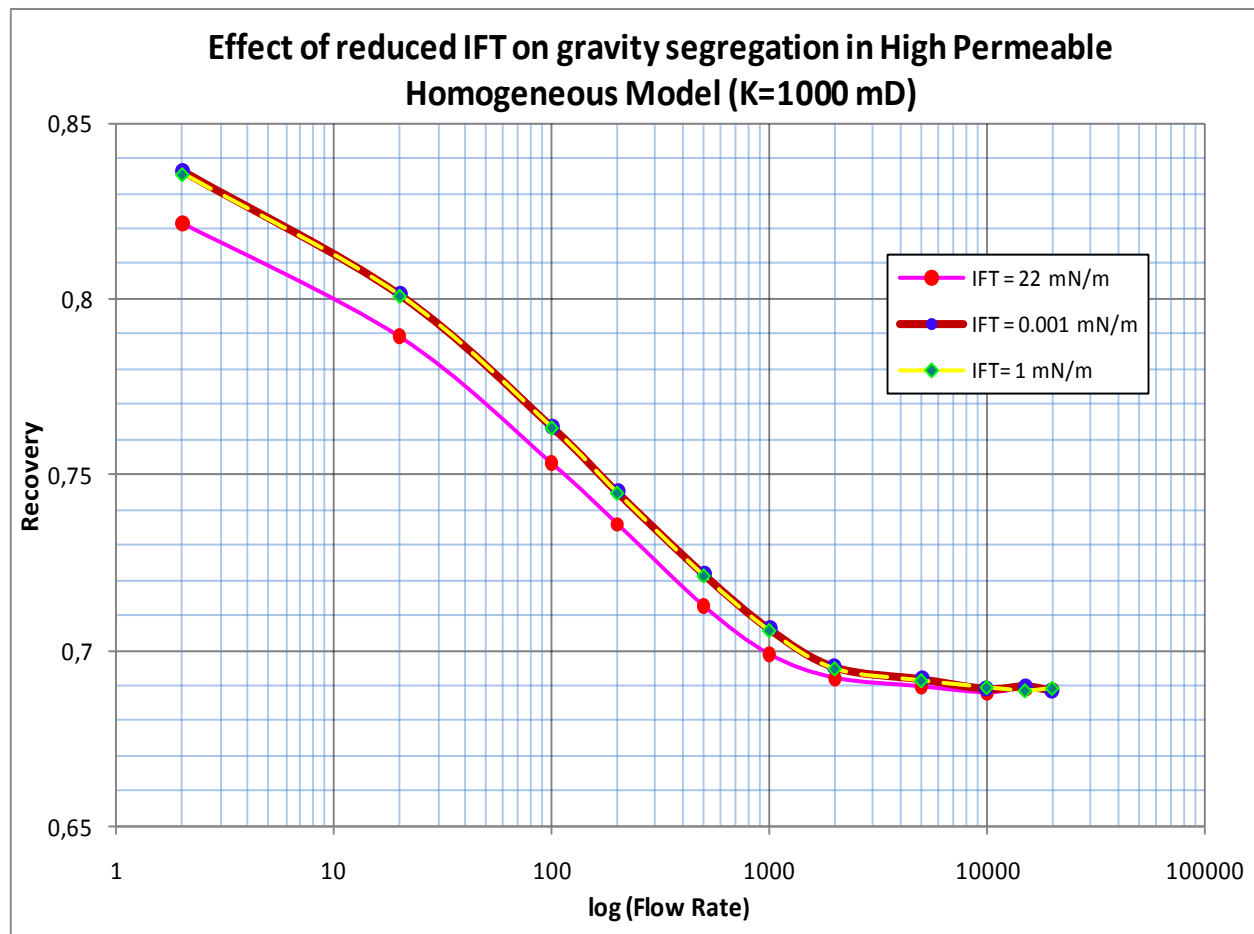
Figure 38: Effect of gravity segregation on oil recovery from homogeneous model

The above plot clearly reveals that a reduction in interfacial tension would assist gravity to segregate oil and water and would ultimately lead to enhanced oil recovery. The lower flattened part of the above recovery curve indicates viscous dominated flow regime whereas the higher recovery part of the curve which starts flattening out indicates gravity plus capillary dominated flow regime. A reduction in interfacial tension from 22 to 1 mN/m indicates an increase in oil recovery. According to above plot, recovery results from IFT of 1 mN/m and 0.001 mN/m are same meaning an inexpensive surfactant or good quality surfactant at low concentration can be used to get same enhanced oil recovery.

4.6.2. Sensitivity Analysis on Permeability

A sensitivity analysis was conducted on permeability to investigate if effect of reduced IFT depends upon permeability of the reservoir or not. The same model as used in previous case is simulated with 100 mD permeability. The difference was found obvious from the simulation results as shown below.

Figure 39: Dependence of reduced IFT effect on permeability of the model

The above graphical comparison clearly reveals that at low permeability, effect of reduced interfacial tension is more significant in comparison to high permeable

models. But at the same time, it shows that this effect is negligible at high rate since gravity does not play much role at high rates. The results from low permeability model indicate that o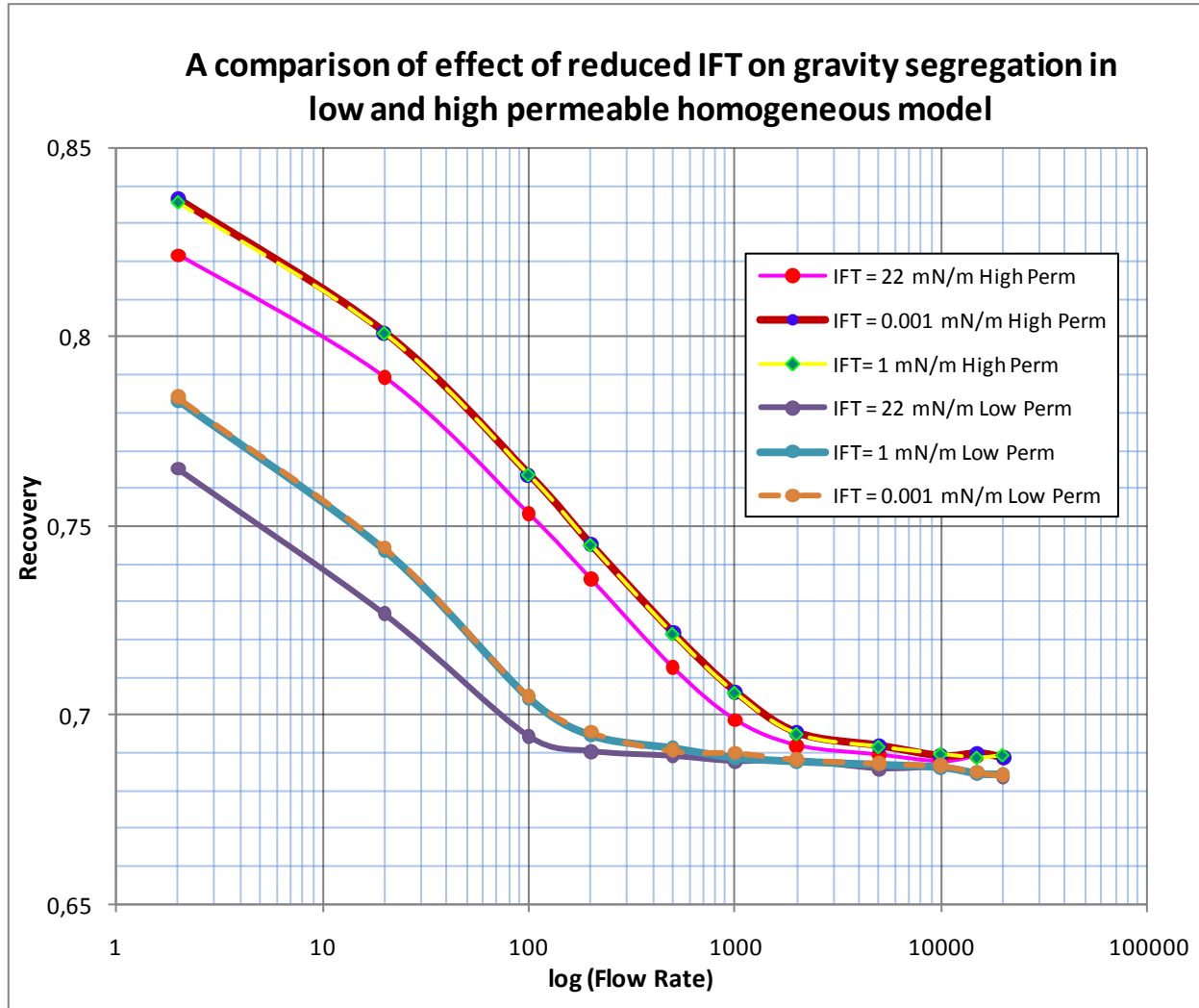il recovery is not enhanced when interfacial tension is reduced from 1 to 0.001 mN/m as depicted by previous simulation results which also validates our earlier results.

4.6.3. Model with Impermeable Shale Streaks

This model is a modification in above model. The above model has been split up into finer layers in vertical direction and three impermeable shale streaks were introduced in the model to investigate the effect of oil accumulation beneath such impermeable streaks on recovery. Model dimensions for new modified homogeneous model are given below

DX = 100, DY = 1, DZ = 52

Length of model = 100 * 5 = 500 m

Width of model = 1 * 10 = 10 m

Isotropic model with a porosity of 25%.

The total number of grid blocks in horizontal direction is half of what we used in previous model to reduce the computational time but block size in horizontal direction is doubled and total vertical thickness of model is kept same in order to get same pore volume so that results from both models could be compared after injection of certain pore volume.

The thickness of layers/grid blocks in vertical direction with their respective connection transmissibility factor (used in simulation) is given in table below.

Table 11: Definition of new homogeneous model including impermeable shale streaks

Layers (Grids in vertical direction)	Grid vertical thickness (m)	Connection Transmissibility Factor
1 to 5	0.1	3.4108
6 to 7	0.5	17.054
8 to 10	1	34.108
11	0.74	25.23992
12	**0.01**	**0**
13 to 17	0.1	3.4108
18 to 19	0.5	17.054
20 to 22	1	34.108
23	0.74	25.23992
24	**0.01**	**0**
25 to 29	0.1	3.4108
30 to 31	0.5	17.054
32 to 34	1	34.108
35	0.74	25.23992
36	**0.01**	**0**
37 to 41	0.1	3.4108
42 to 43	0.5	17.054
44 to 46	1	34.108
47	0.25	8.527
48 to 52	0.1	3.4108

Permeability of surrounding matrix/background rock = 1000 mD

Permeability of shale streaks =0 mD

The three impermeable shale streaks are highlighted in table 11 above with green color. Impermeable streaks were chosen to ascertain restriction of segregated oil so that it could accumulate beneath these impermeable streaks. This is analogous to reducing the thickness of the model or in other words increasing the ratio L_x/L_z where L_x is length of the model and L_z is thickness of the model. Actually in our case the previous model has been split in four different zones by introducing three impermeable layers to investigate the effect of accumulated oil beneath each impermeable layer. The same flow rate sensitivity analysis was conducted as did in previous case without impermeable shale streaks. The simulation results are shown below.

Table 12: Effect of reduced IFT and flow rate to capture gravitational effect in homogeneous model in the presence of impermeable shale streaks

Flow Rate (m^3/day)	Recovery without Impermeable Shale Steaks		
	22E–3 N/m	1E–3 N/m	0.001E–3 N/m
20000	0.69334	0.69409	0.69359
15000	0.69397	0.69457	0.69392
10000	0.69204	0.69621	0.69511
5000	0.69385	0.69994	0.70030
2000	0.70194	0.71338	0.71220
1000	0.71310	0.72724	0.71829
500	0.72422	0.74095	0.73394
200	0.73297	0.74981	0.75133
100	0.74348	0.7625	0.76467
20	0.78763	0.79954	0.79952
2	0.82079	0.83215	0.83521

The comparison of recovery from models with and without impermeable shale streaks at two reduced IFTs is shown below.
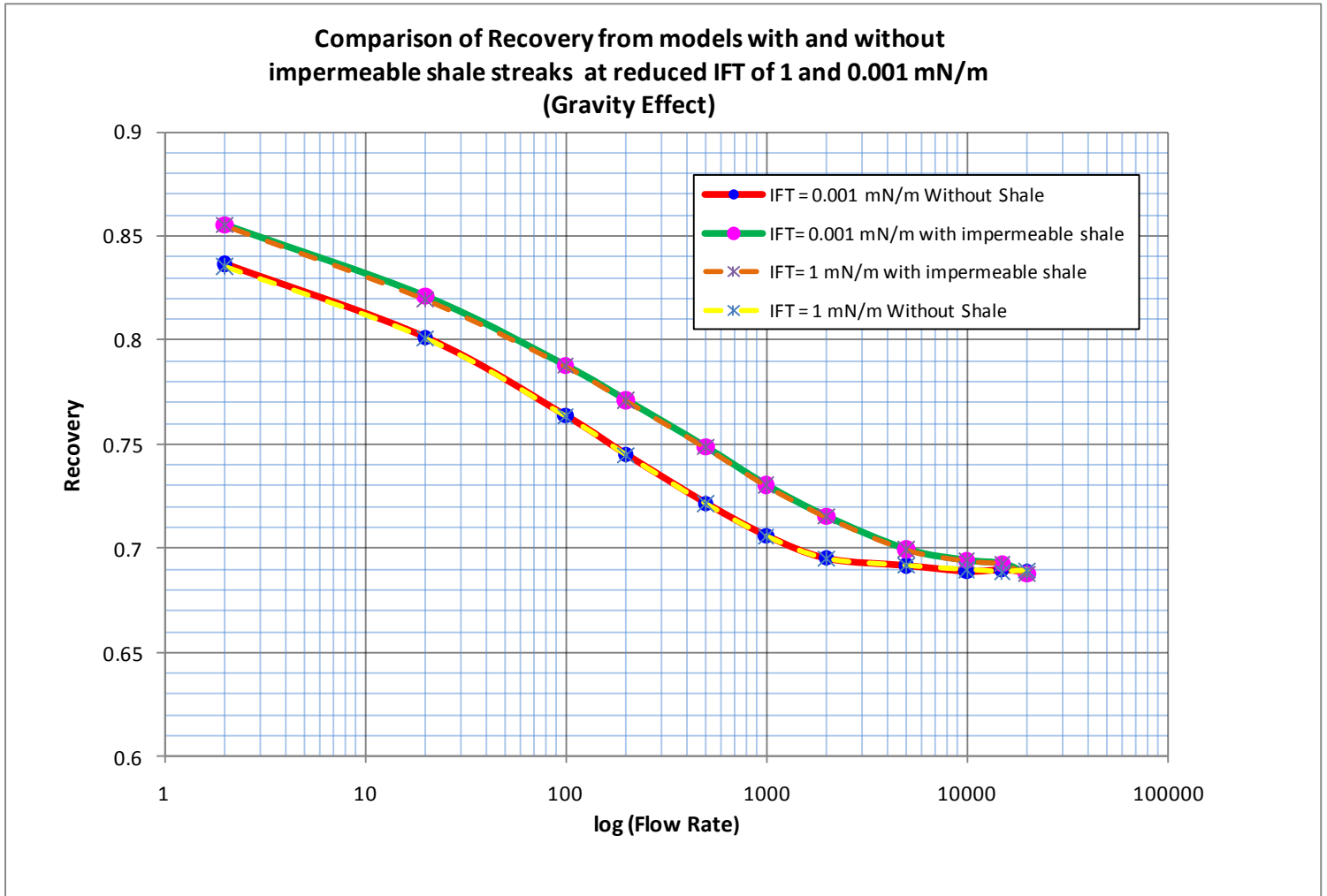
Figure 40: Dependence of reduced IFT effect on presence of impermeable shale streaks

The above plot reveals that recovery is enhanced due to the presence of impermeable shale streaks which were assumed to restrict further vertical movement of oil which is segregated by reduction in interfacial tension. Further

reduction in interfacial tension below 1 mN/m does not seem to enhance oil recovery as concluded earlier.

4.7. Effect of Change in Oil Relative Permeability Curvature

In this case, the sensitivity analysis of flow rate was not conducted and the same flow rate determined earlier through flow rate sensitivity analysis was used representing capillary dominance at the beginning of simulation runs. Simulation of change in oil relative permeability curve requires different miscible and immiscible curves as input to simulation. Same end points for both miscible and immiscible curves were used to make the case simple and results comprehensible. An example of data input file (showing different miscible and immiscible curves with same end points) required for such simulation is provided in Appendix.

The effect of change in oil relative permeability curvature was simulated for homogeneous model and the simplest case of heterogeneity i.e., layered or stratified model (with model dimensions as used before) and the results are shown below for homogeneous model and stratified model respectively.

Table 13: Effect if reduced IFT in homogeneous model considering change in oil relative permeability curvature

IFT (mN/m)	Recovery Factor	N_c	ROS
22	0.69198	2.340E–07	0.261311
1	0.69195	5.154E–06	0.261332
0.1	0.76886	3.190E–05	0.196091
0.01	0.86373	1.993E–04	0.115603
0.001	0.87770	1.893E–03	0.103755

Semilog Plot of IFT Vs. Recovery
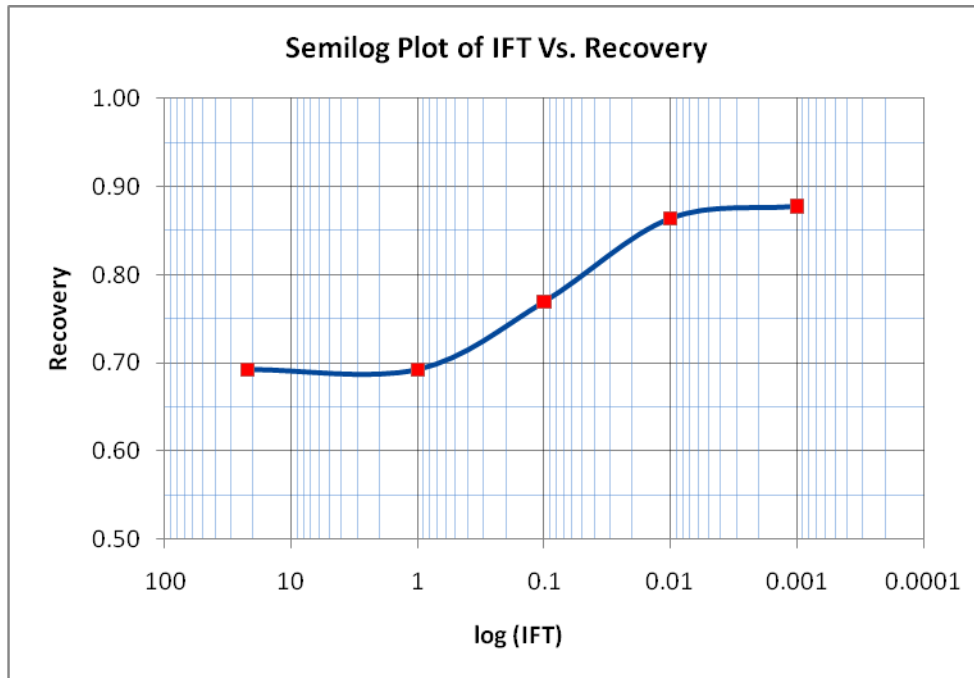
Figure 41: Effect of reduced IFT on recovery considering change in oil relative permeability curvature in homogeneous model

The above plot indicate a significant increase in oil recovery when interfacial tension between oil and water is reduced from 22 to 0.01 mN/m and a same trend could be observed through a semilog plot of capillary number verses remaining oil saturation as shown below.
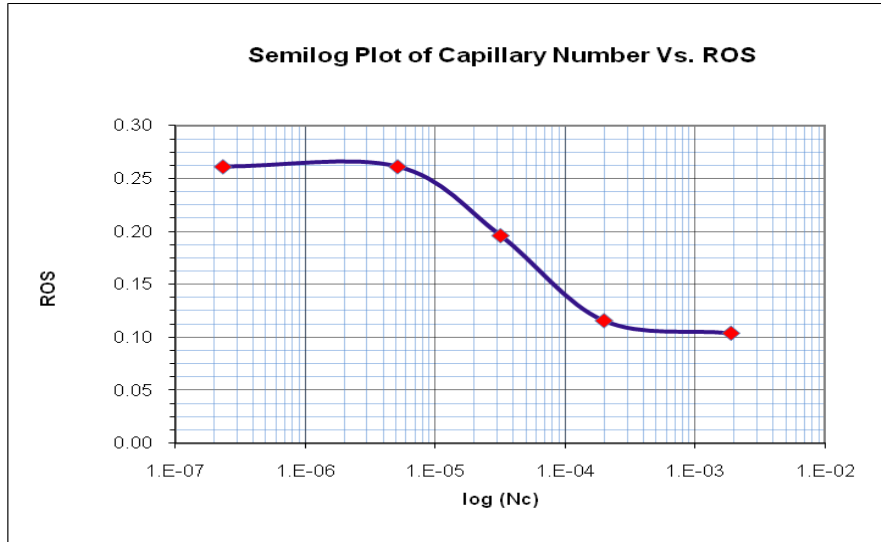
Figure 42: Effect of capillary number (obtained by varying IFT) on remaining oil saturation considering change in oil relative permeability curvature in homogeneous model

For stratified case, the same increase in recovery with reduced IFT and a decrease in remaining oil saturation with increase in capillary number was observed. The resutls are shown below.

Table 14: Effect if reduced IFT in heterogeneous (Layered/Stratified) model considering change in oil relative permeability curvature

IFT (mN/m)	Recovery Factor	N_c	ROS
22	0.64335	1.097E–06	0.301681
1	0.70391	1.953E–05	0.250461
0.1	0.77981	1.335E–04	0.186255
0.01	0.87069	1.186E–03	0.109380
0.001	0.88250	1.163E–02	0.099387
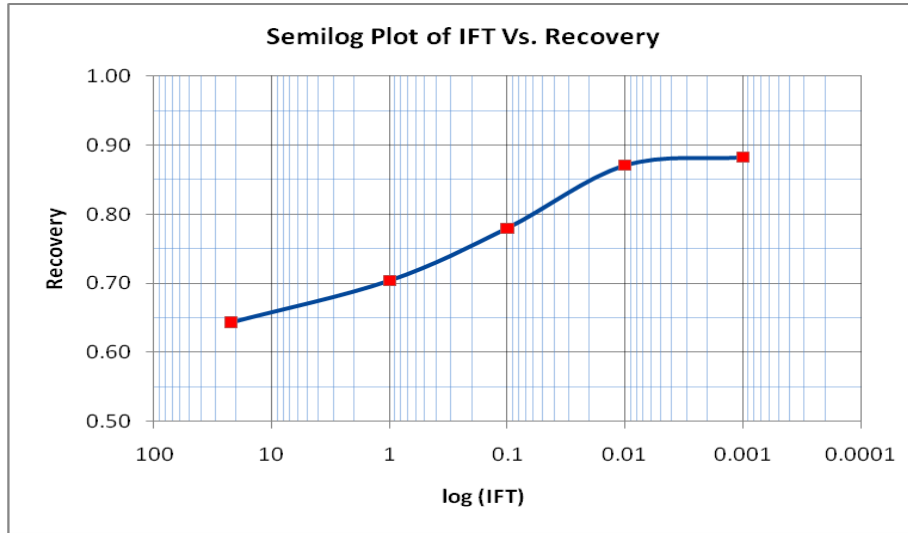
Figure 43: Effect of reduced IFT on recovery considering change in oil relative permeability curvature in stratified model
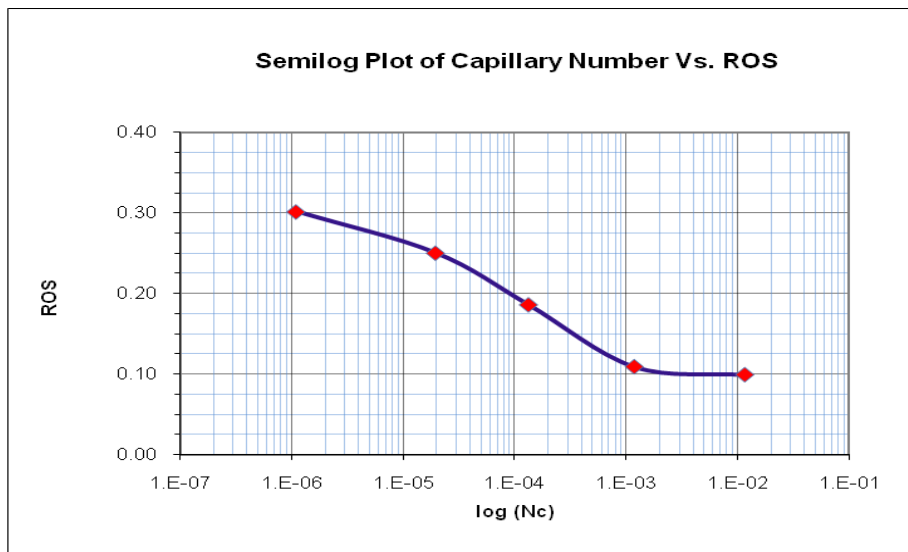
Figure 44: Effect of capillary number (obtained by varying IFT) on remaining oil saturation considering change in oil relative permeability curvature in stratified model

The effect of reduced interfacial tension on recovery as found above was revealed by simulation studies shown below. Only the results for homogeneous model are given.

Comparison of Field Cumulative Oil Production at different IFTs considering change in oil relative permeability curve
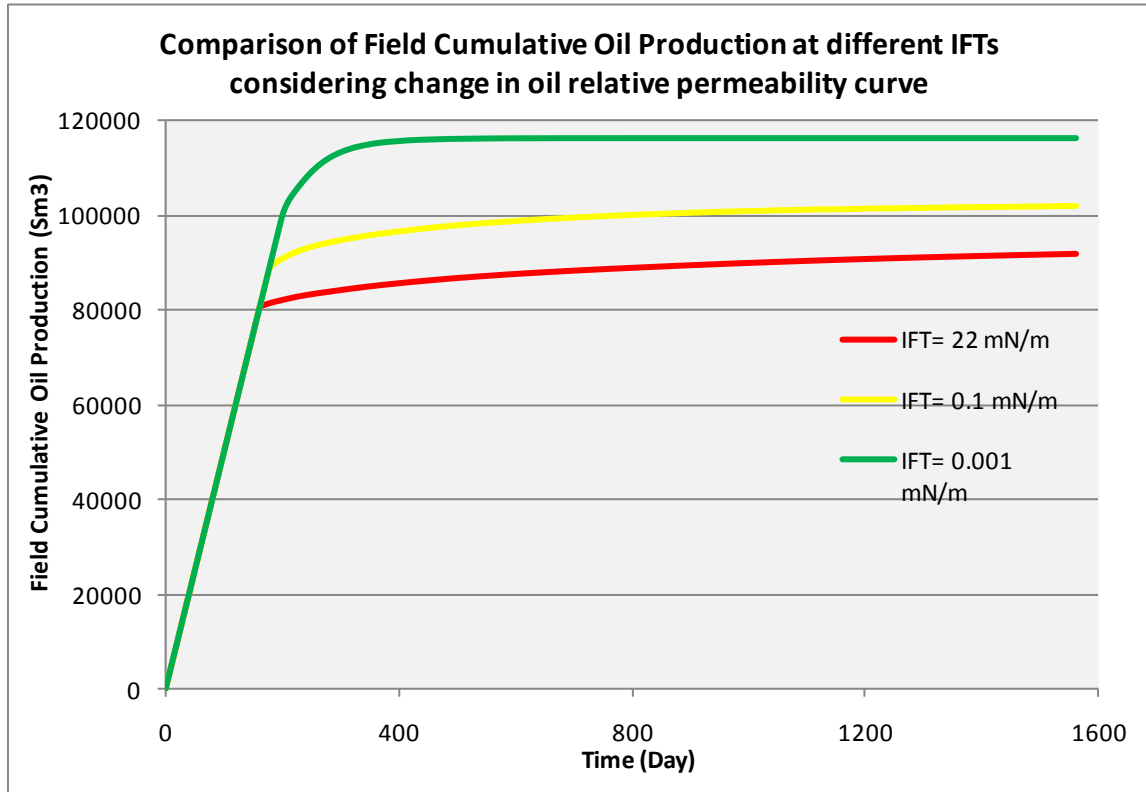
Figure 45: Comparison of field cumulative oil production at different IFTs considering change in oil relative permeability curvature in homogeneous model

A comparison of recovery from homogeneous model with and without gravitational effects is shown below. The figure below clearly indicates a profound gravitational effect causing significant increase in oil recovery. At high interfacial tension (22 to 1 mN/m), water and surfactant flooding gives same resutls because gravity does not play any role at high interfacial tension due to high capillary forces. As the interfacial tension is reduced below 1 mN/m, capillary forces are reduced, release and segregate oil which contribute to increase oil recovery.
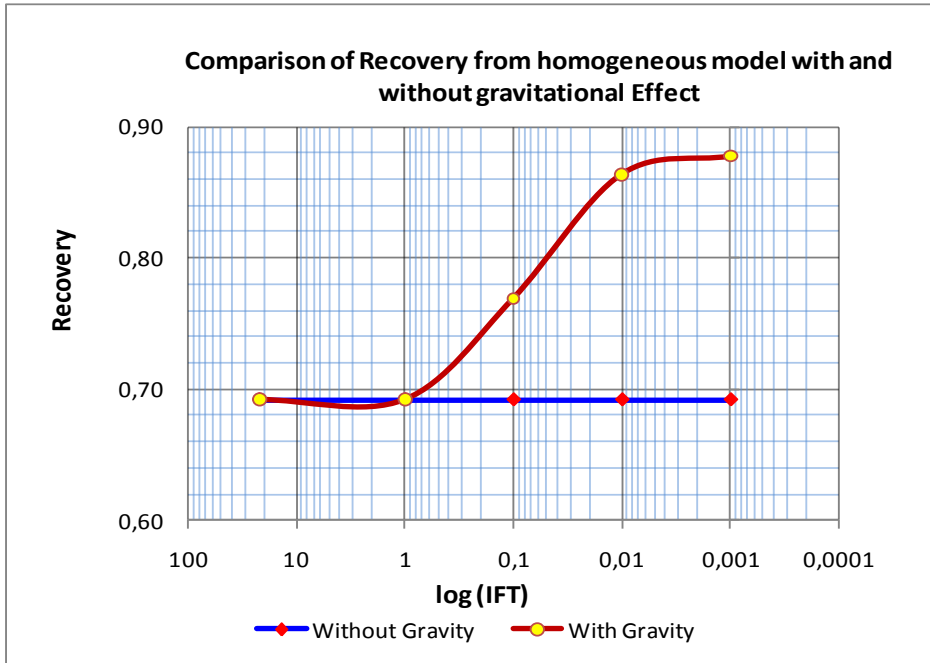
Figure 46: Comparison of Recovery from homogeneous model with and without gravitational effect
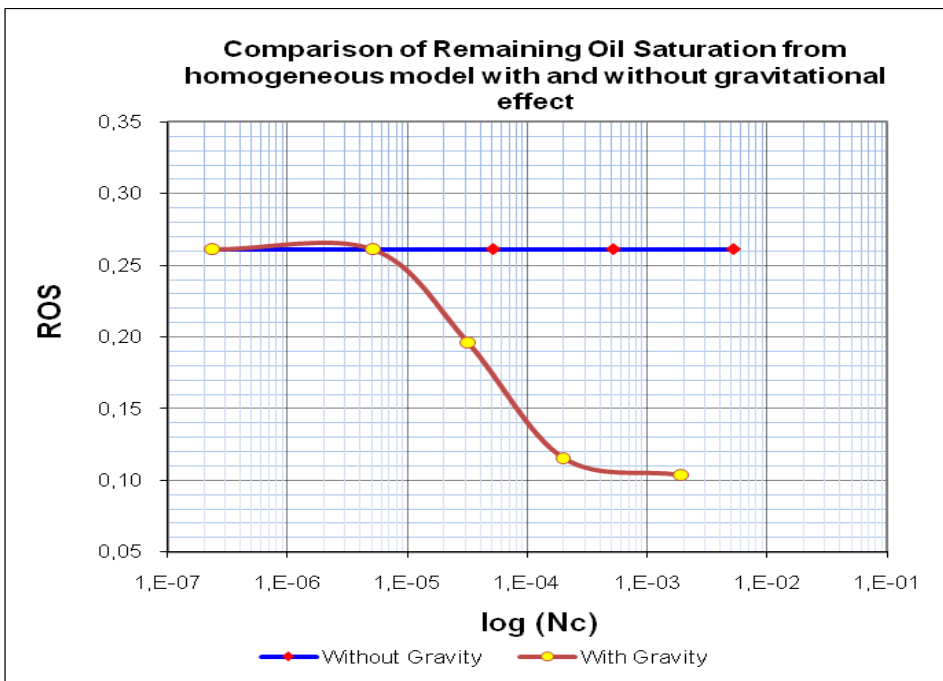
Figure 47: Comparison of Remaining Oil Saturation from homogeneous model with and without gravitational effect

80

4.8. Limitations of Simulation Results

1. Capillary trapping mechanism depends upon properties, some of which are not very well known while others are hard to include in simulation studies. These properties mainly include geometrical distribution of heterogeneities, variation of properties and scale of heterogeneities.

2. We assumed J–Scaling in our simulation studies but at the same time we provided same relative permeability curves for different permeability rocks in simulation models. Relative permeability in our case is independent of permeability since miscible and immiscible curves are same which is, of course, not true. In other words, representation of imbibition capillary pressure is simplified in our simulation models i.e., all rocks (Inclusion and surrounding matrix) in our models regardless of varying permeability follow same imbibition capillary pressure curve. All imbibition capillary pressure curves start from same saturation which is an over simplification.

3. Our simulation studies do not incorporate the effect of surfactant adsorption. In our simulation studies, the surfactant was used to introduce a constant IFT. The behavior of surfactant was not investigated e.g., zero adsorption was considered. In real case of surfactant flooding, IFT would not be constant and would depend upon a number of parameters.

4. The variation in water viscosity due to addition of surfactant is not considered in our case.

5. All rocks have been provided same wettability conditions i.e., background rock and inclusions have been considered mixed–wet which is not always true since low permeable inclusion are usually water–wet.

6. Regarding change in curvature of oil relative permeability, we don't know at which capillary number this change occurs. This needs to be figured out experimentally and then needs to be incorporated in simulation studies.

7. Interpolation between immiscible and miscible curves in Eclipse 100 is based on experience from water–wet cores. The extent to which this linear interpolation is valid for mixed–wet reservoir is unknown.

CHAPTER 5

CONCLUSIONS AND DISCUSSION

The success of oil recovery by waterflooding and miscible displacement is strongly influenced by wettability of the reservoir rocks. The wettability is introduced in reservoir simulation studies in the form of capillary pressure and relative permeability curves. Thus the determination of reservoir rock wettability in any secondary or tertiary recovery project is necessary. A sensitivity analysis on flow rates given at the beginning of simulation results reveals that capillary dominance exists at low flow rates (usually exist close to a well in some high permeable layers) whereas viscous dominance exists at high flow rates (usually encountered away from wells in a low permeable layers where the velocities ratio or capillary number ratio may reach several order of magnitude.

In the absence of gravitational forces and without relative permeability modification, surfactant flooding does not seem to be a viable solution for oil production enhancement from mixed–wet clean sand reservoirs (such as coastal depositional environment i.e., Beach deposition). This is indicated by simulation results from homogeneous model which indicate recovery trend from water and surfactant flooding to overlap. This makes sense since input relative permeability and capillary pressure curves from mixed–wet reservoir were used in simulation studies and in such reservoir oil is not trapped because of snap–off phenomenon which is usually the case in water–wet reservoirs.

In the presence of gravitational forces, reduced interfacial tension as a result of surfactant flooding increases gravity segregation in mix–wet reservoirs which enhances oil recovery. This effect has been investigated and revealed by including gravity effect in same homogeneous model which indicated no effect of reduced

IFT on recovery in absence of gravitational forces. This effect is quantified through a ratio of viscous to gravitational forces which depends upon injection rates, absolute horizontal permeability of reservoir and vertical permeability, density difference. A sensitivity analysis of permeability in this case indicates that effect of reduced interfacial tension is strongly dependent on permeability of the model/reservoir. Results indicate that reduced interfacial tension causes more oil segregation and hence more oil recovery in low permeable reservoirs.

In stratified/layered mixed–wet reservoirs, oil recovery enhancement due to capillary trapping was not found to be very sensitive to variation in interfacial tension. We just considered a simple stratified model with uniform layers of alternating low and high permeability. One may assume that more realistic stratified models with considerable lateral variation in reservoir properties may show increase sensitivity to variation in interfacial tension. This case requires more simulation research since there are many parameters which could influence the effect of reduced interfacial tension. Variation in permeability among different layers of the stratified reservoir, thickness of layers, cross flow among layers, different wettability condition within different layers (we considered all layers as mixed–wet which is not always true) are few factors to mention.

In such case, variation in interfacial tension affects the balance between capillary and viscous cross flow. Viscous cross flow increases with lateral variation in reservoir properties like permeability, porosity etc. Mobility contrast between displacing and displaced fluids in different layers also cause an increase in viscous cross flow which can be reduced by a reduction in interfacial tension.

High saturation contrast between inclusions/heterogeneities and surrounding matrix/background rock at capillary dominance was revealed by our simulation studies. An effect of reduced interfacial tension was found analogous to increase in

flow rate in both low and high permeable inclusion models even though the results from those two models were found to be quite opposite.

In low permeable inclusion case, reduced interfacial tension releases oil from low permeable because this reduction causes capillary pressure between oil and water in low permeable inclusion to decrease and release oil from such inclusions. Reduction in interfacial tension in this case causes a delay in water breakthrough as depicted by results from low permeable inclusion model.

In mixed–wet reservoirs, a reduction in IFT from 22 to 1 mN/m enhances oil recovery but further reduction in interfacial tension seems ineffective or has negligible effect on oil recovery. This suggests that an inexpensive surfactant or a good quality surfactant at low concentration can be injected to get same results.

Surfactant flooding seems to cause entrapment of oil in background/surrounding matrix in high permeable inclusion case. Water prefers to pass through high permeable inclusions/heterogeneities. So surfactant flooding in reservoirs with high permeability inclusions/heterogeneities (e.g. reservoirs with fracture, fissures etc) seems even vulnerable and causes a reduction in ultimate recovery. A bypassing of oil above and below inclusions was also revealed in this case.

Effect of reduced interfacial tension was found more significant in model with low permeable or impermeable shale streaks. Impermeable shale streaks enhance the effect of gravity segregation and hence oil recovery. The results depends upon the geometrical distribution of the shale streaks i.e., continuous or discontinuous shale streaks, vertical restriction offered by shale streaks to segregated oil, frequency of shale streaks etc. It also depends upon the type of saturation dependent properties (relative permeability and capillary pressure) provided to low permeability streaks. In our case same oil–wet relative permeability and capillary pressure curves were provided to both background rock

and shale streaks. This is not always true since low permeability shale streaks are preferentially water–wet since clay minerals are more prone to water. So if the water–wet table of K_r and P_c are provided to low permeable streaks, the results would be different.

The change in oil relative permeability curvature was found to enhance oil recovery both in homogeneous model and layered/stratified model. This mechanism could be combined with two other mechanisms i.e., capillary trapping and gravity segregation very easily by introducing different immiscible and miscible curves. We used same end points for both immiscible and miscible curve but it could be different.

RECOMMENDATIONS FOR FUTURE WORK

In this thesis, effect of reduced IFT on different mechanisms which could possibly occur in mixed–wet reservoirs is investigated. Only the effect of reduced interfacial tension has been investigated and no attention has been paid to wettability alteration which could be a consequence of surfactant flooding. The area of wettability modification in mixed–wet reservoirs by surfactant flooding needs to be addressed. We believe that our results are still not quite conclusive and a further extensive simulation research is required before surfactant flooding in mixed–wet reservoirs is recommended since there are many uncertainties related to surfactant flooding in such reservoirs. Modeling the change in wettability by surfactant being the area needed to be explored further.

We used same relative permeability and imbibition capillary pressure curves in low and high permeable inclusion models. In future work, we recommend to introduce hysteresis effect i.e., use different imbibition capillary pressure curves for different permeability rocks. How the curvature of oil relative permeability changes at high capillary number is not addressed in our simulation studies and requires further research.

The factors which could possibility influence the change in curvature of oil relative permeability include reduced IFT and wettability alteration, the extent by which they influence this curvature change needs to be determined. The effect of surfactant adsorption and change in water viscosity due to addition of surfactant is recommended to be incorporated in future simulation studies.

REFERENCES

Al–Hashim, H.S., Obiora, V., Al–Yousef, H. Y., Fernandez, F., and Nofal, W., *"Alkaline Surfactant Polymer Flooding Formulation for Saudi Arabian Carbonate Reservoirs",* Tulsa, OK, Apr., 1996.

Anderson, W.G., *"Wettability Literature Survey–Part 1: Rock/Oil/Brine Interactions, and the Effects of Core Handling on Wettability",* JCPT, Oct., 1986.

Anderson, W.G., *"Wettability Literature Survey – Part 4: Effects of Wettability on Capillary Pressure"*, JPT, 1283–1300, Oct., 1987.

Arihara, N., Yoneyama, Akita, Y., and Lu, X., *"Oil Recovery Mechanism of Alkali–Surfactant–Polymer Flooding"*, SPE 54330 prepared for presentation at SPE Asia Pacific Oil and Gas Conference and Exhibition, Jakarta, Indonesia, Apr., 1999.

Baviere, M., Glenat, P., Plazanet, V., and Labrid, J., *"Improvement of the Efficiency/Cost Ratio of Chemical EOR Processes by Using Surfactants, Polymers, and Alkalis in Combination",* SPE 27821 presented at the SPE/DOE Ninth Symposium on Improved Oil Recovery, Tulsa, OK, Apr., 1994.

Baviere, M., Glenat, P., Plazanet, V., and Labrid, J., C. A. Miller and P. Neogi, *"Improved EOR by Use of Interfacial Phenomena,"* Marcel Dekker Inc., New York, 1985.

Brownell, L.E. and Katz, D.L., *"Flow of fluids throught porous media – Part II, Simultaneous flow of two homogeneous phases"*, Chem. Eng. Progr., 43, 601–612, 1947.

Chatzis, I., Morrow, N. R., *"Correlation of Capillary Number Relationships for Sandstone",* SPE10114, 1984.

Craig, F.F., *"The Reservoir Engineering Aspects of Waterflooding,"* SPE Monograph Series, Dallas, p. 21, 1971.

Craig, F. F., Sanderlin, J. L., Moore, D. W. and Geffen, T. M., *"A Laboratory Study of Gravity Segregation in Frontal Drives",* Trans., AIME, Vol. 210, 275, 1957.

Denekas, M.O., C. C. and Davis, G.T., *"Effects of Crude Oil Components on Rock Wettability",* Trans. AIME No. 216, pp 330–333, 1959.

Don W. Green and G. Paul Willhite., *Enhanced Oil Recovery*, Textbook series, SPE, Vol. 6, Richardson, TX, 1998.

Donaldson, E. C., Thomas, R. D., and Lorenz, P. B., *"Wettability Determination and Its Effect on Recovery Efficiency",* SPEJ, Mar., 1969.

Emery, L. W., Mungan, N., and Nicholson, R. W., *"Caustic Slug Injection in the Singleton Field",* JPT, 1569–1576, Dec., 1970.

Falls, A. H., Thigpen, D. R., Nelson, R. C. et al., *"A Field Test of Cosurfactant–Enhanced Alkaline Flooding",* SPE 24117 presented at the SPE/DOE Eighth Symposium on Enhanced Oil Recovery, Tulsa, OK, 1992.

Foster, W.R., *"A low tension waterflooding process",* SPE 3803, JPT, 205–210, 1973.

French, T. R., *"A Method for Simplifying Field Application of ASP Floodin",* SPE 35354 presented at the Tenth Symposium on Improved Oil Recovery, Tulsa, OK, Apr., 1996.

French, T. R., and Burchfield, T. E., *"Design and Optimization of Alkaline Flooding Formulation",* SPE 20238 presented at the SPE/DOE Seventh Symposium on Enhanced Oil Recovery, Tulsa, OK, 1990.

Gao, S., Li, H., and Li, H., *"Laboratory Investigation of Combination of Alkali/Surfactant/Polymer Technology for Daqing EOR",* SPERE, 194–197, Aug., 1995.

Gao, S., Li, H., Yang, Z., Pitts, M. J., Surkalo, H., and Wyatt, K., *"Alkaline/Surfactant/Polymer Pilot Performance of the West Central Saertu, Daqing Oil Field",* SPERE, 181–188, Aug., 1996.

Green, D. W., and Willhite, G.P., *Enhanced Oil Recovery*, 240–300, SPE Textbook Series Vol. 6, SPE inc., Richardson, TX, 1998.

Gupta, S.P. and TRUSHENSKI, S.P., *"Micellar Flooding – Compositional Effects on Oil Displacement"*, SPEJ, 116–128, Apr., 1979.

Hernandez, C., Chacon, L. J., Anselmi, L., Baldonedo, A., Qi, J., Dowling, P. C., and Pitts M. J., *"ASP System Design for an Offshore Application in the La Salina Field, Lake Maracaibo"*, SPE 69544 presented at the SPE Latin America and Caribbean Petroleum Engineering Conference, Buenos Aires, Argentina, Mar., 2001.

J.J. Taber, *Research on Enhanced Oil Recovery: Past, Present, and Future*. Symposium on Surface Phenomenon in Enhanced Oil Recovery. Stockholm, Sweden, Aug., 1979.

Klins, M.A., *"Carbon Dioxide Flooding – Basic Mechanism and Project Design"*, International Human Resources Development Corporation, Boston, 1984.

Krumrine, P.H., J.S. Falcone, Jr., and T.C. Campbell., *"Surfactant Flooding II: "The Effect of Alkaline Additives on Permeability and Sweep Efficiency"*, SPEJ., 983–992, Dec., 1982.

Larry W. Lake., *"Enhanced Oil Recovery"*, Textbook, Prentice Hall, Englewood Cliffs, New Jersey 07632, 1989.

Larson, R. G., Davis, H. T., and Scriven, L. E., *"Displacement of residual nonwetting phase from porous media,"* Chem. Eng. Sci.,75–85, 1981.

Leal, L. G., *"Advanced Transport Phenomena"*, New York: Cambridge University Press, 2007.

Lefebvre du Prey, E.J., *"Factors Affecting Liquid–Liquid Relative Permeabilities of a Consolidated Porous Media"*, SPEJ., vol. 13, 39, Feb., 1973.

Lefebvre du Prey, E. G., SPEJ, vol. 13, 39–47, 1973.

Leverett, M.C., *"Flow of oil–water mixtures through unconsolidated sands"*, Trans. AIME, 149–171, 1939.

Leverett, M.C., *"Capillary Behaviour in Porous Solids,"* Trans AIME, Vol. 142, 1941.

Lo, H.Y., *"The Effect of Interfacial Tension on Oil–Water Relative Permeabilities"*, Research Report, Petroleum Recovery Institute, Nov., 1976.

Manrique, E. J., de Carvajal, G. G., Anselmi, L., Romero, C., and Chacon, L. J., *"Alkali/Surfactant/Polymer use at VLA 6/9/21 Field in Maracaibo Lake"*, SPE 59363 presented at the SPE/DOE Improved Oil Recovery Symposium, Tulsa, OK, Apr., 2000.

Martin, F. D., and Oxley, J. C., *"Effect of Various Alkaline Chemicals on Phase Behavior of Surfactant/Brine/Oil Mixtures"*, SPE 13575 presented at the international Symposium on Oilfield and Geothermal Chemistry, Phoenix, AR, Apr., 1985.

Martin, F. D., and Oxley, J.C., and Lim, H., *"Enhanced Recovery of a "J" Sand Crude Oil with a Combination of Surfactant and Alkaline Chemicals"*, SPE 14293 presented at the 60th Annual Technical Conference and Exhibition of SPE, Las Vegas, NV, Sep., 1985.

Mat Hussin Yunan, *"An Experimental Study on the Mechanism of Waterflood Residual Oil Mobilization"*, M.Sc. Thesis, University of New South Wales, 1988.

Mayer, E.H., Berg, R.L., Carmichael, J.D., and Weinbrandt, R.M., *"Alkaline Injection for Enhanced Oil Recovery – A Status Report"*, JPT, 209–221, Jan., 1983.

McCaffery, F.G. and Bennion, D.W., *"The Effect of Wettability on Two–Phase Relative Permeabilities"*, The Journal of Canadian Petroleum Technology, vol. 13, 42–53, 1974.

McDougall, S. R., and Sorbie, K. S., *"The Impact of Wettability on Waterflooding: Pore–Scale Simulation"*, SPERE, 208–213, Aug., 1995.

Melrose, J.C. and C.F. Brandner., *"Role of Capillary Forces in Determining Microscopic Displacement Efficiency for Oil Recovery by Waterflooding"*, J. Can. Pet. Tech., v.13, 54, Oct.–Dec., 1974.

Moore, T.F. and Slobod, R.L., *"The effect of viscosity and capillarity on the displacement of oil by water,"* Producer's Monthly, 20–30, 1956.

Morrow, N.R., Tang, G., Valat, M. and Xie, X., *"Prospects of improved oil recovery related to Wettability and Brine Composition,"* J. Pet. Sci. Eng., 267–276, Jun., 1998.

Morrow, N. R., *"Wettability and Its Effects on Oil Recovery"*, JPT, 1476–1484, Dec., 1990.

Mungun, N., *"Role of Wettability and Interfacial Tension in Water Flooding"*, SPEJ, 115–123, Jun., 1964.

Mungan, N., *"Certain Wettability Effects in Laboratory Waterfloods"*, JPT, 247–252, Feb., 1966.

Nelson, R.C., Lawson, J.B., Thigpen, D.R., Stegemeier, G.L., *"Cosurfactant–enhanced alkaline flooding"*, SPE/DOE 12672 presented at the SPE/DOE Fourth Symposium on Enhanced Oil Recovery, Tulsa, OK, 1984.

Olsen, D. K., Hicks, M.D., Hurd, B. G., Sinnokrot, A. A., and Sweigart, C.N., *"Design of a Novel Flooding System for an Oil–Wet Central Texas Carbonate Reservoir"*, SPE 20224 presented at the SPE Seventh Symposium on Enhanced Oil Recovery, Tulsa, OK, 1990.

Owens, W.W. and Archer, D.L., *"The Effect of Rock Wettability on Oil–Water Relative Permeability Relationships,"* JPT, 873–878, Jul., 1971.

P. Shen, B. Zhu, B. Li, and Y. S., *"The Influence of Interfacial Tension on Water/Oil Two–Phase Relative Permeability"* SPE 95405–MS, prepared for presentation at SPE/DOE Symposium on Improved Oil Recovery, Tulsa, Oklahoma, 22–26 Apr., 2006.

Qiao, ., Gu, H., Li, D., and Dong, L., *"The Pilot Test of ASP Combination Flooding in Karamay Oil Field"*, SPE 64726 presented at the International Oil and Gas Conference and Exhibition in China, Beijing, China, Nov., 2000.

Rosman, A. and E. Zana, *"Experimental Studies of Low IFT Displacement by CO_2 Injection"*, SPE 6723 presented at 52nd Annual Fall Tech. Conference and Exhibition, Denver, Colorado, 9–12 Oct., 1977.

Saffman, P.G. and Taylor, G., *"The penetration of a fluid into a porous medium or Hele–Shaw cell containing a more viscous liquid,"* Proc. Roy. Soc. London A, 312–329, 1958.

Salathiel, R. A., *"Oil Recovery by Surface Film Drainage in Mixed–wettability Rocks",* JPT, 1216–1224, Oct., 1973.

Shuler, P. J., Kuehne, D. L., and Lerner, R. M., *"Improving Chemical Flood Efficiency with Micellar/Alkaline/Polymer Processes",* JPT, 80–88, Jan., 1989.

Skjaeveland, S.M. et al., *"Relative Permeability Correlation for Mixed–Wet Reservoirs,"* SPEREE, Feb., 2000.

Song, W., Yang, C., Han, D., Qu, Z., Wang, B., and Jia, W., *"Alkaline–Surfactant– Polymer Combination Flooding for Improving Recovery of the Oil with High Acid Value",* SPE 29905 presented at the International Meeting on Petroleum Engineering, Beijing, China, Nov., 1995.

Stegemeier, G.L., *"Mechanisms of Entrapment and Mobilization of Oil in Porous Media",* Improved Oil Recovery by Surfactant and Polymer Flooding, 55–92, Academic Press, New York City, 1977.

Subhash C. A., *"Surfactant Induced Relative Permeability Modifications for Oil Recovery Enhancement",* M.Sc. Thesis, Louisiana State University, 2002.

Taber, J.J., *"Dynamic and Static Forces Required to Remove a Discontinuous Oil Phase from Porous Media Containing both Oil and Water",* SPE 2098 presented at SPE European Regional Meeting, Milano, Italy, Apr., 1968.

Taber, J.J., Martin, F.D., and Seright, R.S., EOR screening criteria revisited – Part I: *"Introduction, to screening criteria and enhanced recovery field projects",* SPE Reservoir Engineering. v. 12, 189–198, 1997.

Talash, A.W., *"Experimental and calculated relative permeability data for systems containing tension additives",* SPEJ., 177–188, 1976.

Talash, A.W., *"Experimental and Calculated Relative Permeability Data for Systems Containing Tension Additives",* SPE 5810, Improved Oil Recovery Symposium of SPE of AIME, Tulsa, OK., Mar., 22.–24., 1976.

Tiab, D. a., Petrophysics. Houston, Gulf Publishing Company, 1999.

Tong, Z., Yang, C., Wu, G., Yuan, H., Yu, L., and Tian, G., SPE 39662 presented at the SPE/DOE Improved Oil Recovery Symposium, Tulsa, OK, Apr., 1998.

Treiber, L.E., Archer, D.L. and Owens, W.W., *"A Laboratory Evaluation of the Wettability of Fifty Oil–Producing Reservoirs",* SPEJ, 531–540, Dec., 1972.

Vargo, J., Turner, J., Vergnani, B., Pitts, M. J., Wyatt, K., Surkalo, H., and Patterson, D., *"Alkaline–Surfactant–polymer Flooding of the Cambridge Minnelusa Field",* SPERE&E, 552–557, Dec., 2000.

Virnovsky, G. A., Lohne, A. and Lerdahl, T. R., *"Coarse Scale Capillary Pressure in Heterogeneous Reservoirs"*, published in Transport in Porous Media Journal, Dec., 2008.

Wang, D., Cheng, J., Wu, J., Yang, Z., Yao, Y., and Li, H., *"Summary of ASP Pilot in Daqing Oil Field",* SPE 57288 presented at the SPE Asia Pacific Improved Oil Recovery Conference, Kuala Lumpur, Malaysia, Oct., 1999.

Wang, D., Zhang, Z., Cheng, J., Yang, J., Gao, S., and Li, L., *"Pilot Tests for Alkaline/Surfactant/Polymer Flooding in Daqing Oil Field,"* SPERE, 229–233, Nov., 1997.

Wanger O.R. and R.O. Leach, *"Effect of Interfacial Tension on Displacement Efficiency",* SPEJ., vol. 6, 335, Dec., 1966.

Wanger, O.R., and Leach, R.O., *"Improving Oil Displacement Efficiency by Wettability Adjustment,"* Petroleum Transactions, AIME, 65–72, 1959.

Willhite, G. P., *Waterflooding*, Textbook series, SPE, Richardson, TX, 1986.

APPENDIX

Simulation Data Input File for Homogeneous Model without Gravity Effect

RUNSPEC
==============================

TITLE

 Water flooding in homogeneous model (Base Case)

DIMENS
  200 1 50 /

NONNC

OIL

WATER

SURFACT
METRIC

TABDIMS
  2 1 100 20 1 /

ENDSCALE
  NODIR REVERS /

WELLDIMS
  2 50 1 2 /

START

1 JAN 2000 /

NSTACK
 50 /

GRID
==========================

INIT

DXV
 200*2.5 /

DYV
 1*10 /

DZ
 10000*2.5 /

== Reservoir Pore Volume = (200*2.5 * 1*10 * 50*2.5)* 0.25 = 156250 m3
== 5 * Pore Volume (Volume to be Injected) = 5 * 156250 = 781250 m3

PERMX
 10000*100/

== Isotropic Model

COPY
 PERMX PERMY/
 PERMX PERMZ/
/

PORO
 10000*0.25 /
TOPS

```
   200*2600 /


JFUNC
  WATER  22.0 /


RPTGRID
  DX  DY  PERMX  PORO  KOVERD
TRANX /


PROPS
============================


SWFN
```

== S_w	K_{rw}	$J(S_w)$
0.148000	0.00000000	200.0000
0.149590	0.00000001	23.83791
0.153375	0.00000002	6.147762
0.160945	0.00000004	2.258275
0.168515	0.00000009	1.309519
0.176085	0.00000021	0.888995
0.183655	0.00000036	0.653511
0.191225	0.00000054	0.503619
0.198795	0.00000081	0.400102
0.206365	0.00000121	0.324441
0.213935	0.00000176	0.266779
0.221505	0.00000255	0.221397
0.229075	0.00000369	0.184753
0.244215	0.00000755	0.129192
0.259355	0.00001484	0.088996
0.274495	0.00002852	0.058471
0.289635	0.00005262	0.034401
0.304775	0.00009491	0.014834
0.335055	0.00027820	–0.015400
0.365335	0.00071893	–0.038200
0.395615	0.00165294	–0.056640
0.425895	0.00349981	–0.072480
0.447636	0.00578936	–0.082900
0.469377	0.00923191	–0.09289
0.491118	0.01434285	–0.10273
0.512859	0.02171011	–0.11267
0.534600	0.03157445	–0.12296
0.556341	0.04460744	–0.13386
0.578082	0.06139899	–0.14570
0.599823	0.08195209	–0.15884
0.621564	0.10528319	–0.17378
0.643305	0.13247879	–0.19114
0.665046	0.16376902	–0.21182
0.686787	0.19981156	–0.23710
0.708528	0.24134976	–0.26888
0.730269	0.28903769	–0.31019
0.752010	0.34284329	–0.36598
0.773751	0.40138466	–0.44506
0.795492	0.46591559	–0.56445
0.817233	0.53621018	–0.76117
0.838974	0.60968389	–1.13094
0.860716	0.68594618	–2.00247
0.868286	0.71379943	–2.62999
0.875856	0.74223685	–3.68938
0.890996	0.79588497	–10.9333
0.898566	0.82414609	–34.9465
0.902351	0.83865077	–132.058
0.903108	0.84158220	–218.707
0.903865	0.84452387	–470.499
0.905000	0.84747583	–600.000

```
/
```

0.148000	0.00000000	200.0000
0.149590	0.00000001	23.83791
0.153375	0.00000002	6.147762
0.160945	0.00000004	2.258275
0.168515	0.00000009	1.309519
0.176085	0.00000021	0.888995
0.183655	0.00000036	0.653511
0.191225	0.00000054	0.503619
0.198795	0.00000081	0.400102
0.206365	0.00000121	0.324441
0.213935	0.00000176	0.266779
0.221505	0.00000255	0.221397
0.229075	0.00000369	0.184753
0.244215	0.00000755	0.129192
0.259355	0.00001484	0.088996

0.274495	0.00002852	0.058471
0.289635	0.00005262	0.034401
0.304775	0.00009491	0.014834
0.335055	0.00027820	−0.015400
0.365335	0.00071893	−0.038200
0.395615	0.00165294	−0.056640
0.425895	0.00349981	−0.07248
0.447636	0.00578936	−0.08290
0.469377	0.00923191	−0.09289
0.491118	0.01434285	−0.10273
0.512859	0.02171011	−0.11267
0.534600	0.03157445	−0.12296
0.556341	0.04460744	−0.13386
0.578082	0.06139899	−0.14570
0.599823	0.08195209	−0.15884
0.621564	0.10528319	−0.17378
0.643305	0.13247879	−0.19114
0.665046	0.16376902	−0.21182
0.686787	0.19981156	−0.23710
0.708528	0.24134976	−0.26888
0.730269	0.28903769	−0.31019
0.752010	0.34284329	−0.36598
0.773751	0.40138466	−0.44506
0.795492	0.46591559	−0.56445
0.817233	0.53621018	−0.76117
0.838974	0.60968389	−1.13094
0.860716	0.68594618	−2.00247
0.868286	0.71379943	−2.62999
0.875856	0.74223685	−3.68938
0.890996	0.79588497	−10.9333
0.898566	0.82414609	−34.9465
0.902351	0.83865077	−132.058
0.903108	0.84158220	−218.707
0.903865	0.84452387	−470.499
0.905000	0.84747583	−600.000

/

SOF2

== S_o	K_{ro}
0.09500	0.00000001
0.12528	0.00000077

0.15556	0.00000491
0.18584	0.00002617
0.21610	0.00011603
0.2464	0.00042824
0.27668	0.00131584
0.30696	0.00336597
0.33724	0.00716820
0.36752	0.01275780
0.3978	0.02070515
0.42808	0.03237853
0.45836	0.04878788
0.48864	0.07083417
0.51892	0.09909457
0.5492	0.13357739
0.57948	0.17349708
0.60976	0.21713381
0.64004	0.26475376
0.67032	0.32144566
0.7006	0.38839826
0.73088	0.46703697
0.76116	0.55889411
0.79144	0.66559810
0.82172	0.78885812
0.8520	0.93044349

/

0.0950	0.00000001
0.12528	0.00000077
0.15556	0.00000491
0.18584	0.00002617
0.21612	0.00011603
0.2464	0.00042824
0.27668	0.00131584
0.30696	0.00336597
0.33724	0.00716820
0.36752	0.01275780
0.39780	0.02070515
0.42808	0.03237853
0.45836	0.04878788
0.48864	0.07083417
0.51892	0.09909457

```
0.5492      0.13357739                      10   1.0 /
0.57948     0.17349708                     –9    0.0
0.60976     0.21713381                     –4.5  0.0
0.64004     0.26475376                     –2    1.0
0.67032     0.32144566                      10   1.0 /
0.7006      0.38839826
0.73088     0.46703697          RPTPROPS
0.76116     0.55889411              DX    ROCKTAB    STOW
0.79144     0.66559810          SURFVISC SWFN /
0.82172     0.78885812
0.8520      0.93044349          REGIONS
/                               ===========================

PVTW                            SATNUM
   1  1.000  4.6E–6   0.34  0.0 /   10000*1 /

PVDO                            SURFNUM
   200     1.00000   0.47        10000*2 /
   280     0.99999   0.47
   100000  0.99998   0.47 /     SOLUTION
                                ===========================
ROCK
   1  .3E–6 /                   EQUIL
                                   2600  1  2625  5 /
DENSITY
   999.9999  1000   10 /        SUMMARY
                                ===========================
SURFVISC
   0     0.34                   FWIR
   30    0.34 /                 FOPR
                                FOPT
SURFST                          FWPR
   0    22                      FWCT
   0.1   0.1                    FOIP
   30    0.1 /                  FWIP
                                WBHP
 SURFCAPD                       'I' /
   –9    0.0                    EXCEL
   –4.5  0.0
   –2    1.0
```

SCHEDULE

============================

RPTSCHED

'PRES'   'SOIL'   'SWAT' 'CPU=1'
'FIP=1' 'KRO' 'KRW'
'PCOW'   'POILD'   'RESTART=2'
'SUMMARY=1' 'WELLS=2'
'FIPSURF=2' ' SURFBLK' 'VWAT'   /

WELSPECS
 'P' 'G' 200 1   2600   'OIL' 0.0 /
 'I' 'G' 1   1   2600   'WAT' 0.0 /
/

COMPDAT
 'P'   200   1   1   50 'OPEN'   0
17.054   /
 'I' 1   1   1 50 'OPEN' 0   17.054
/
/

WCONPROD
 'P' 'OPEN' 'BHP'   5*   0.1 /
      /

WCONINJE
   'I'   'WAT' 'OPEN' 'RESV'   1*
  500 100000 /
   /

TUNING
 1 100 0.01 0.015   /
                                /
 2* 500 3 50 2* 0.01   /

TSTEP
 1562.5 /
END

Simulation Data Input File for Change in Oil Relative Permeability Curvature

RUNSPEC

============================

TITLE

Simulation of Change in Oil Relative Permeability Curvature

DIMENS
  200 1   50 /

NONNC

OIL

WATER

SURFACT

METRIC

TABDIMS
  2 1 100 20 1 /

ENDSCALE
NODIR REVERS /

WELLDIMS
  2 50 1 2 /

START
  1 JAN 2000 /

NSTACK
 50   /

GRID

============================

INIT

DXV
 200*2.5 /

DYV
 1*10 /

DZ
 10000*2.5 /

== Reservoir Pore Volume = (200*2.5 *
1*10 * 50*2.5)* 0.25 = 156250 m3
== 5 * Pore Volume (Volume to be
Injected) = 5 * 156250 = 781250 m3

PERMX
 10000*100/

== Isotropic Model

COPY
 PERMX PERMY/
 PERMX PERMZ/
   /

PORO
 10000*0.25 /

TOPS
 200*2600 /

JFUNC
   WATER 22.0 /

RPTGRID

DX DY PERMX PORO KOVERD
TRANX /

PROPS

=========================

SWFN

== S_w	K_{rw}	$J(S_w)$
0.148000	0.00000000	200.0000
0.149590	0.00000001	23.83791
0.153375	0.00000002	6.147762
0.160945	0.00000004	2.258275
0.168515	0.00000009	1.309519
0.176085	0.00000021	0.888995
0.183655	0.00000036	0.653511
0.191225	0.00000054	0.503619
0.198795	0.00000081	0.400102
0.206365	0.00000121	0.324441
0.213935	0.00000176	0.266779
0.221505	0.00000255	0.221397
0.229075	0.00000369	0.184753
0.244215	0.00000755	0.129192
0.259355	0.00001484	0.088996
0.274495	0.00002852	0.058471
0.289635	0.00005262	0.034401
0.304775	0.00009491	0.014834
0.335055	0.00027820	−0.015400
0.365335	0.00071893	−0.038200
0.395615	0.00165294	−0.056640
0.425895	0.00349981	−0.07248
0.447636	0.00578936	−0.08290
0.469377	0.00923191	−0.09289
0.491118	0.01434285	−0.10273
0.512859	0.02171011	−0.11267
0.534600	0.03157445	−0.12296
0.556341	0.04460744	−0.13386
0.578082	0.06139899	−0.14570
0.599823	0.08195209	−0.15884
0.621564	0.10528319	−0.17378
0.643305	0.13247879	−0.19114

0.665046	0.16376902	–0.21182
0.686787	0.19981156	–0.23710
0.708528	0.24134976	–0.26888
0.730269	0.28903769	–0.31019
0.752010	0.34284329	–0.36598
0.773751	0.40138466	–0.44506
0.795492	0.46591559	–0.56445
0.817233	0.53621018	–0.76117
0.838974	0.60968389	–1.13094
0.860716	0.68594618	–2.00247
0.868286	0.71379943	–2.62999
0.875856	0.74223685	–3.68938
0.890996	0.79588497	–10.9333
0.898566	0.82414609	–34.9465
0.902351	0.83865077	–132.058
0.903108	0.84158220	–218.707
0.903865	0.84452387	–470.499
0.905000	0.84747583	–600.000

/

0.148000	0.00000000	200.000
0.905000	0.84747583	–600.000

/

SOF2

— S_o	K_{ro}
0.09500	0.00000001
0.12528	0.00000077
0.15556	0.00000491
0.18584	0.00002617
0.21612	0.00011603
0.2464	0.00042824
0.27668	0.00131584
0.30696	0.00336597
0.33724	0.00716820
0.36752	0.01275780
0.3978	0.02070515
0.42808	0.03237853
0.45836	0.04878788
0.48864	0.07083417
0.51892	0.09909457

0.5492	0.13357739
0.57948	0.17349708
0.60976	0.21713381
0.64004	0.26475376
0.67032	0.32144566
0.7006	0.38839826
0.73088	0.46703697
0.76116	0.55889411
0.79144	0.66559810
0.82172	0.78885812
0.8520	0.93044349

/

0.0950	0.00000001
0.8520	0.93044349

/

PVTW
  1 1.000 4.6E–6   0.34   0.0 /
 PVDO
   200   1.00000   0.47
   280   0.99999   0.47
   100000 0.99998   0.47 /

ROCK
  1   .3E–6 /

DENSITY
  999.9999 1000 10 /

SURFVISC
   0   0.34
   30   0.34 /

SURFST
   0   0.022
   0.1 0.000001
   30   0.000001 /

SURFCAPD
 –9   0.0

```
 –4.5  0.0
 –2    1.0
  10   1.0 /
 –9    0.0
 –4.5  0.0
 –2    1.0
  10   1.0 /
```

RPTPROPS
     DX   ROCKTAB   STOW
SURFVISC SWFN /

REGIONS
============================

SATNUM
 10000*1 /

SURFNUM
 10000*2 /

SOLUTION
============================

EQUIL
   2600 1 2625 5 /

SUMMARY
============================

FWIR
FOPR
FOPT
FWPR
FWCT
FOIP
FWIP
WBHP
'I' /
EXCEL

SCHEDULE
============================

RPTSCHED

'PRES'   'SOIL'   'SWAT' 'CPU=1'
'FIP=1' 'KRO' 'KRW'
'PCOW'   'POILD'   'RESTART=2'
'SUMMARY=1' 'WELLS=2'
'FIPSURF=2' ' SURFBLK' 'VWAT'
/

WELSPECS
 'P' 'G' 200 1   2600   'OIL' 0.0
/
 'I' 'G' 1   1   2600   'WAT' 0.0
/
/

COMPDAT
 'P'   200 1   1   50   'OPEN'   0
17.054   /
 'I'   1   1   1   50   'OPEN'   0
17.054   /
/

WCONPROD
 'P' 'OPEN' 'BHP'   5*   0.1 /
/

WCONINJE
 'I' 'WAT' 'OPEN' 'RESV' 1*
500 100000 /
/

WSURFACT
 'I' 30.0 /
 /

TUNING
```

```
 1   100   0.01  0.015                    /
                                          /
 2*  500  3  50   2*  0.01                /


TSTEP

 1562.5

END
```

VITA

Usman Aslam was born in Sargodha, Pakistan on August 24, 1984, the son of Aslam Siddiqui and Saida Aslam. After completing his high school studies at Air Base Inter College Sargodha, Pakistan, he entered one of the prestigious universities of Pakistan, University of Engineering & Technology Lahore, in August 2003 to pursue his bachelor's degree in Petroleum Engineering. He was declared "Best Student" in Petroleum Engineering Department in his B.Sc. degree and was awarded with two gold medals. After completing his B.Sc. degree, he worked as a trainee petroleum engineer with a national oil and gas exploration and production company, Pakistan Petroleum Limited, for about one year. In August 2008, he was sponsored by ConocoPhillips after a world level competition to pursue his master's degree in Petroleum Engineering from University of Stavanger, Norway. The degree of Master of Science in Petroleum Engineering will be conferred in June 2010.

**